POST-AGB STARS AS TRACERS OF THE ORIGIN OF ELEMENTS AND ISOTOPES IN THE UNIVERSE

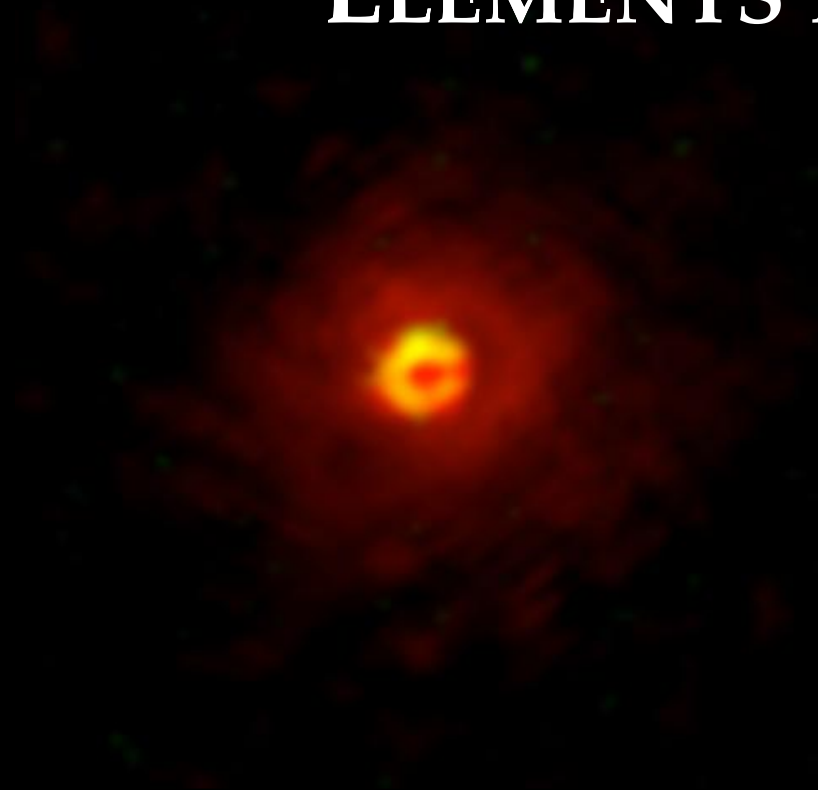

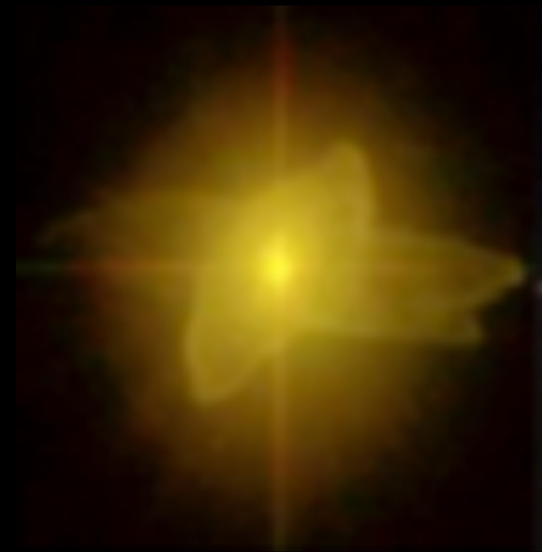

Devika Kamath

MACQUARIE University SYDNEY·AUSTRALIA

Australian Government Australian Research Council

H. Van Winckel, P. Ventura, F. Dell'Agli, M. Mohorian, S. Tosi, K. Andrych, M. Menon, J. Kluska, A. Karakas, Z. Osborn, A. Garcia Hernandez

- Tracing AGB Nucleosynthesis using observations of post-AGBs

- Tracing AGB Nucleosynthesis using observations of post-AGBs
- The revelation of chemical diversities in AGB nucleosynthesis

- Tracing AGB Nucleosynthesis using observations of post-AGBs
- The revelation of chemical diversities in AGB nucleosynthesis
- Our attempts to understand the observed diversities

- Tracing AGB Nucleosynthesis using observations of post-AGBs

AGB Nucleosynthesis

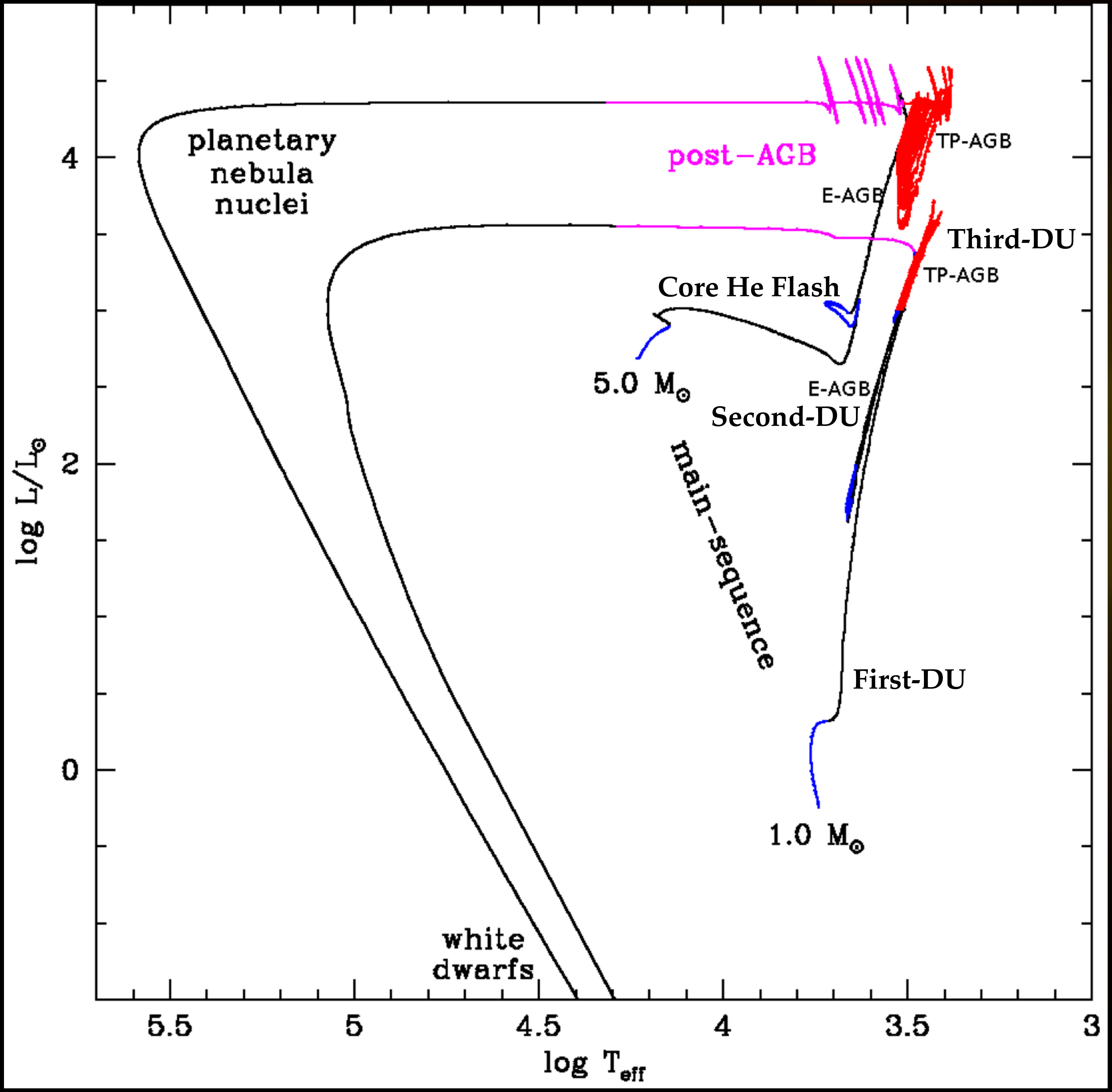

Hot Bottom Burning
(in M > ~3 Msun)
decrease in 12C
increase in 13C and 14N
7Li, Na, Al

Second-DU (in M > ~3 Msun)
increase in 4He and 14N

Third-DU
increase in 12C, some 16O and heavy elements (s-process elements)

First-DU
increase in 4He, 13C, 14N, 17O
decrease in 12C, 16O and 18O

Observational Constraints From AGB Stars

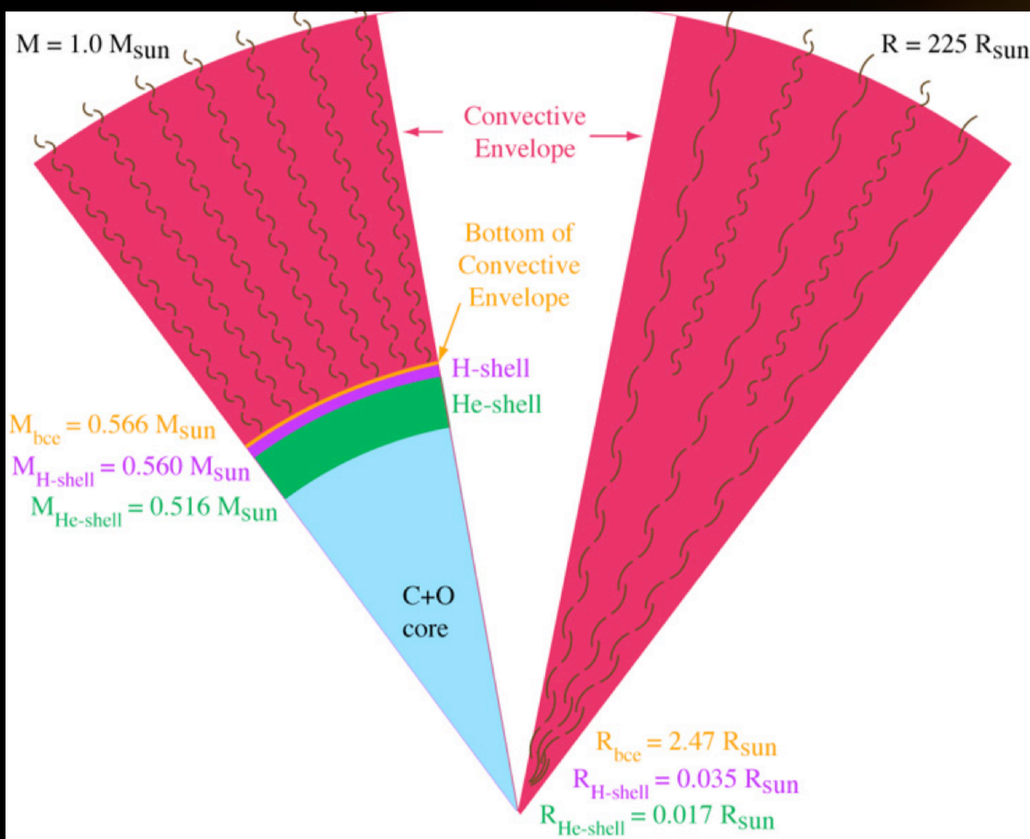

Schematic Structure of an AGB Star

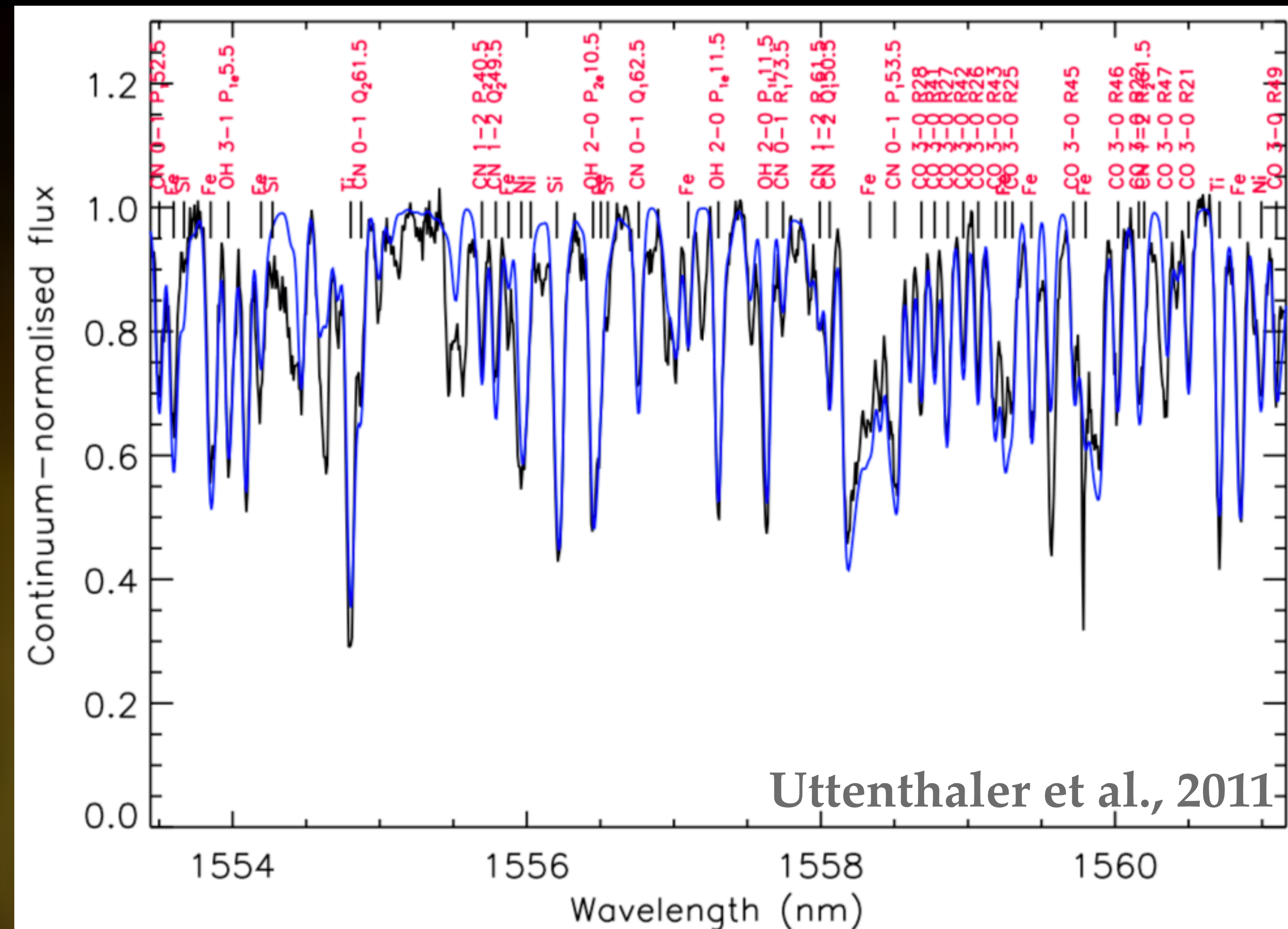

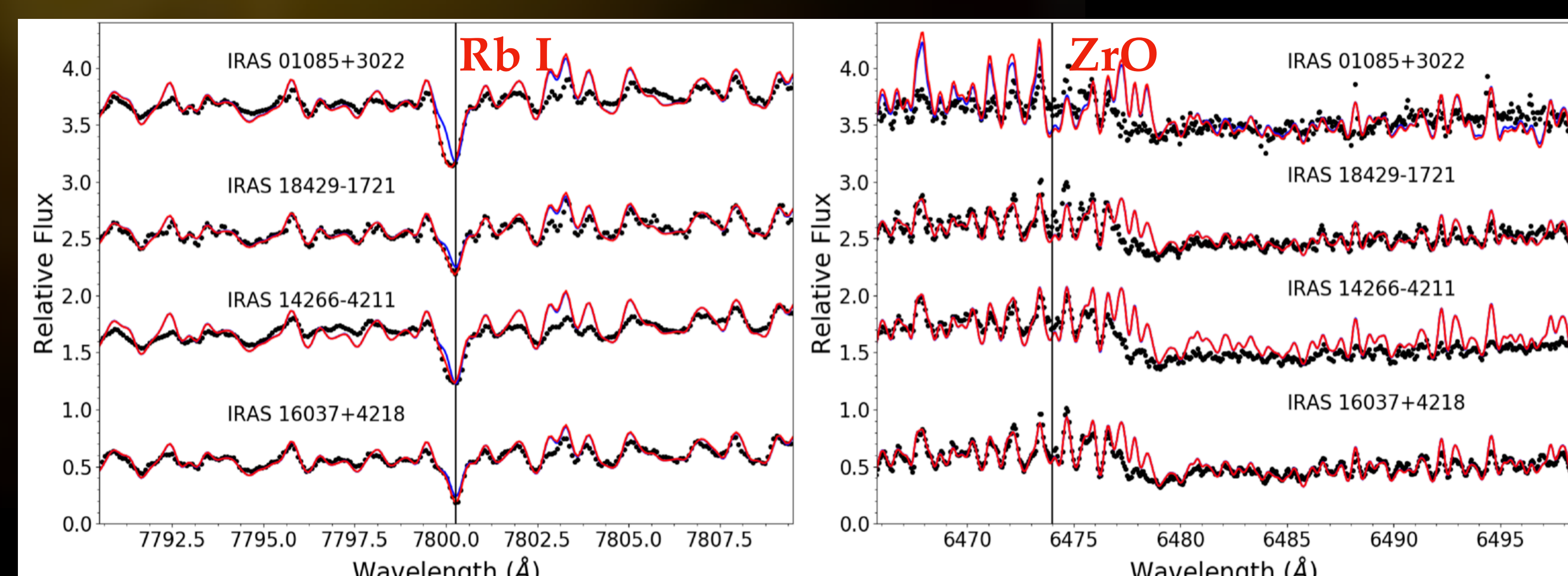

García-Hernández, D. A et al., 2011; 2017

POST-AGB EVOLUTION (SINGLE STARS)

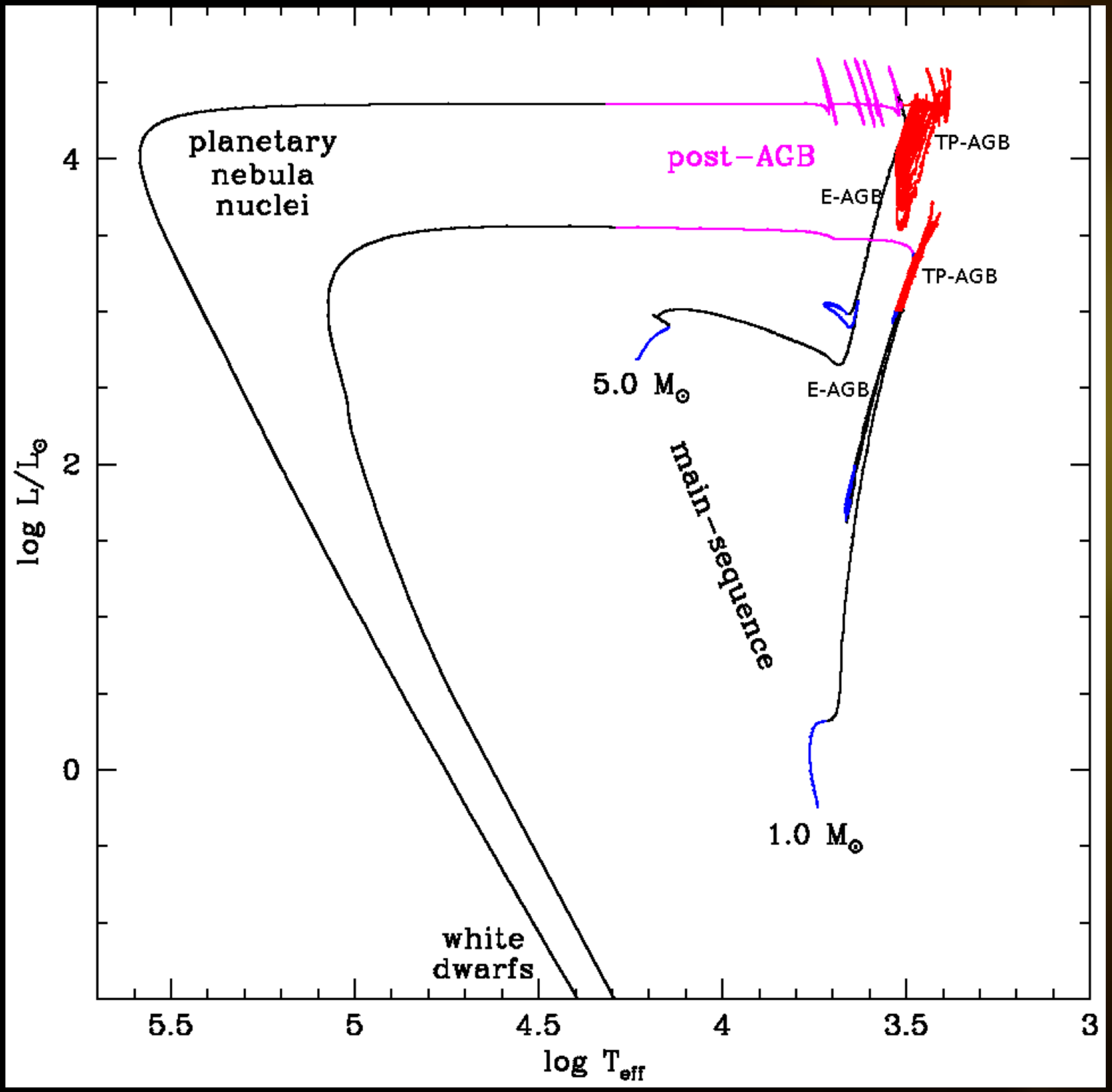

Post-AGB Evolution (Single Stars)

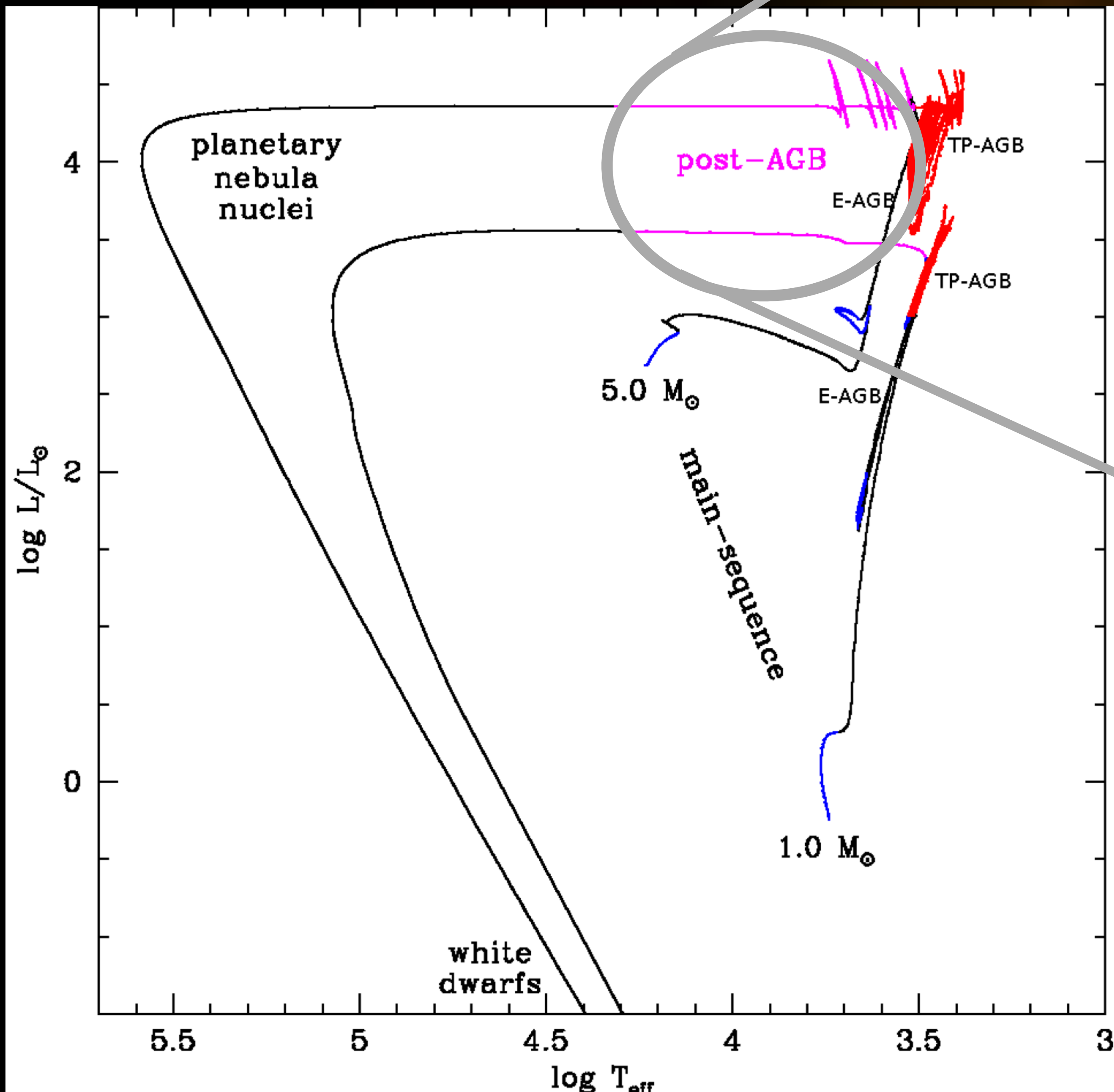

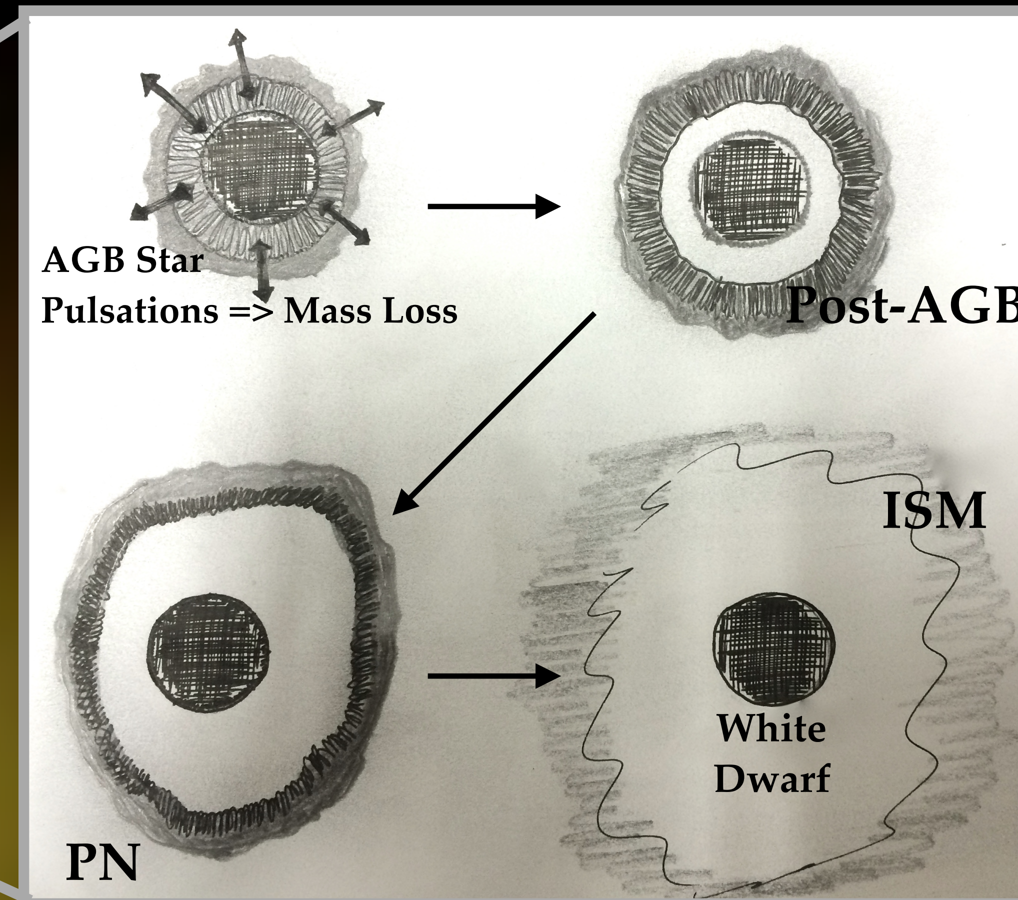

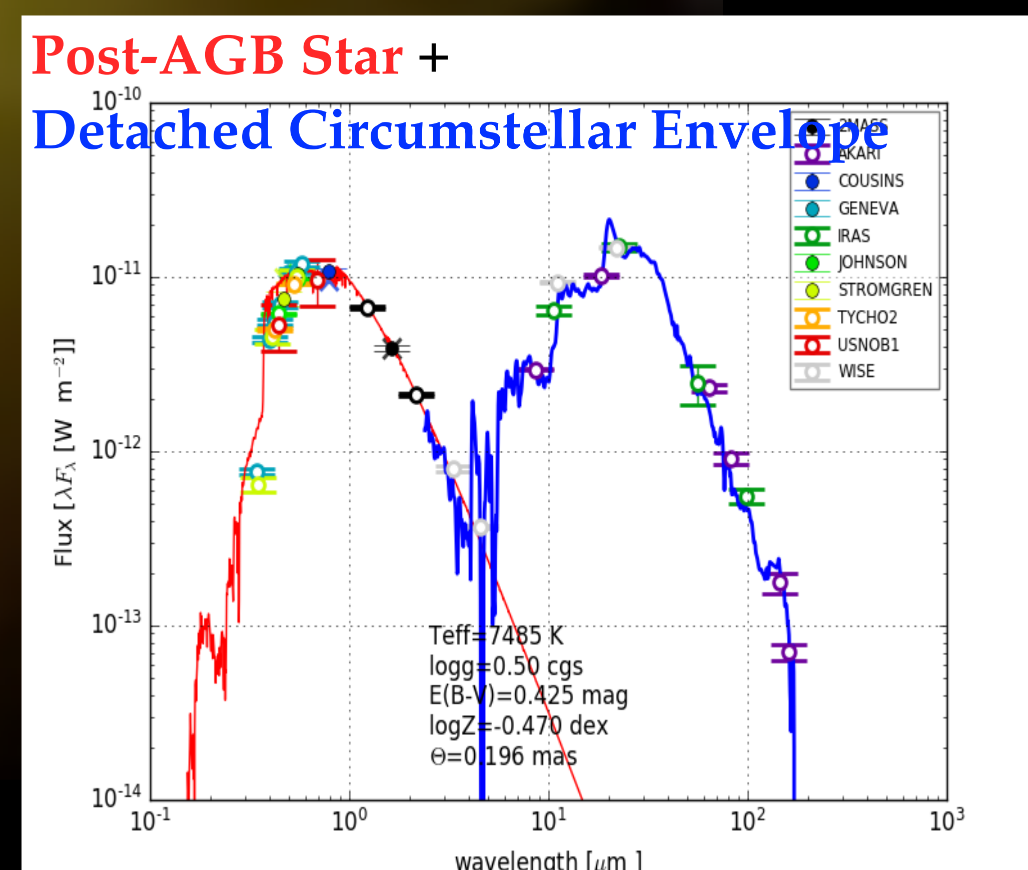

- A-K Spectral Types
- Low Log g (0 to ~1.5 dex)
- Low Metallicity

POST-AGB STARS AS EXQUISITE TRACERS FOR CNO, FE-PEAK, AND *S*-PROCESS ELEMENTS

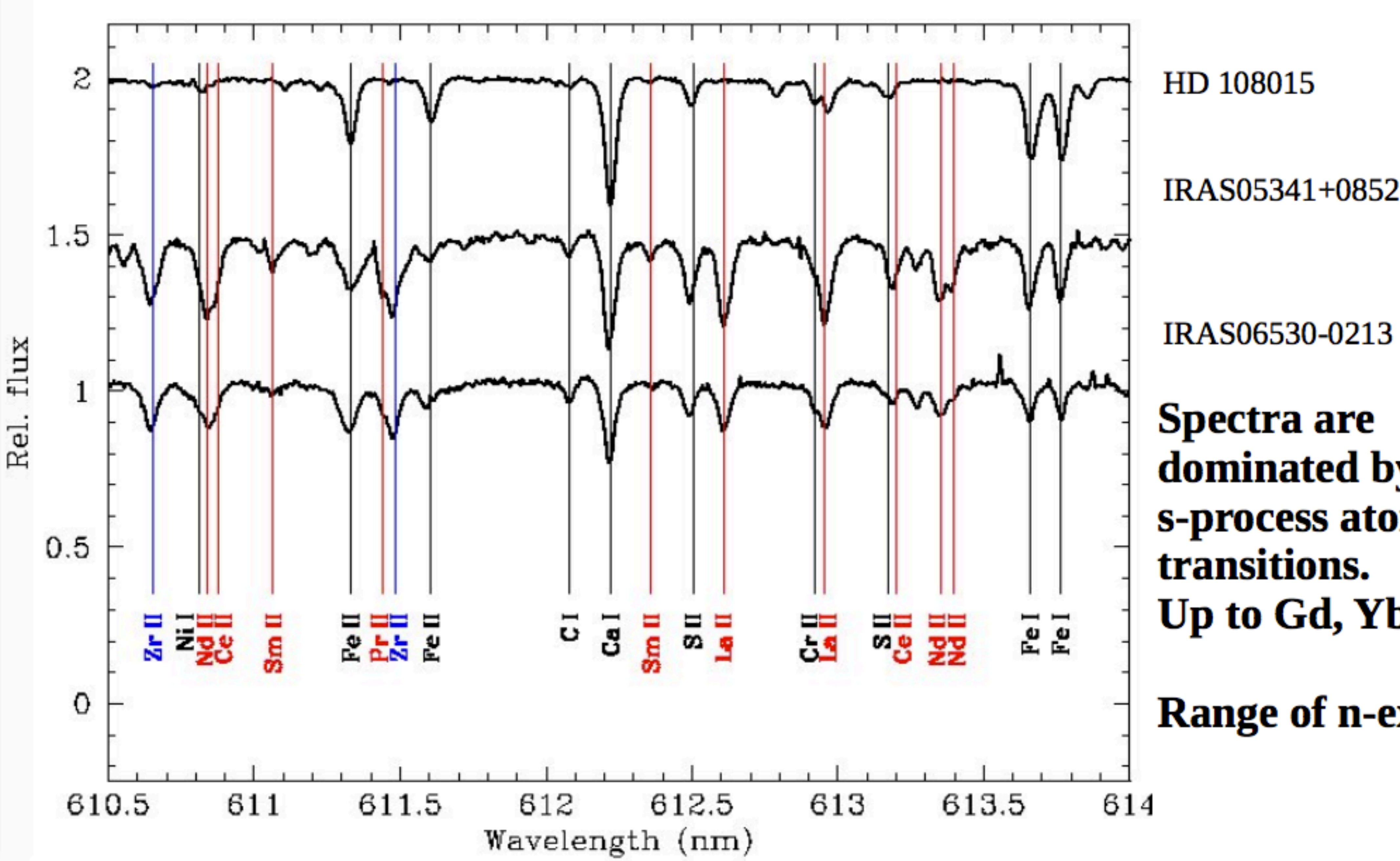

Spectra are dominated by s-process atomic transitions.
Up to Gd, Yb, Lu, W

Range of n-exposures

POST-AGB STARS AS EXQUISITE TRACERS FOR CNO, FE-PEAK, AND *S*-PROCESS ELEMENTS

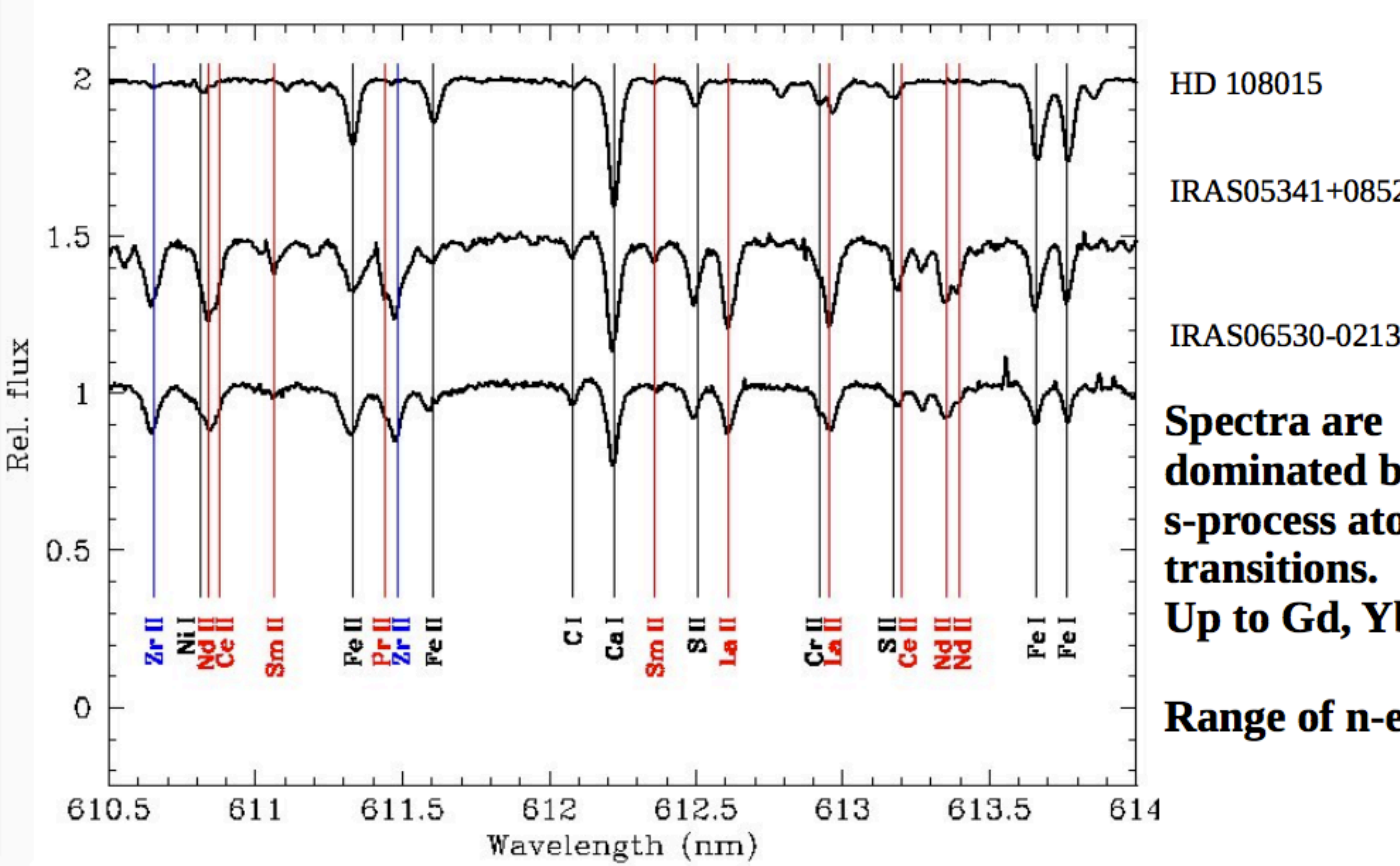

Spectra are dominated by s-process atomic transitions.
Up to Gd, Yb, Lu, W

Range of n-exposures

+ LUMINOSITY (PROGENITOR MASS)

The Hunt for Post-AGB stars:

MilkyWay
LMC
SMC

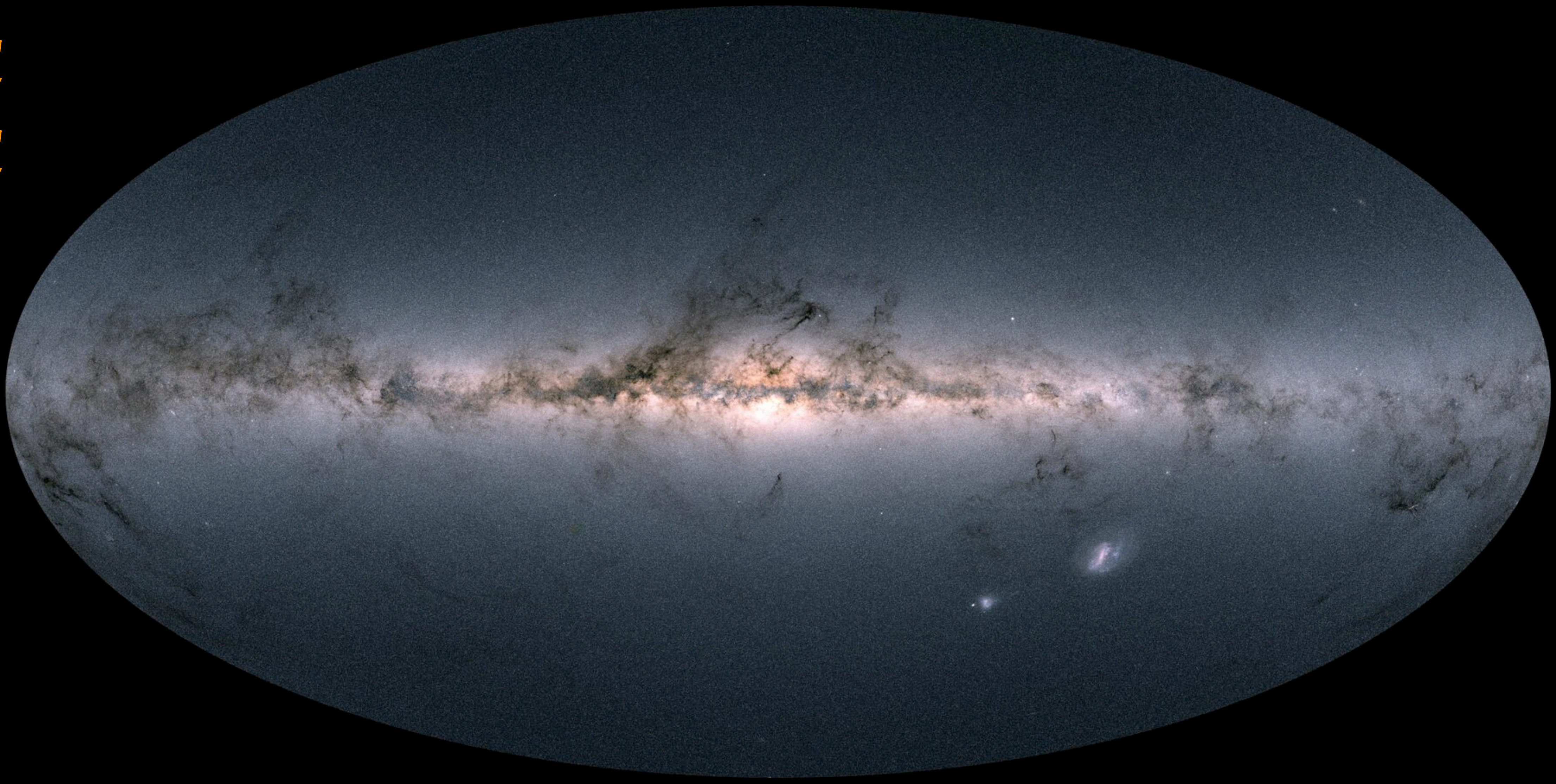

Galaxy: Van Winckel 2003; Szczerba et al., 2007; Oomen et al., 2018; Kamath et al., 2022; Kluska et al., 2022

LMC/SMC: Van Aarle et al., 2011; Kamath et al., 2014, 2015

POST-AGB STARS AS EXQUISITE TRACERS FOR CNO, FE-PEAK, AND *S*-PROCESS ELEMENTS

Carbon and *s*-process rich stars:

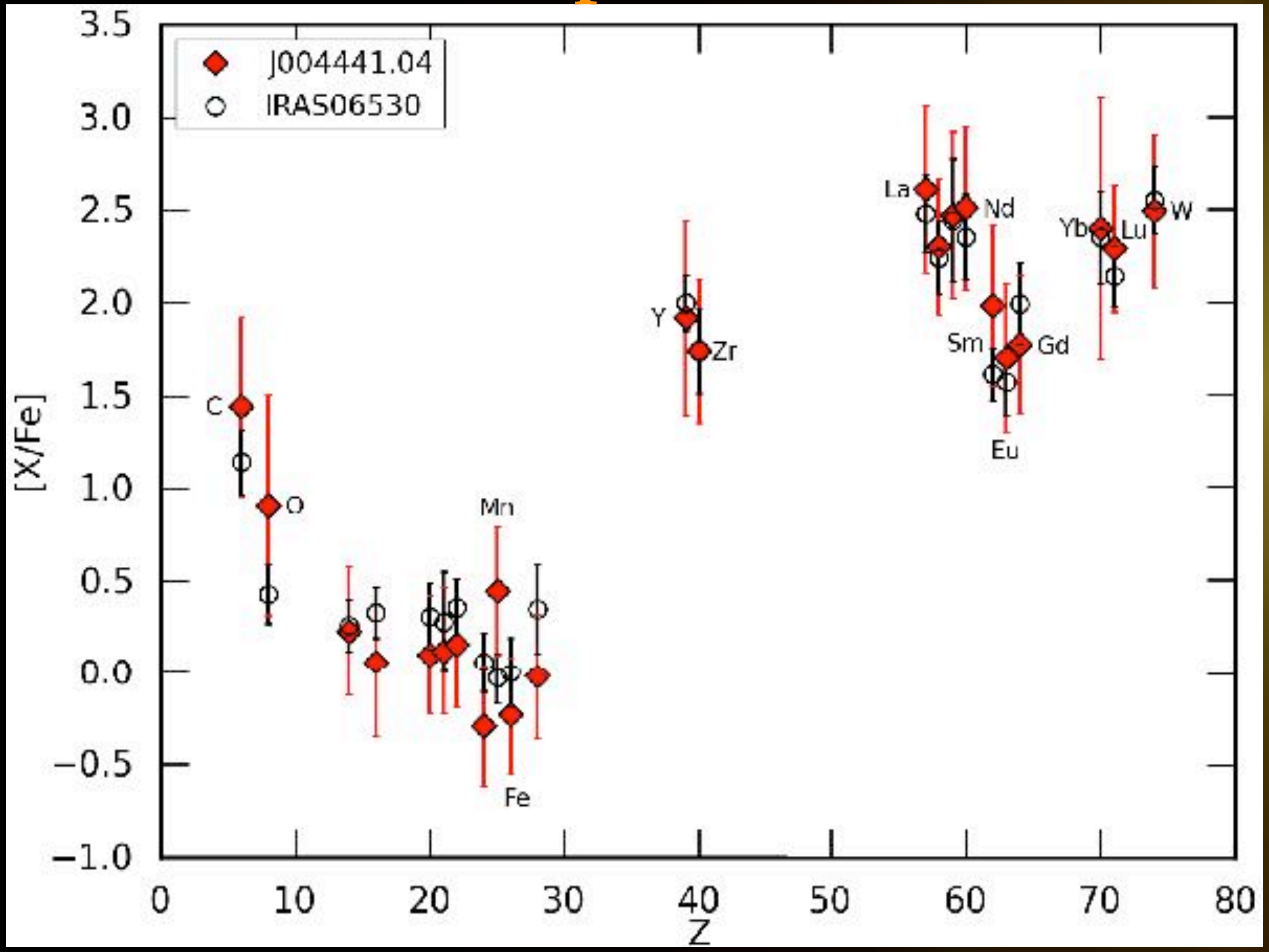

De Smedt et al., 2012, 2015

$M_{initial}$ ~ 1 to 1.5 Msun
[Fe/H] = -1.0 to -1.5
Z ~ 0.001
T_{eff} ~6000 K
Log g ~1 to 1.5 dex

POST-AGB STARS AS EXQUISITE TRACERS FOR CNO, FE-PEAK, AND *S*-PROCESS ELEMENTS

Carbon and *s*-process rich stars:

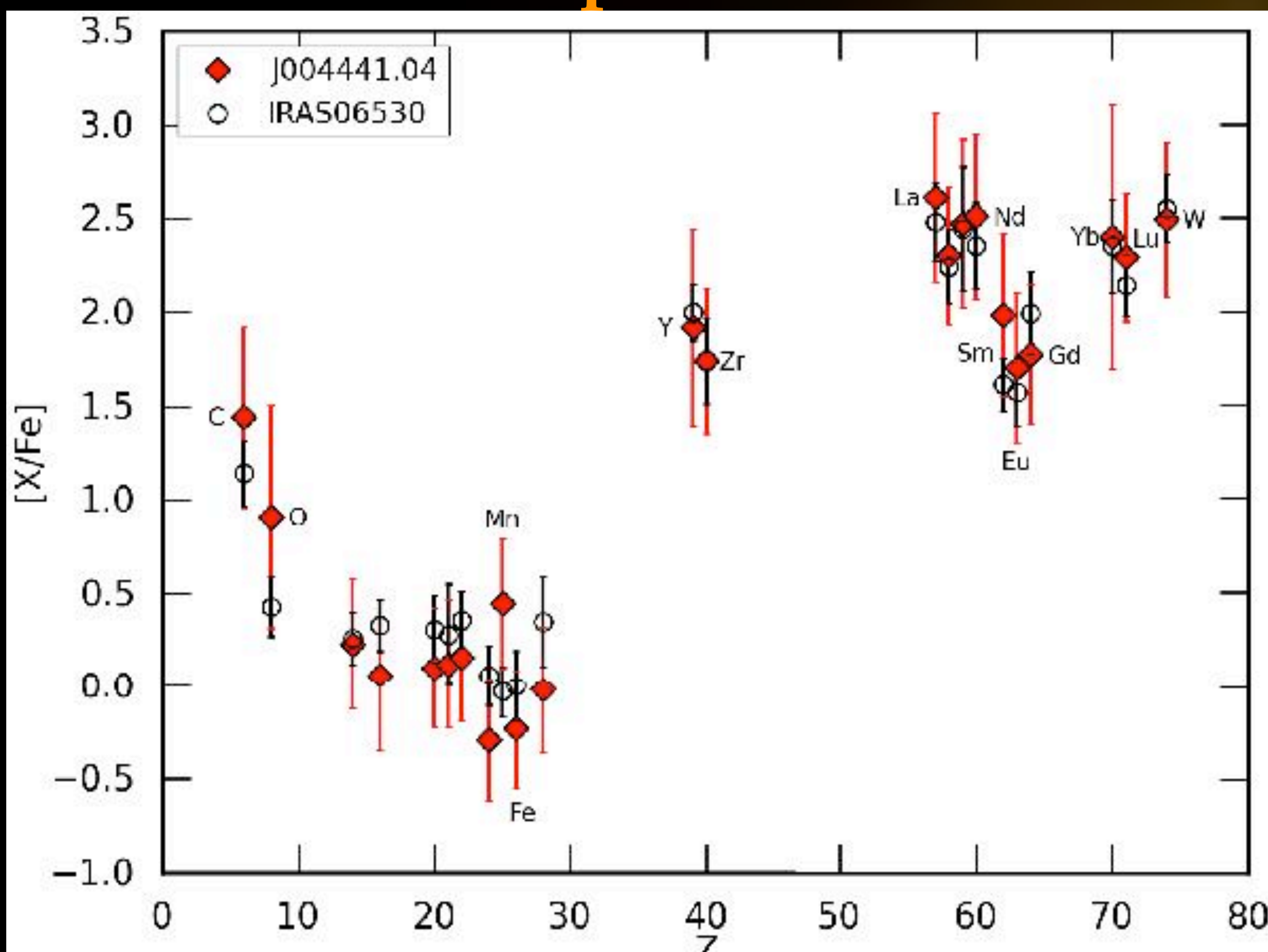

De Smedt et al., 2012, 2015

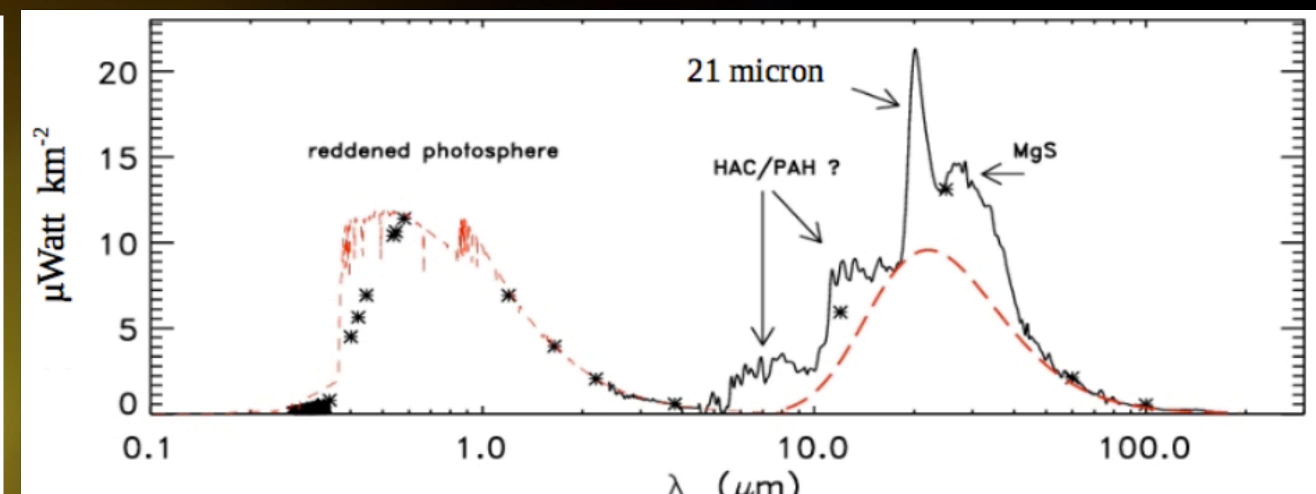

Van Winckel 2003

All C-rich and *s*-process rich post-AGB stars show the 21-micron feature

$M_{initial}$ ~ 1 to 1.5 Msun
[Fe/H] = -1.0 to -1.5
Z ~ 0.001
T_{eff} ~6000 K
Log g ~1 to 1.5 dex

- The revelation of chemical diversities in AGB nucleosynthesis

Complexities in Single Star AGB Nucleosynthesis

Failed third dredge-up

- ⋆ Lack of carbon production during the AGB phase for stars that are predicted to have efficient TDU

  Kamath et al., 2017

Diverse AGB nucleosynthesis

- ⋆ **Non-uniform *s*-process production**

  Van Winckel 2003; Kamath et al.,2022a; Kamath et al., 2022b to-be-submitted

Chemical Diversity within the Galactic Single Star Sample

s-process rich versus non-enriched:

s-process rich
non s-process enriched

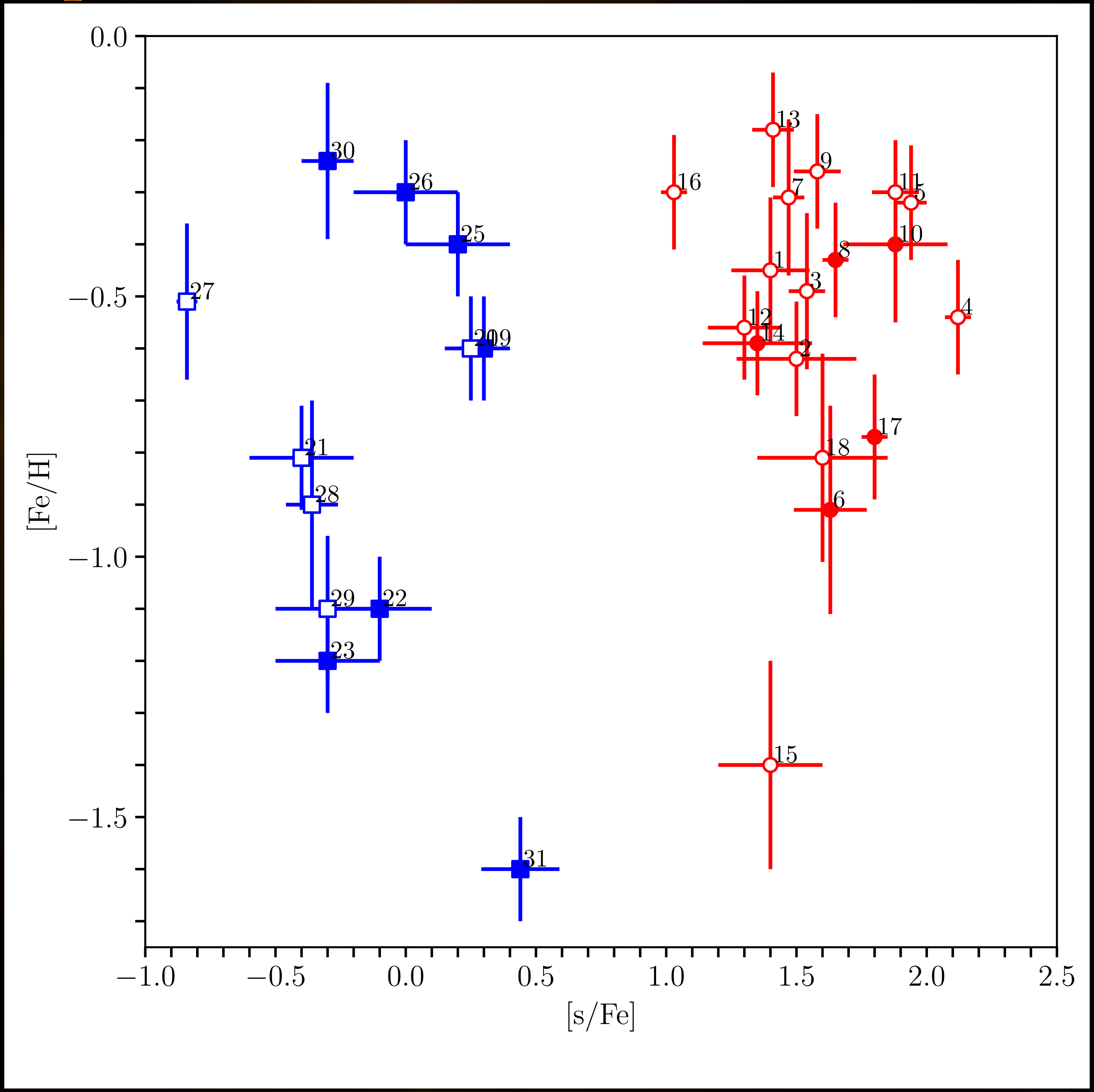

Chemical Diversity within the Galactic Single Star Sample

s-process rich versus non-enriched:

s-process rich
non s-process enriched

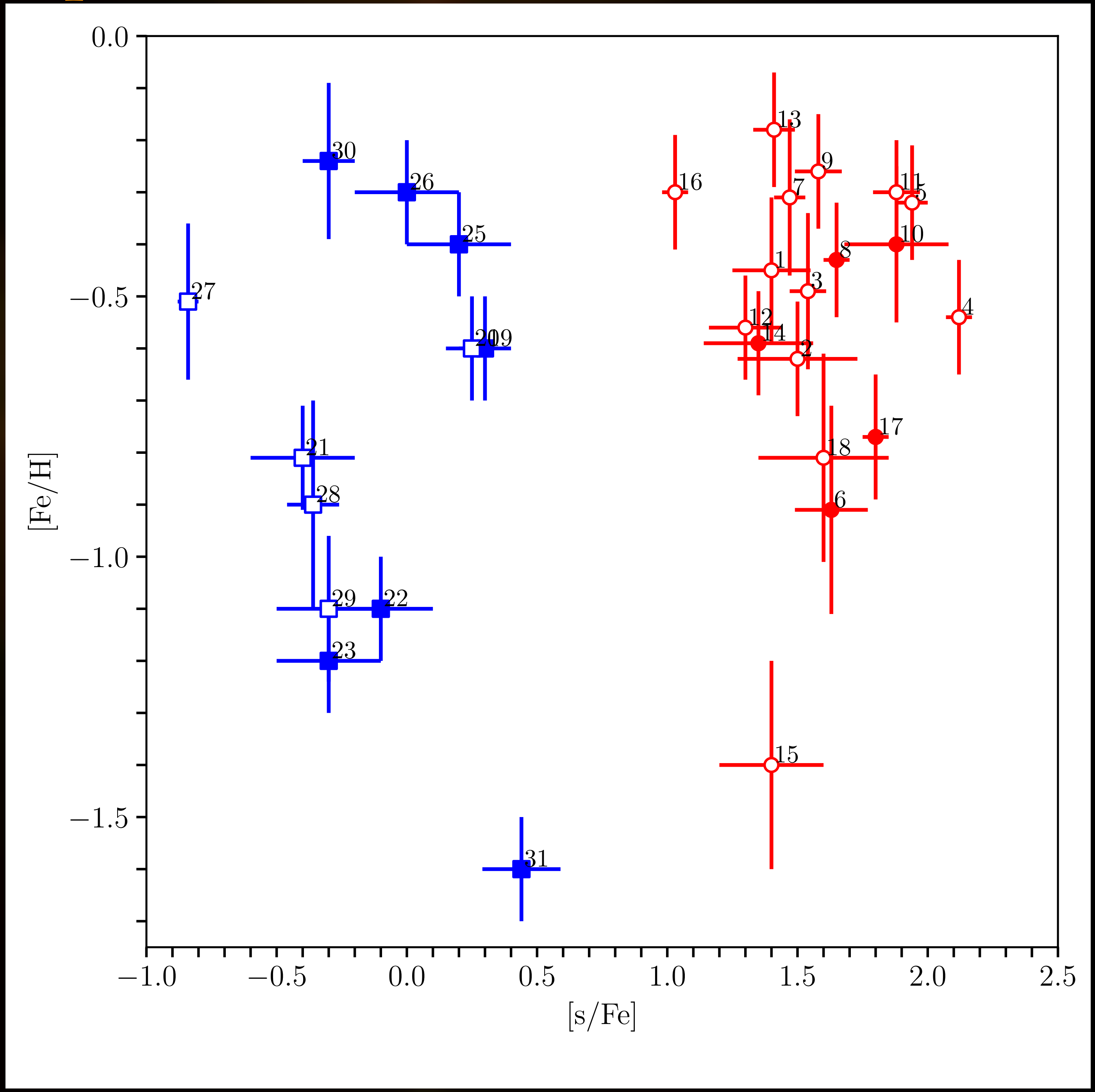

AGB Nucleosynthesis is NOT homogenous!

Red: s-process enriched
Blue: non s-process rich

- ⋆ A chemical dichotomy in the C and *s*-process abundances: enriched and non-enriched (in disagreement with models!)
- ⋆ No obvious trends in O and N

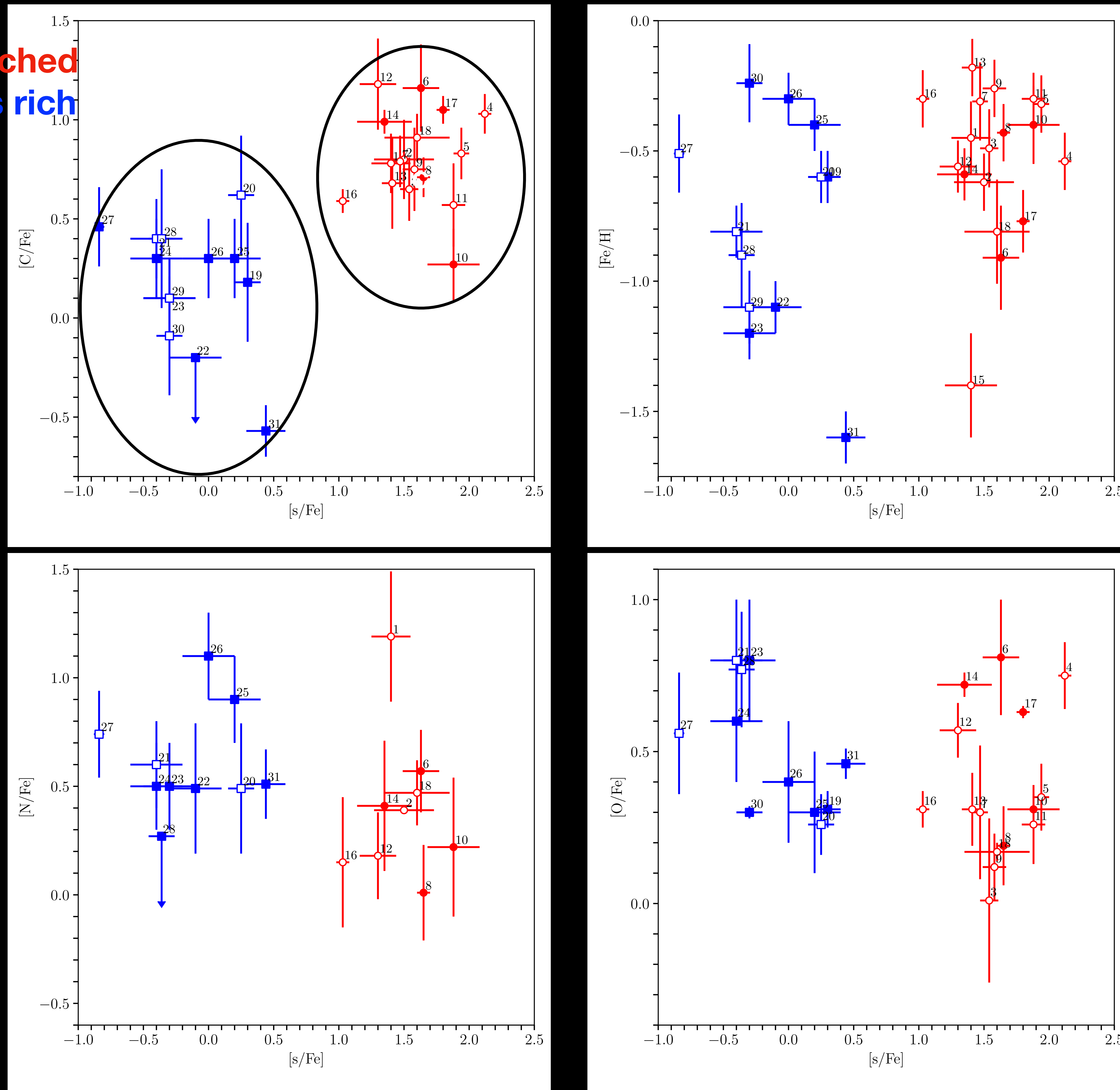

LUMINOSITIES FOR SINGLE GALACTIC POST-AGBS FROM GAIA DR3

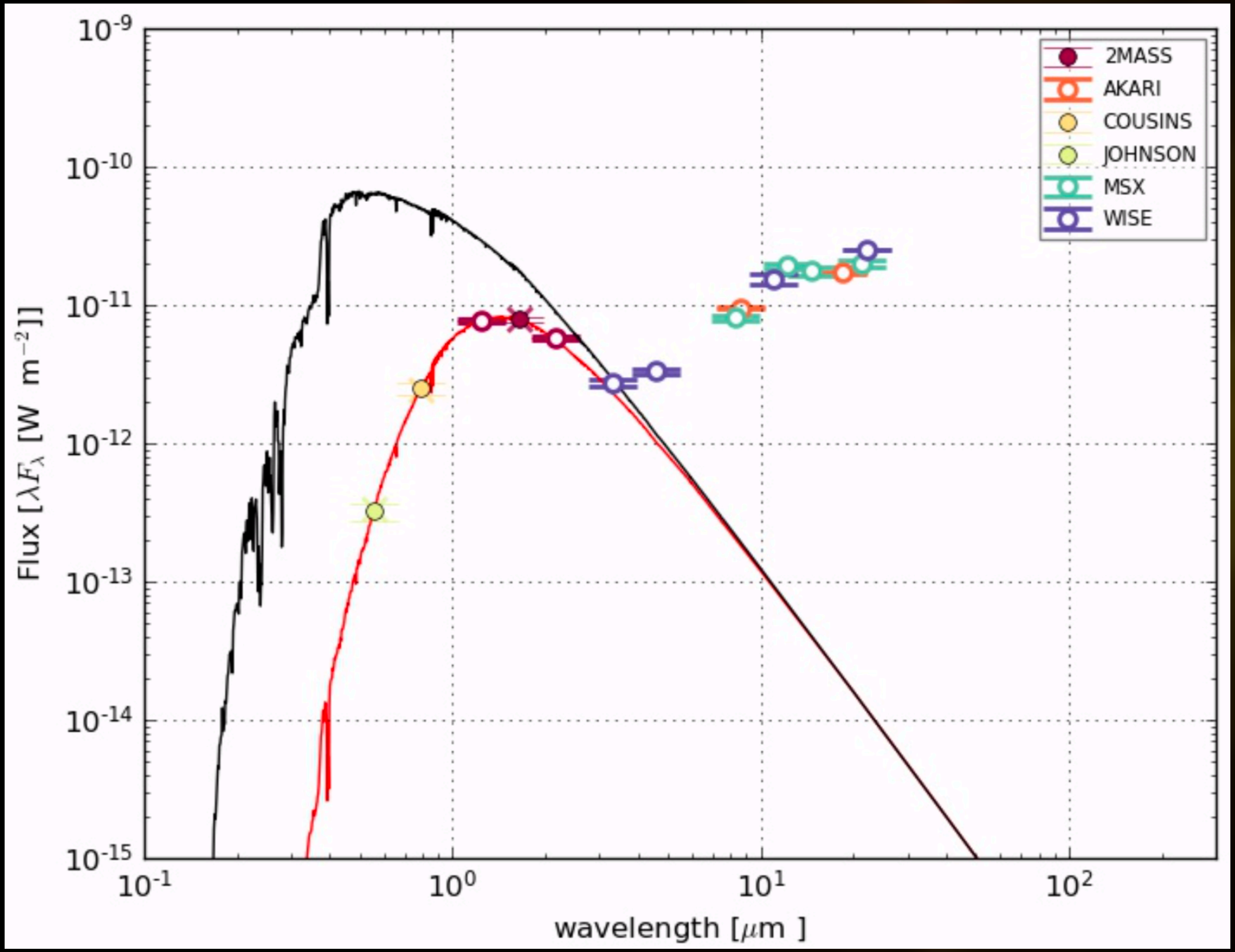

- ⋆ Parallaxes from Gaia EDR3
- ⋆ Geometric distances from Bailer Jones et al., 2021
- ⋆ SED Fitting:
  - ⋆ E(B-V)

    ↓
  - ⋆ Luminosity

Position of the Galactic Post-AGBs in the HR-Diagram

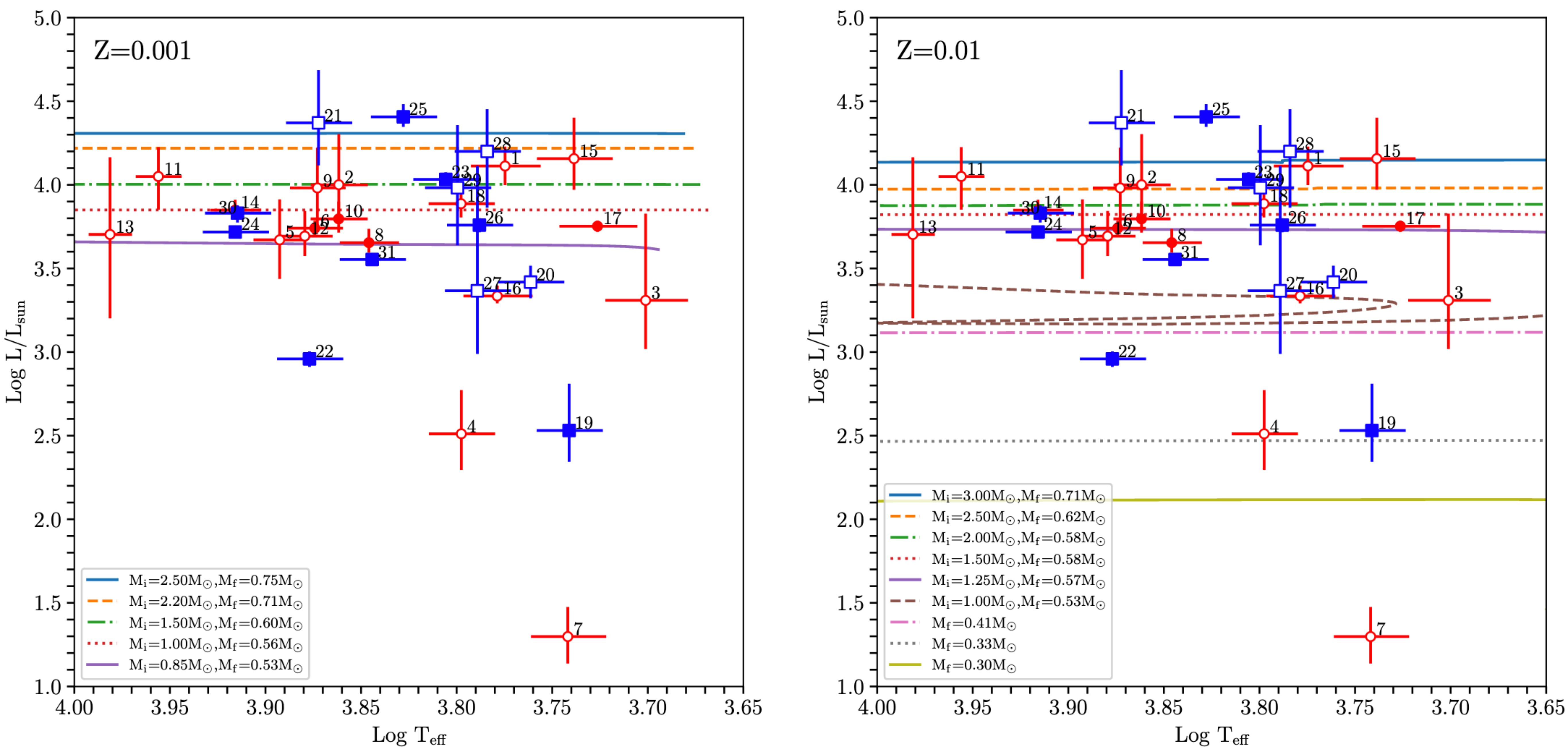

Filled: Quality 1 - Filled, Open: Quality 2 (based on GAIA astrometric data)

Red circles: s-process enriched Blue squares: non s-process rich

Kamath et al., 2022

Position of the Galactic Post-AGBs in the HR-Diagram

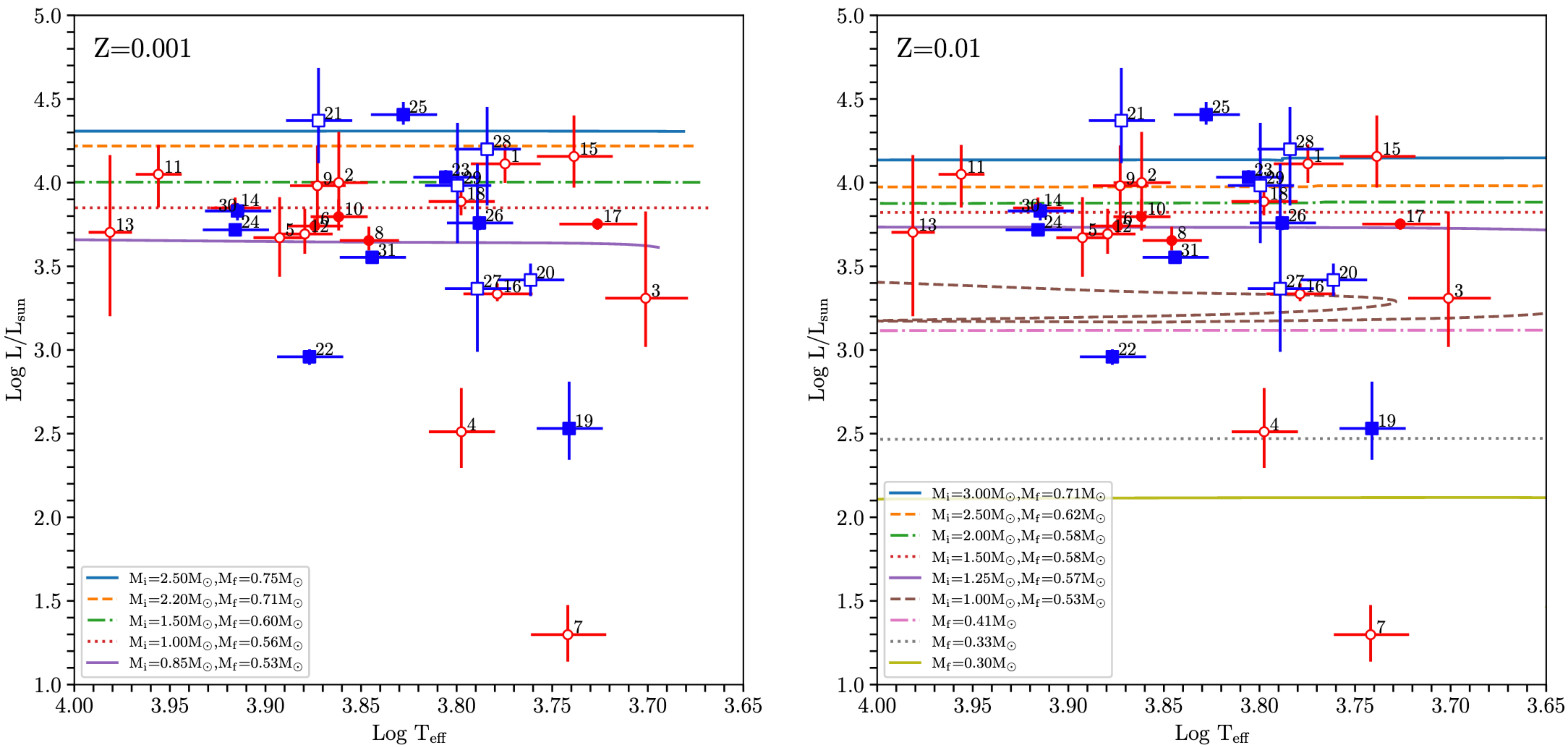

Filled: Quality 1 - Filled, Open: Quality 2 (based on GAIA astrometric data)

Red circles: s-process enriched Blue squares: non s-process rich

Chemical diversity NOT entirely a mass or initial metallicity effect!

Kamath et al., 2022

- Our attempts to understand the observed chemical diversities and AGB nucleosynthesis

NEW POST-AGB STAR MODELS AS TOOLS TO UNDERSTAND THE OBSERVED COMPLEXITIES

Kamath et al., 2022b to-be-submitted

$M/M_\odot$	$L/L_\odot$	$M_{core}/M_\odot$	[C/Fe]	[N/Fe]	[O/Fe]
		$Z=8\times10^{-3}$			
0.75	4000	0.55	0.0	0.30	0.20
0.80	4200	0.557	0.0	0.30	0.20
0.85	5100	0.564	0.0	0.30	0.20
0.90	5550	0.574	0.0	0.30	0.20
0.95	5500	0.571	0.58	0.30	0.20
1.00	6200	0.584	0.44	0.32	0.22
1.25	6500	0.59	0.60	0.30	0.23
1.50	7450	0.602	0.59	0.36	0.24
1.75	8300	0.632	0.69	0.39	0.20
2.0	8200	0.617	0.80	0.44	0.20
2.5	8600	0.606	1.12	0.55	0.26
3.0	9300	0.66	1.14	0.57	0.50
3.5	21500	0.79	0.35	1.55	0.36
4.0	23000	0.87	0.22		

- ATON stellar evolutionary code (Ventura et al., 2018)
- Metallicities 10^-3 < Z < 0.014
- AGB computations extended until the very end of the post-AGB phase
- For M ≤ 2 Msun, M/Msun is the mass of the stars at the start of the AGB phase

A reminder of the Sample: Single Galactic Post-AGBs

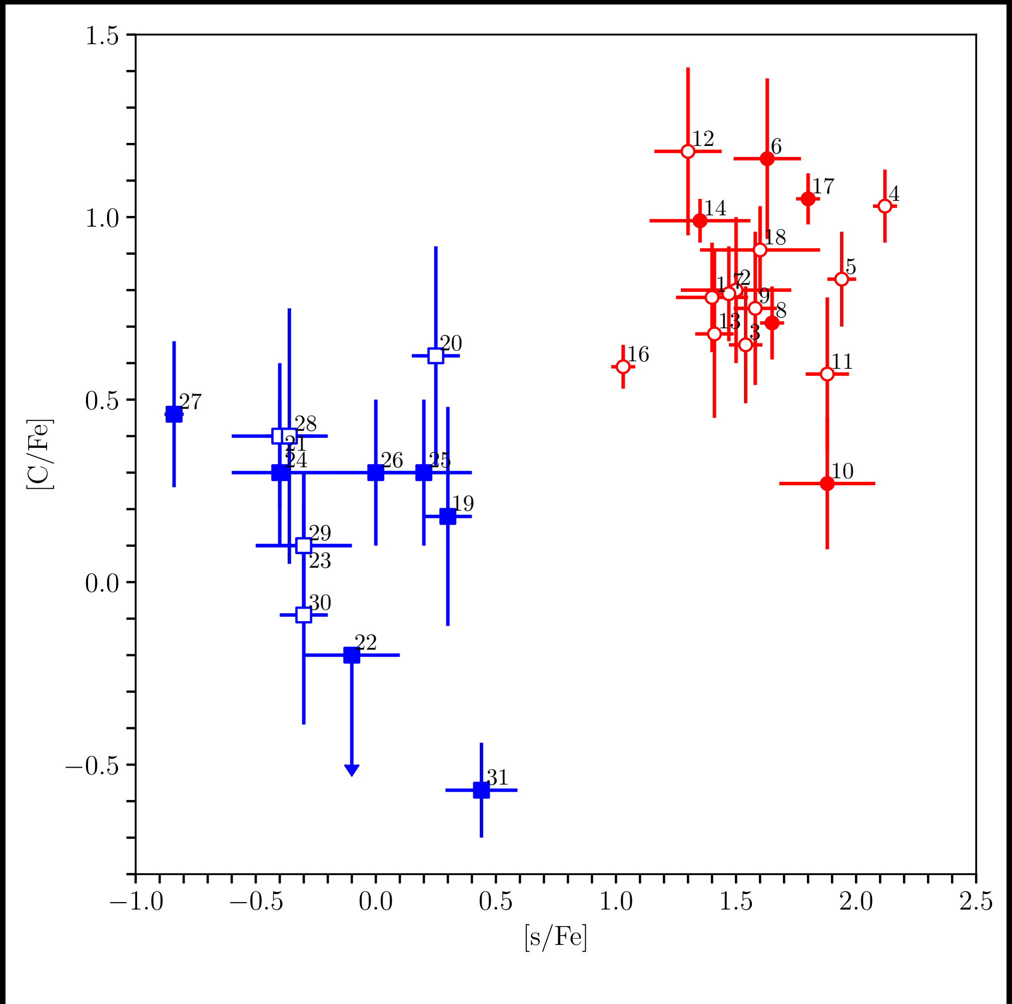

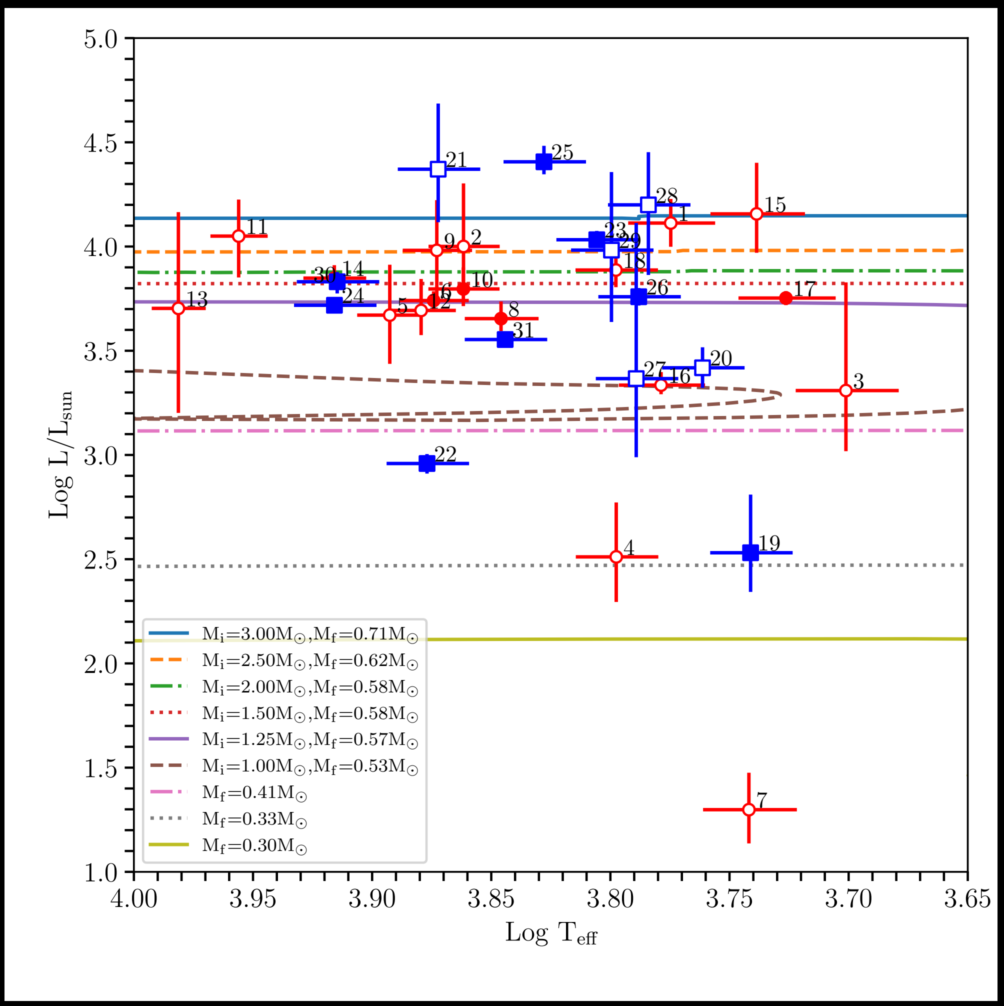

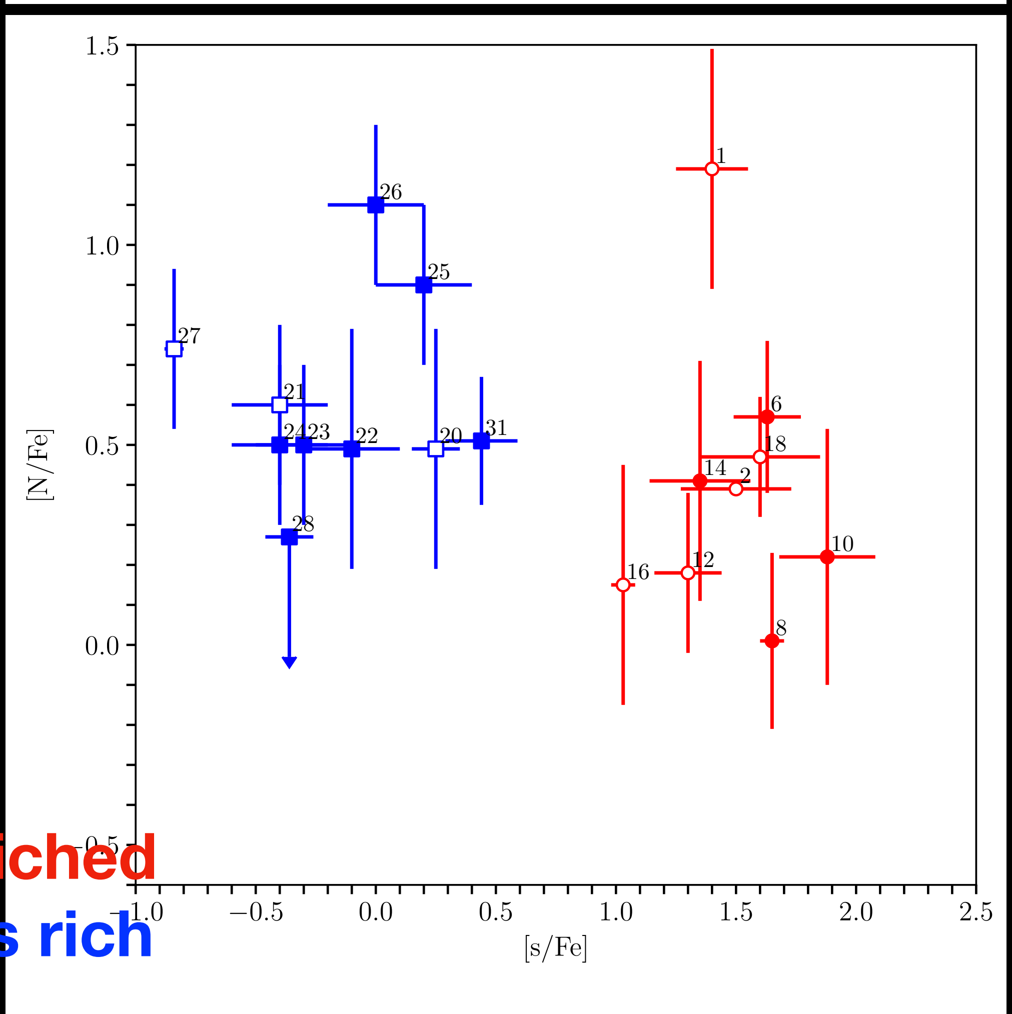

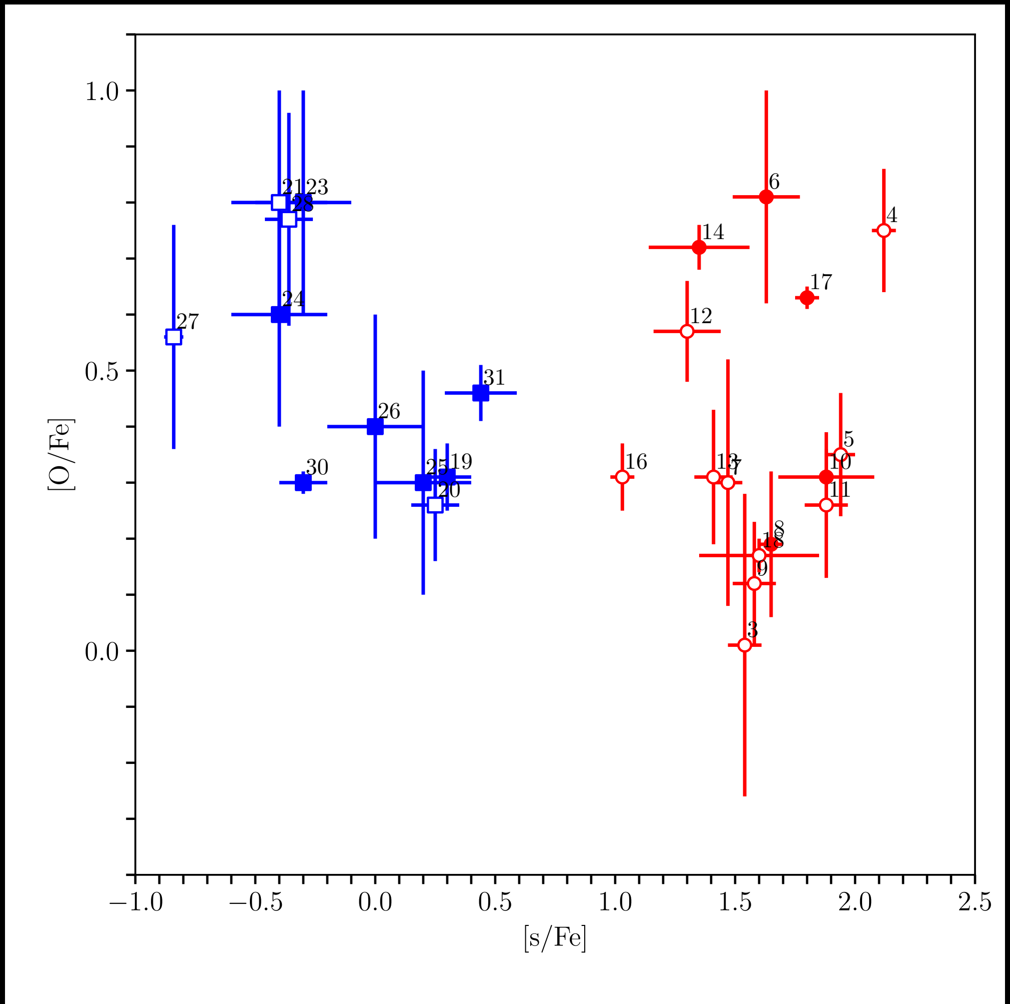

Red: s-process enriched

Blue: non s-process rich

Chemistry of Stars Evolving from AGB to Post-AGB

STANDARD AGB EVOLUTION AND NUCLEOSYNTHESIS SCENARIOS

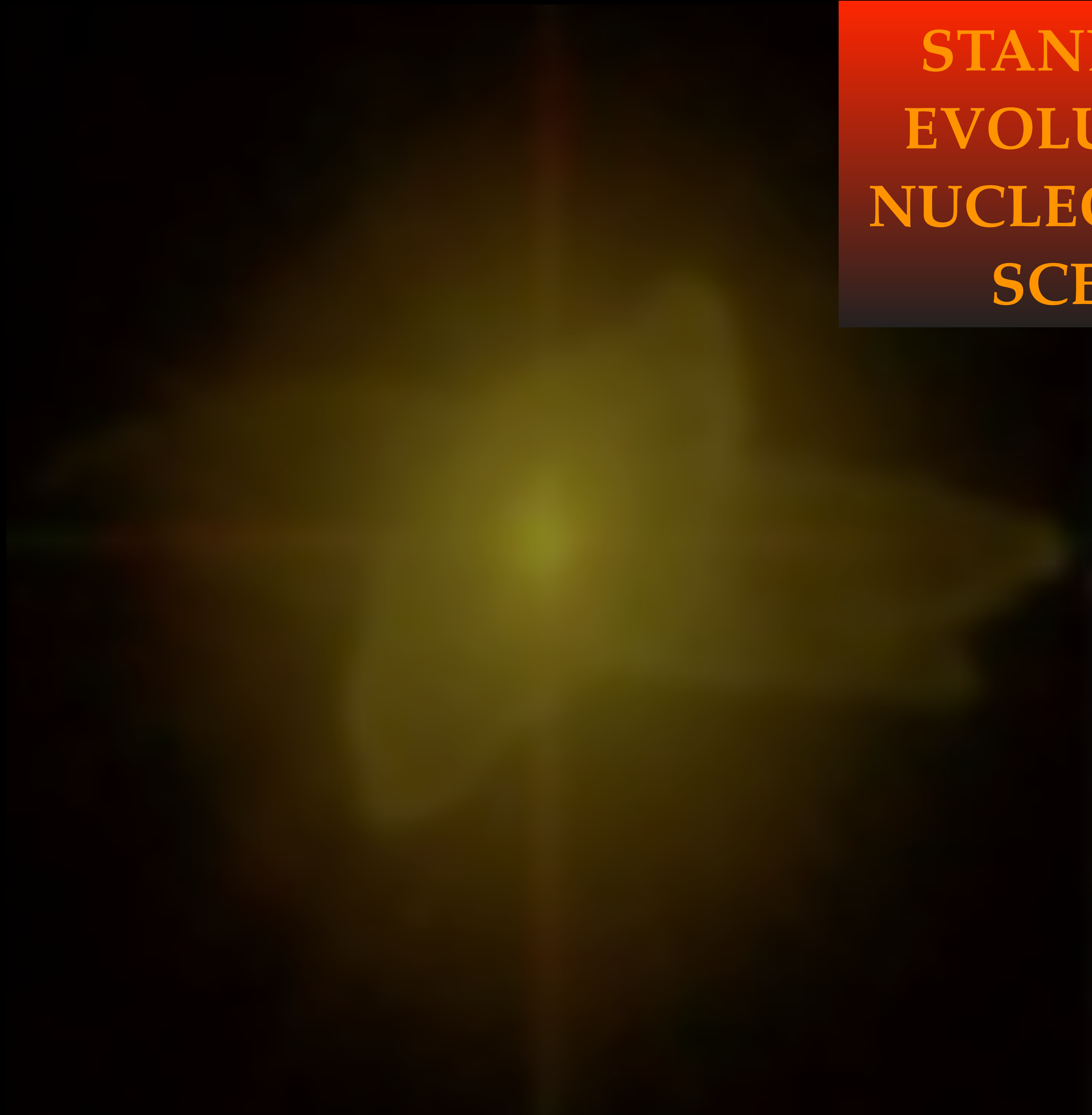

Chemistry of Stars Evolving from AGB to Post-AGB

- **Case 1: Progenitor mass below ~1 Msun (FDU)**
  - Few thermal pulses before envelope is lost
  - Evolve as M-stars
  - Little to no C and *s*-process
  - Some N (~0.5 dex) from FDU

STANDARD AGB EVOLUTION AND NUCLEOSYNTHESIS SCENARIOS

Chemistry of Stars Evolving from AGB to Post-AGB

- **Case 1: Progenitor mass below ~1 Msun (FDU)**
  - Few thermal pulses before envelope is lost
  - Evolve as M-stars
  - Little to no C and *s*-process
  - Some N (~0.5 dex) from FDU

STANDARD AGB EVOLUTION AND NUCLEOSYNTHESIS SCENARIOS

- **Case 2: Progenitor mass of ~1 - 3 Msun (TDU)**
  - Series of thermal pulses
  - Evolve as C-stars
  - Significant C and *s*-process
  - Some N (from FDU), mild O-enrichment

Chemistry of Stars Evolving from AGB to Post-AGB

Standard AGB Evolution and Nucleosynthesis Scenarios

- **Case 1: Progenitor mass below ~1 Msun (FDU)**
  - Few thermal pulses before envelope is lost
  - Evolve as M-stars
  - Little to no C and *s*-process
  - Some N (~0.5 dex) from FDU

- **Case 2: Progenitor mass of ~1 - 3 Msun (TDU)**
  - Series of thermal pulses
  - Evolve as C-stars
  - Significant C and *s*-process
  - Some N (from FDU), mild O-enrichment

Chemistry of Stars Evolving from AGB to Post-AGB

Standard AGB Evolution and Nucleosynthesis Scenarios

- **Case 1: Progenitor mass below ~1 Msun (FDU)**
  - Few thermal pulses before envelope is lost
  - Evolve as M-stars
  - Little to no C and *s*-process
  - Some N (~0.5 dex) from FDU

- **Case 2: Progenitor mass of ~1 - 3 Msun (TDU)**
  - Series of thermal pulses
  - Evolve as C-stars
  - Significant C and *s*-process
  - Some N (from FDU), mild O-enrichment

- **Case 3: Progenitor mass of ~3 - 4 Msun (TDU + HBB)**
  - Experience both TDU and HBB
  - Enhanced in C and *s*-process.
  - N is ~a factor of 10 higher than initial

Chemistry of Stars Evolving from AGB to Post-AGB

STANDARD AGB EVOLUTION AND NUCLEOSYNTHESIS SCENARIOS

- **Case 1: Progenitor mass below ~1 Msun (FDU)**
  - Few thermal pulses before envelope is lost
  - Evolve as M-stars
  - Little to no C and *s*-process
  - Some N (~0.5 dex) from FDU
- **Case 2: Progenitor mass of ~1 - 3 Msun (TDU)**
  - Series of thermal pulses
  - Evolve as C-stars
  - Significant C and *s*-process
  - Some N (from FDU), mild O-enrichment
- **Case 3: Progenitor mass of ~3 - 4 Msun (TDU + HBB)**
  - Experience both TDU and HBB
  - Enhanced in C and *s*-process.
  - N is ~a factor of 10 higher than initial

Chemistry of Stars Evolving from AGB to Post-AGB

Standard AGB Evolution and Nucleosynthesis Scenarios

- **Case 1: Progenitor mass below ~1 Msun (FDU)**
  - Few thermal pulses before envelope is lost
  - Evolve as M-stars
  - Little to no C and *s*-process
  - Some N (~0.5 dex) from FDU
- **Case 2: Progenitor mass of ~1 - 3 Msun (TDU)**
  - Series of thermal pulses
  - Evolve as C-stars
  - Significant C and *s*-process
  - Some N (from FDU), mild O-enrichment
- **Case 3: Progenitor mass of ~3 - 4 Msun (TDU + HBB)**
  - Experience both TDU and HBB
  - Enhanced in C and *s*-process.
  - N is ~a factor of 10 higher than initial
- **Case 4: Progenitor mass of > 4 Msun (HBB)**
  - Dominated by HBB
  - N enhancement, neither C nor *s*-process

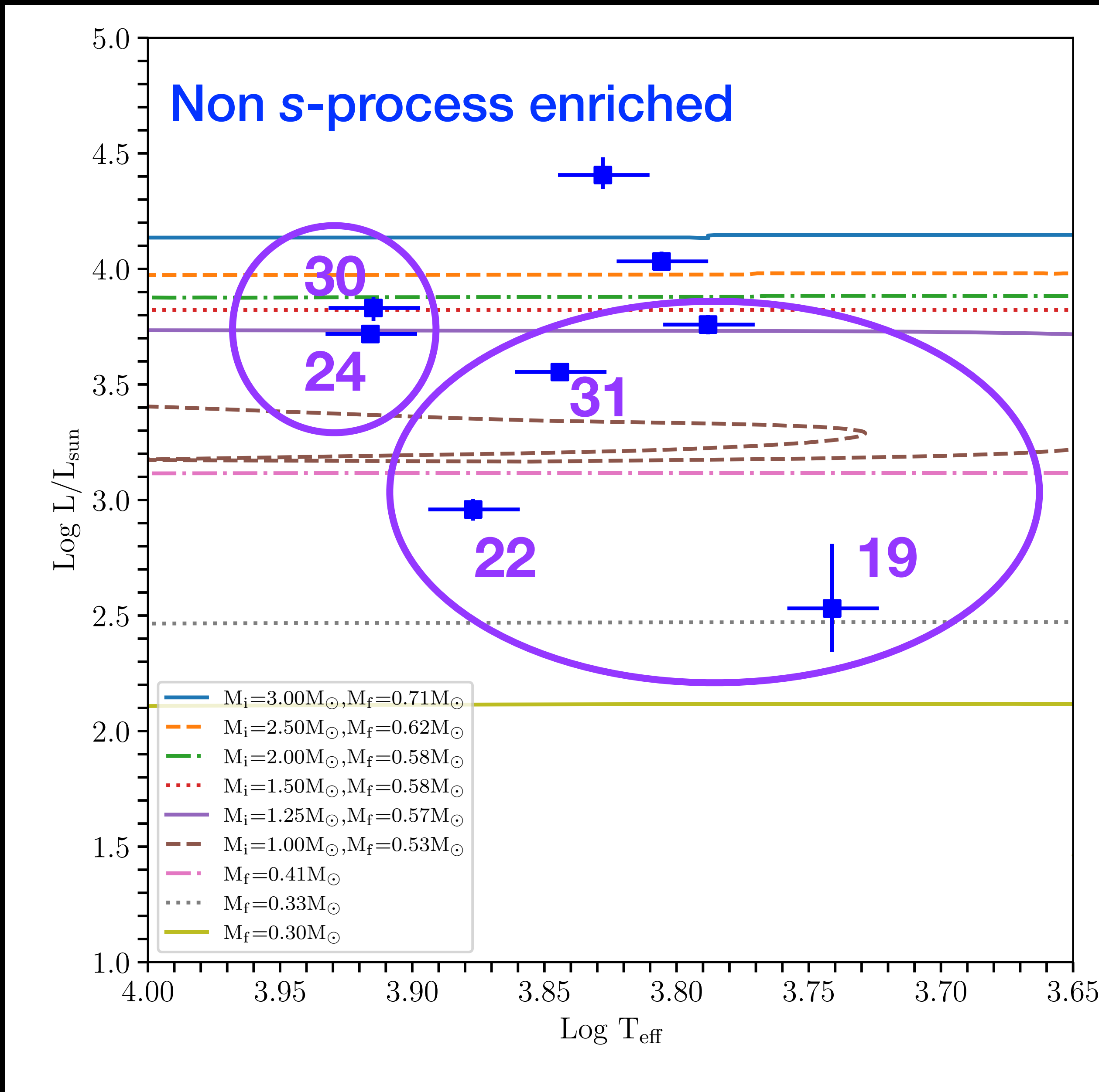

- **Case 1: First Dredge-Up (FDU)**
- **Progenitor mass below ~1 Msun**
  - Few thermal pulses before envelope is lost
  - Evolve as M-stars
  - Little to no C and *s*-process
  - Some N (~0.5 dex) from FDU

Index	Object	T_{eff}	$L/L_{\odot}$	[C/Fe]	[N/Fe]	[O/Fe]	Flag	M_{init}	chemistry
19	IRAS 01259+6823	5510 ± 250	340	0.18 ± 0.15	...	0.31 ± 0.06	Q1	$0.5 - 0.6\ M_{\odot}$	FDU
22	HD 107369	7533 ± 250	910	< -0.2	0.49 ± 0.3	0 ± 0.2	Q1	$0.5 - 0.6\ M_{\odot}$	FDU
24	HD 133656	8238 ± 250	5227	0.3 ± 0.2	0.5 ± 0.2	0.6 ± 0.2	Q1	$0.8 - 1\ M_{\odot}$	FDU
30	IRAS 19475+3119	8216 ± 250	6775	-0.09 ± 0.30	...	0.30 ± 0.02	Q1	$0.8 - 1\ M_{\odot}$	FDU
31	HR 7671	6985 ± 250	3579	-0.57 ± 0.13	0.51 ± 0.16	0.46 ± 0.05	Q1	$0.5 - 0.6\ M_{\odot}$	FDU

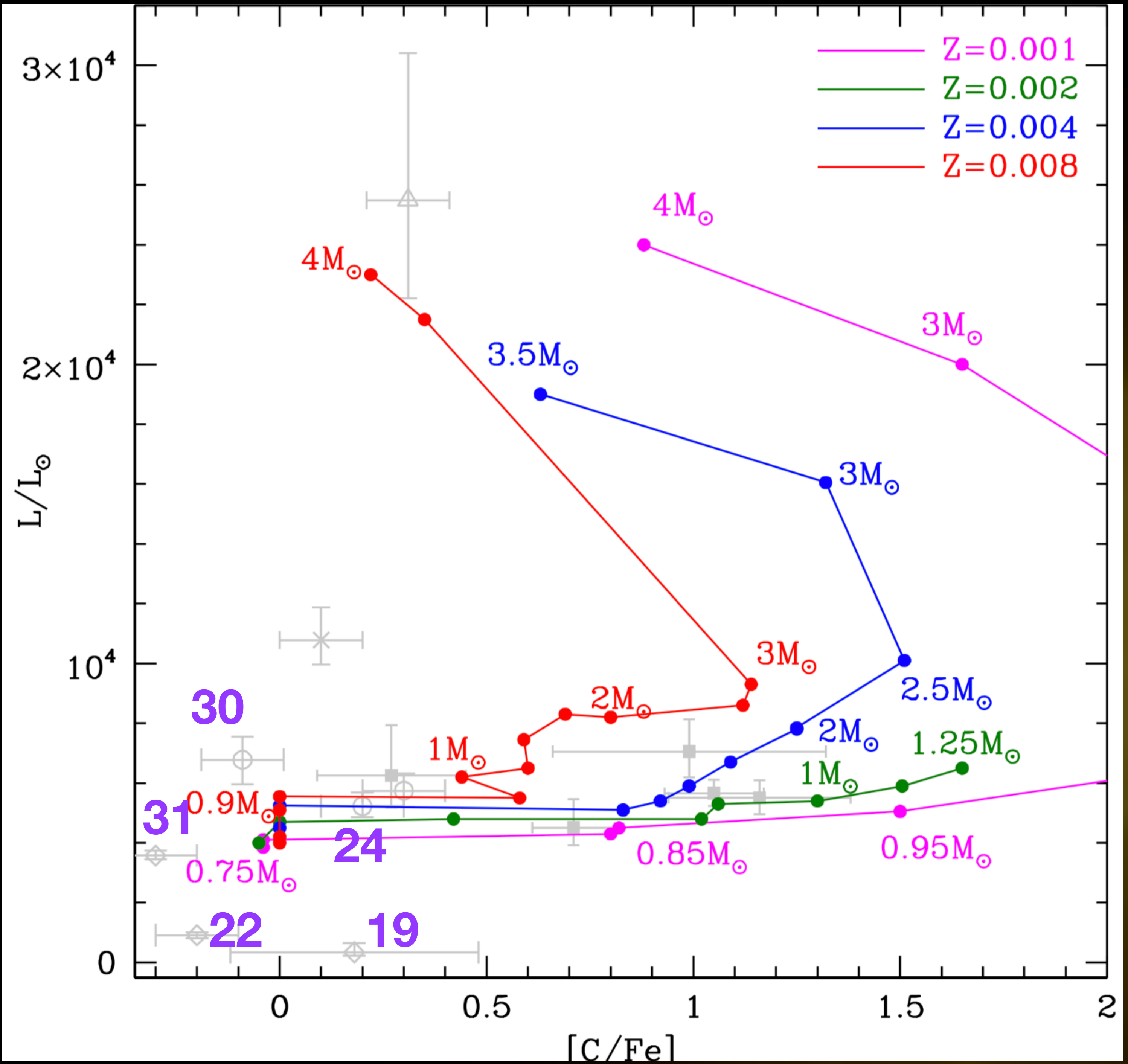

Case 1: First Dredge-Up (FDU)

Progenitor mass below ~1 Msun

- Few thermal pulses before envelope is lost
- Evolve as M-stars
- Little to no C and *s*-process
- Some N (~0.5 dex) from FDU

Index	Object	T_{eff}	$L/L_\odot$	[C/Fe]	[N/Fe]	[O/Fe]	Flag	M_{init}	chemistry
19	IRAS 01259+6823	5510 ± 250	340	0.18 ± 0.15	...	0.31 ± 0.06	Q1	$0.5 - 0.6\ M_\odot$	FDU
22	HD 107369	7533 ± 250	910	< -0.2	0.49 ± 0.3	0 ± 0.2	Q1	$0.5 - 0.6\ M_\odot$	FDU
24	HD 133656	8238 ± 250	5227	0.3 ± 0.2	0.5 ± 0.2	0.6 ± 0.2	Q1	$0.8 - 1\ M_\odot$	FDU
30	IRAS 19475+3119	8216 ± 250	6775	-0.09 ± 0.30	...	0.30 ± 0.02	Q1	$0.8 - 1\ M_\odot$	FDU
31	HR 7671	6985 ± 250	3579	-0.57 ± 0.13	0.51 ± 0.16	0.46 ± 0.05	Q1	$0.5 - 0.6\ M_\odot$	FDU

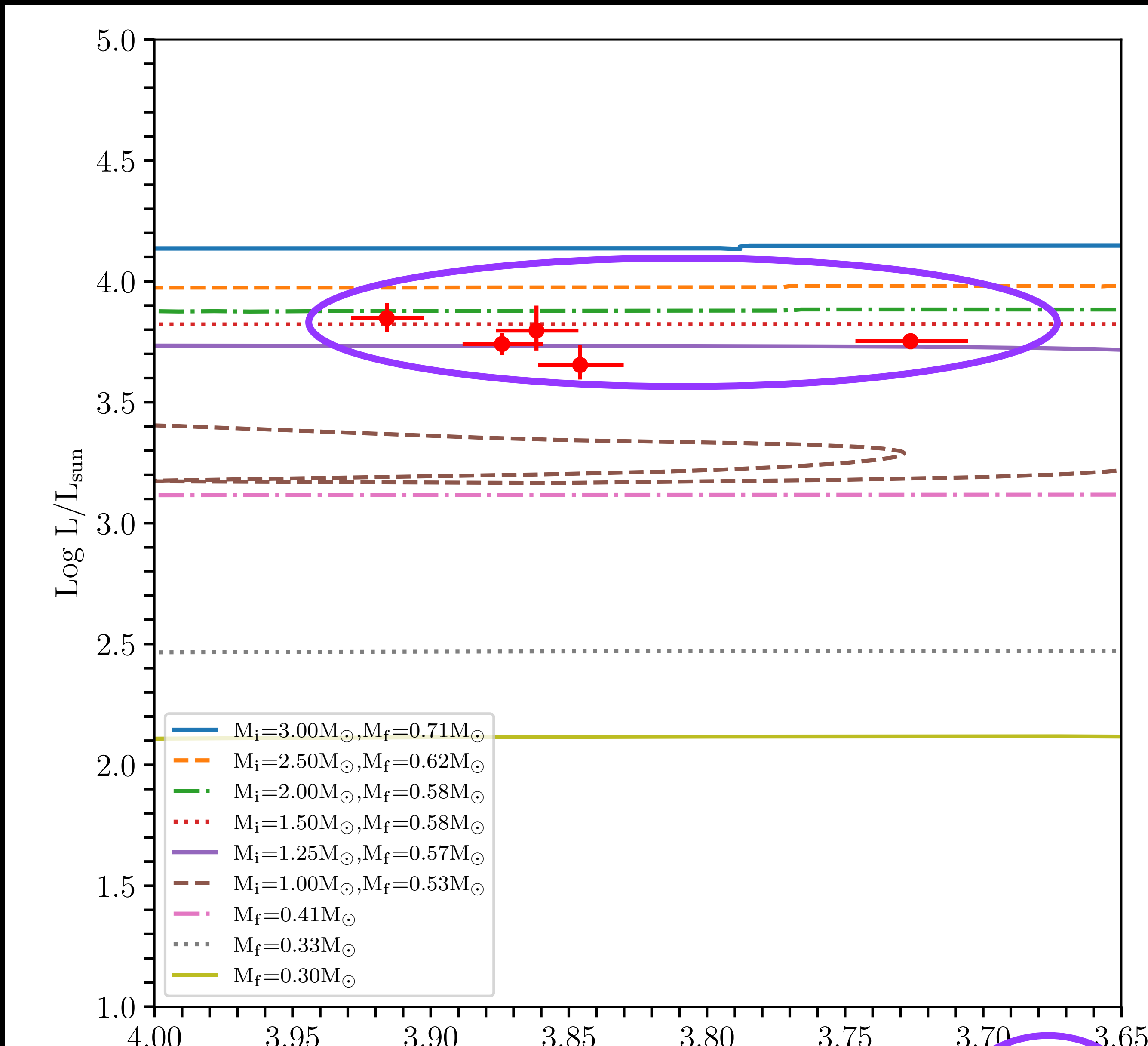

- **Case 2: Third Dredge-Up (TDU)**
- **Progenitor mass of ~1 - 3 Msun**
  - Series of thermal pulses
  - Evolve as C-stars
  - Significant C and *s*-process
  - Some N (from FDU), mild O-enrichment

Object		T_{eff}	$L/L_{\odot}$	[C/Fe]	[N/Fe]	[O/Fe]	Flag	M_{init}	chemistry
8	IRAS 08143-4406	7013 ± 250	4509	0.71 ± 0.10	0.01 ± 0.22	0.19 ± 0.13	Q1	$1 - 1.5\ M_{\odot}$	TDU
9	IRAS 08281-4850	7462 ± 250	9584	0.75 ± 0.21	...	0.12 ± 0.11	Q2	$1.5 - 2\ M_{\odot}$	TDU
10	IRAS 12360-5740	7273 ± 250	6258	0.27 ± 0.18	0.22 ± 0.32	0.31 ± 0.05	Q1	$1 - 1.5\ M_{\odot}$	TDU
11	IRAS 13245-5036	9037 ± 250	11221	0.57 ± 0.21	...	0.26 ± 0.13	Q2	$1.5 - 2\ M_{\odot}$	TDU
12	IRAS 14325-6428	7256 ± 250	4935	1.18 ± 0.23	0.18 ± 0.20	0.57 ± 0.09	Q2	$1.5 - 2\ M_{\odot}$	TDU
13	IRAS 14429-4539	9579 ± 250	5049	0.68 ± 0.23	...	0.31 ± 0.12	Q2	$1.5 - 2\ M_{\odot}$	TDU
14	IRAS 19500-1709	8239 ± 250	7053	0.99 ± 0.06	0.41 ± 0.30	0.72 ± 0.04	Q1	$1.5 - 2\ M_{\odot}$	TDU

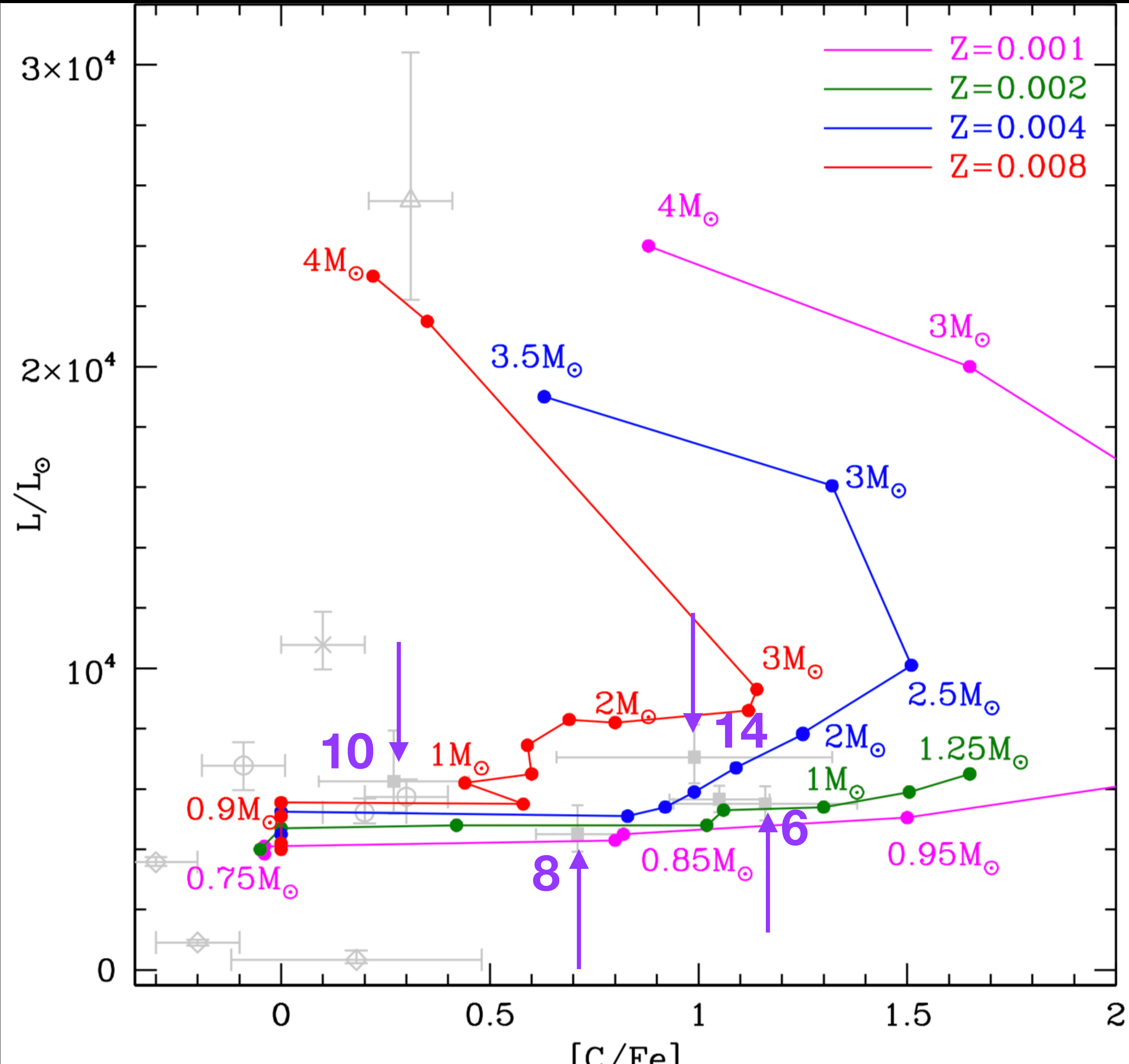

Case 2: Third Dredge-Up (TDU)

Progenitor mass of ~1 - 3 Msun

- Series of thermal pulses
- Evolve as C-stars
- Significant C and *s*-process
- Some N (from FDU), mild O-enrichment

Object		T_{eff}	$L/L_\odot$	[C/Fe]	[N/Fe]	[O/Fe]	Flag	M_{init}	chemistry
8	IRAS 08143-4406	7013 ± 250	4509	0.71 ± 0.10	0.01 ± 0.22	0.19 ± 0.13	Q1	$1 - 1.5\ M_\odot$	TDU
9	IRAS 08281-4850	7462 ± 250	9584	0.75 ± 0.21	...	0.12 ± 0.11	Q2	$1.5 - 2\ M_\odot$	TDU
10	IRAS 12360-5740	7273 ± 250	6258	0.27 ± 0.18	0.22 ± 0.32	0.31 ± 0.05	Q1	$1 - 1.5\ M_\odot$	TDU
11	IRAS 13245-5036	9037 ± 250	11221	0.57 ± 0.21	...	0.26 ± 0.13	Q2	$1.5 - 2\ M_\odot$	TDU
12	IRAS 14325-6428	7256 ± 250	4935	1.18 ± 0.23	0.18 ± 0.20	0.57 ± 0.09	Q2	$1.5 - 2\ M_\odot$	TDU
13	IRAS 14429-4539	9579 ± 250	5049	0.68 ± 0.23	...	0.31 ± 0.12	Q2	$1.5 - 2\ M_\odot$	TDU
14	IRAS 19500-1709	8239 ± 250	7053	0.99 ± 0.06	0.41 ± 0.30	0.72 ± 0.04	Q1	$1.5 - 2\ M_\odot$	TDU

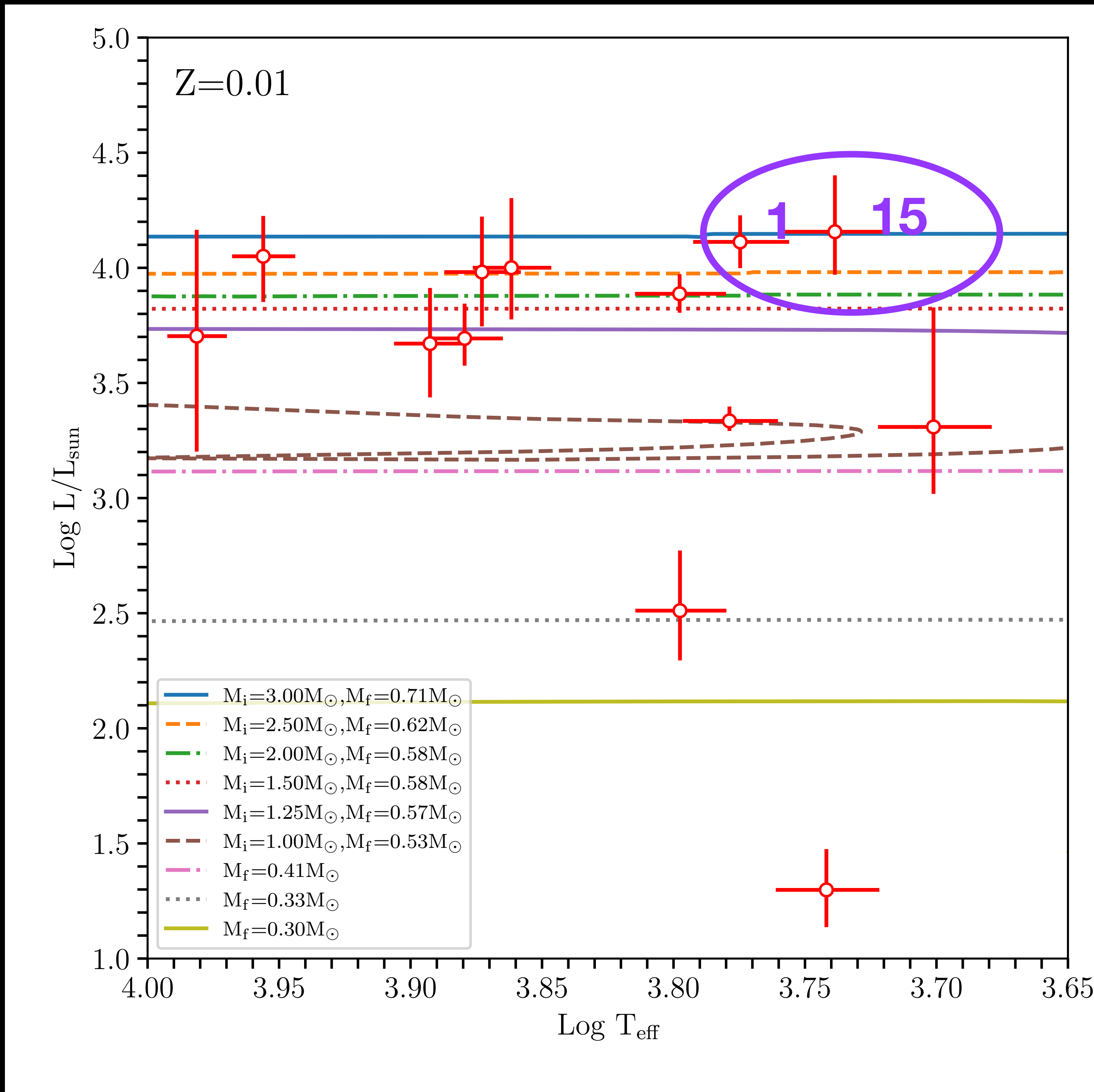

- **Case 3: TDU + HBB**
- **Progenitor mass of ~3 - 4 Msun**
  - Experience both TDU and HBB
  - Enhanced in C and *s*-process.
  - N is ~a factor of 10 higher than initial

Index	Object	T_{eff}	$L/L_\odot$	[C/Fe]	[N/Fe]	[O/Fe]	Flag	M_{init}	chemistry
				s-process enriched stars					
1	IRAS Z02229+6208	5952 ± 250	12959	0.78 ± 0.15	1.19 ± 0.15	...	Q2	$3 - 3.5\ M_\odot$	TDU+HBB
15	IRAS 20000+3239	5478 ± 250	14342	1.7 ± 0.2	2.1 ± 0.2	...	Q2	$3 - 3.5\ M_\odot$	TDU+HBB

- **Case 3: TDU + HBB**
- **Progenitor mass of ~3 - 4 Msun**
  - Experience both TDU and HBB
  - Enhanced in C and *s*-process.
  - N is ~a factor of 10 higher than initial

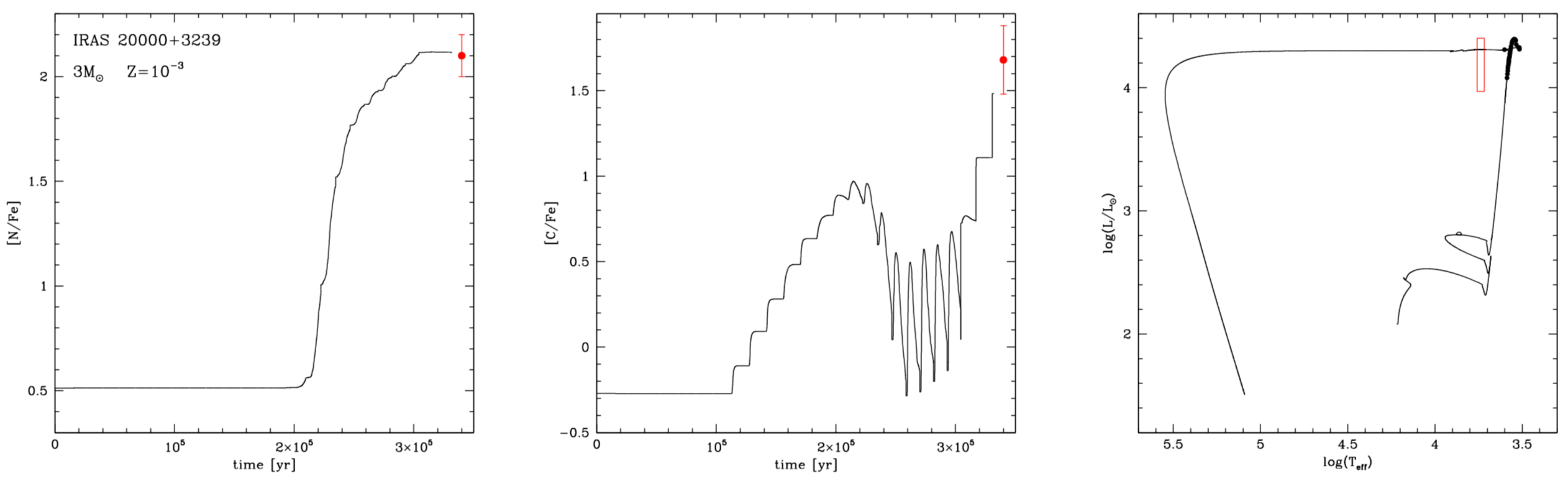

Case 4: HBB

Progenitor mass of > 4 Msun

- Dominated by HBB
- N enhancement, neither C nor *s*-process

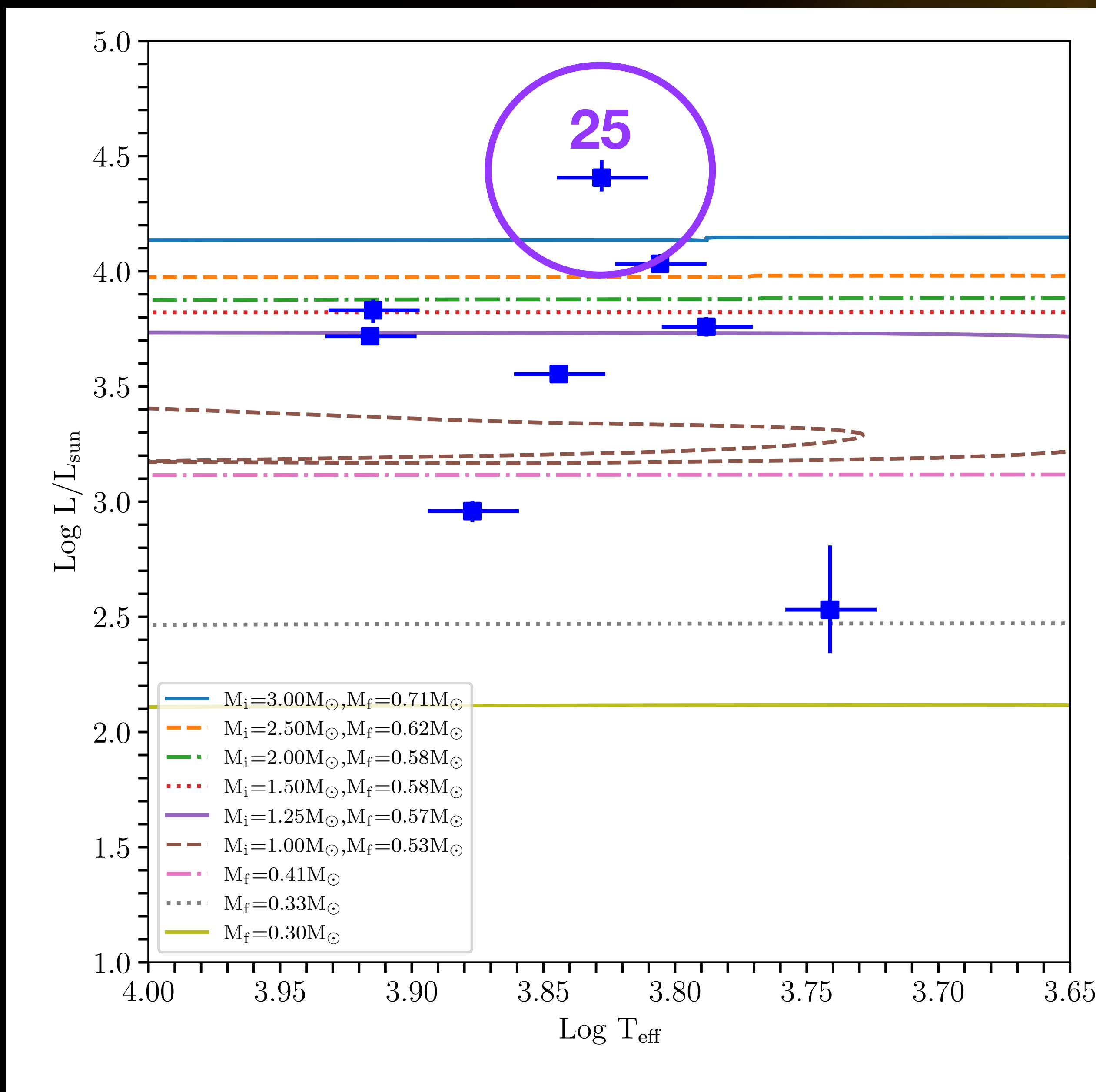

Index	Object	T_{eff}	$L/L_\odot$	[C/Fe]	[N/Fe]	[O/Fe]	Flag	M_{init}	chemistry
25	HR 6144	6728 ± 250	25491	0.3 ± 0.2	0.9 ± 0.2	0.3 ± 0.2	Q1	$4-5\ M_\odot$	HBB

- **Case 4: HBB**
- **Progenitor mass of > 4 Msun**
  - Dominated by HBB
  - N enhancement, neither C nor *s*-process

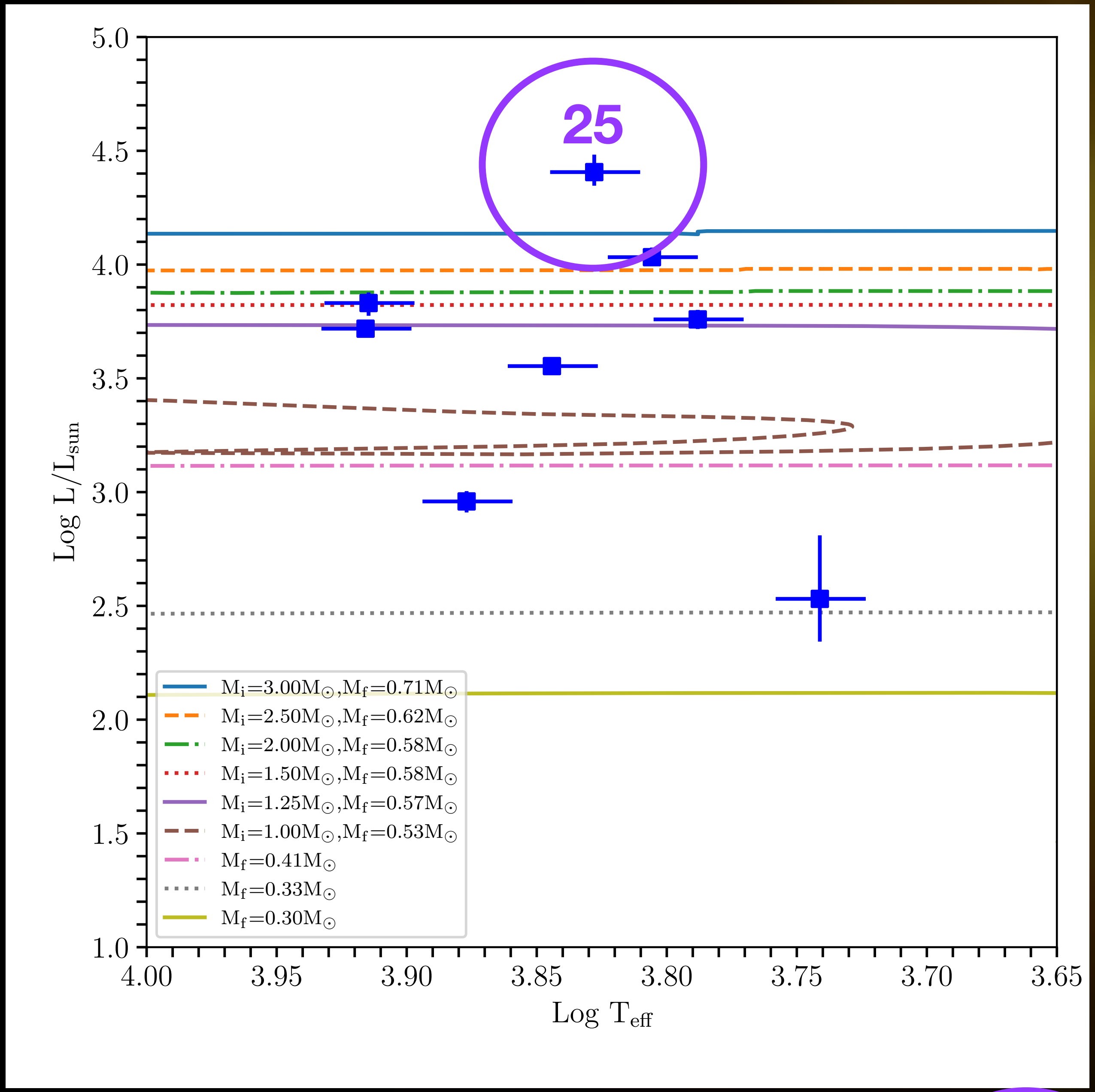

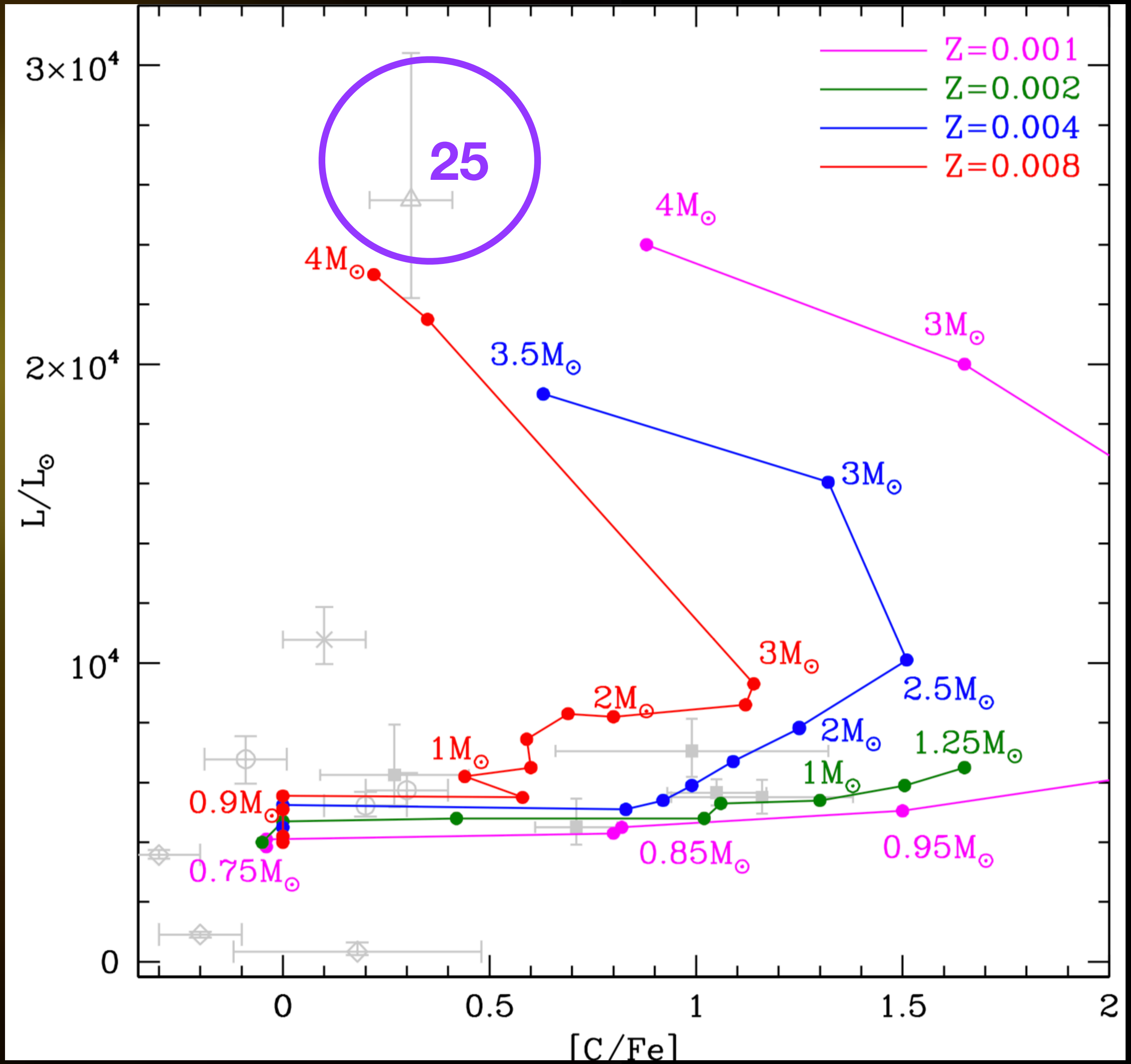

Index	Object	T_{eff}	$L/L_\odot$	[C/Fe]	[N/Fe]	[O/Fe]	Flag	M_{init}	chemistry
25	HR 6144	6728 ± 250	25491	0.3 ± 0.2	0.9 ± 0.2	0.3 ± 0.2	Q1	$4 - 5\ M_\odot$	HBB

- **Case 4: HBB**
- **Progenitor mass of > 4 Msun**
  - Dominated by HBB
  - N enhancement, neither C nor *s*-process

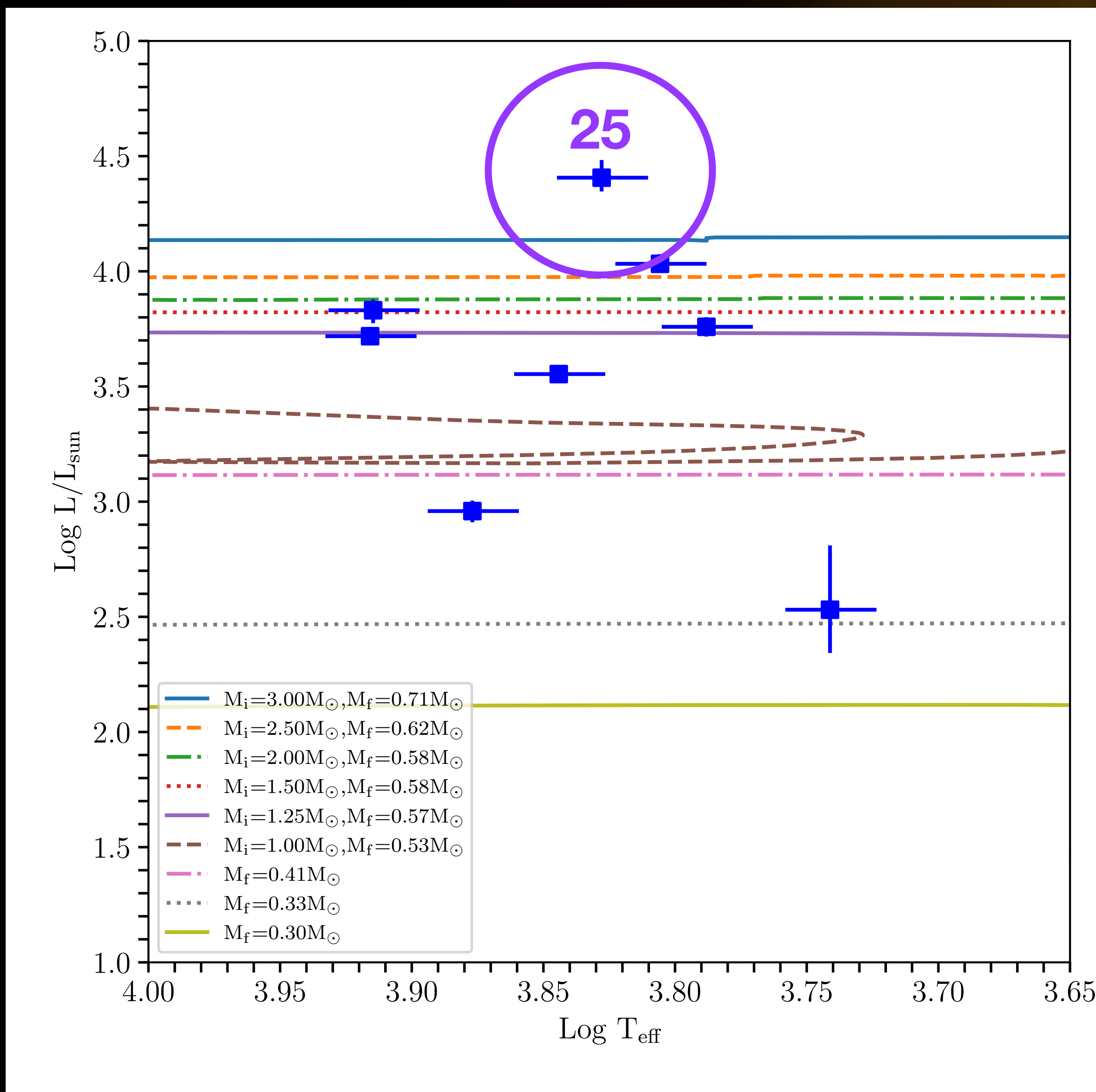

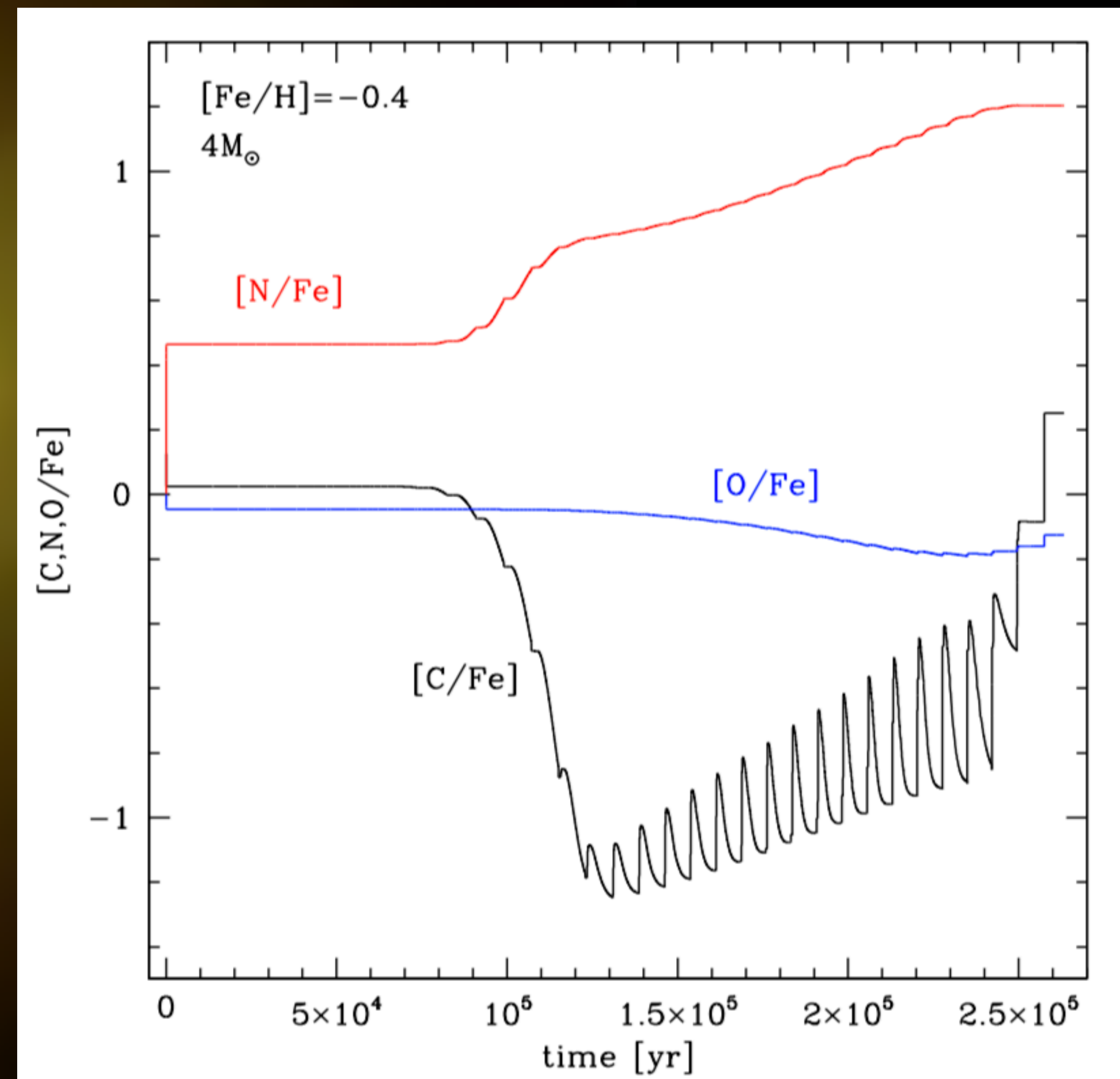

Index	Object	T_{eff}	$L/L_\odot$	[C/Fe]	[N/Fe]	[O/Fe]	Flag	M_{init}	chemistry
25	HR 6144	6728 ± 250	25491	0.3 ± 0.2	0.9 ± 0.2	0.3 ± 0.2	Q1	$4 - 5\ M_\odot$	HBB

Chemistry of Stars Evolving from AGB to Post-AGB

Chemistry of Stars Evolving from AGB to Post-AGB

NON - STANDARD AGB EVOLUTION AND NUCLEOSYNTHESIS SCENARIOS

A SIGNATURE OF DEEP MIXING DURING THE RGB?

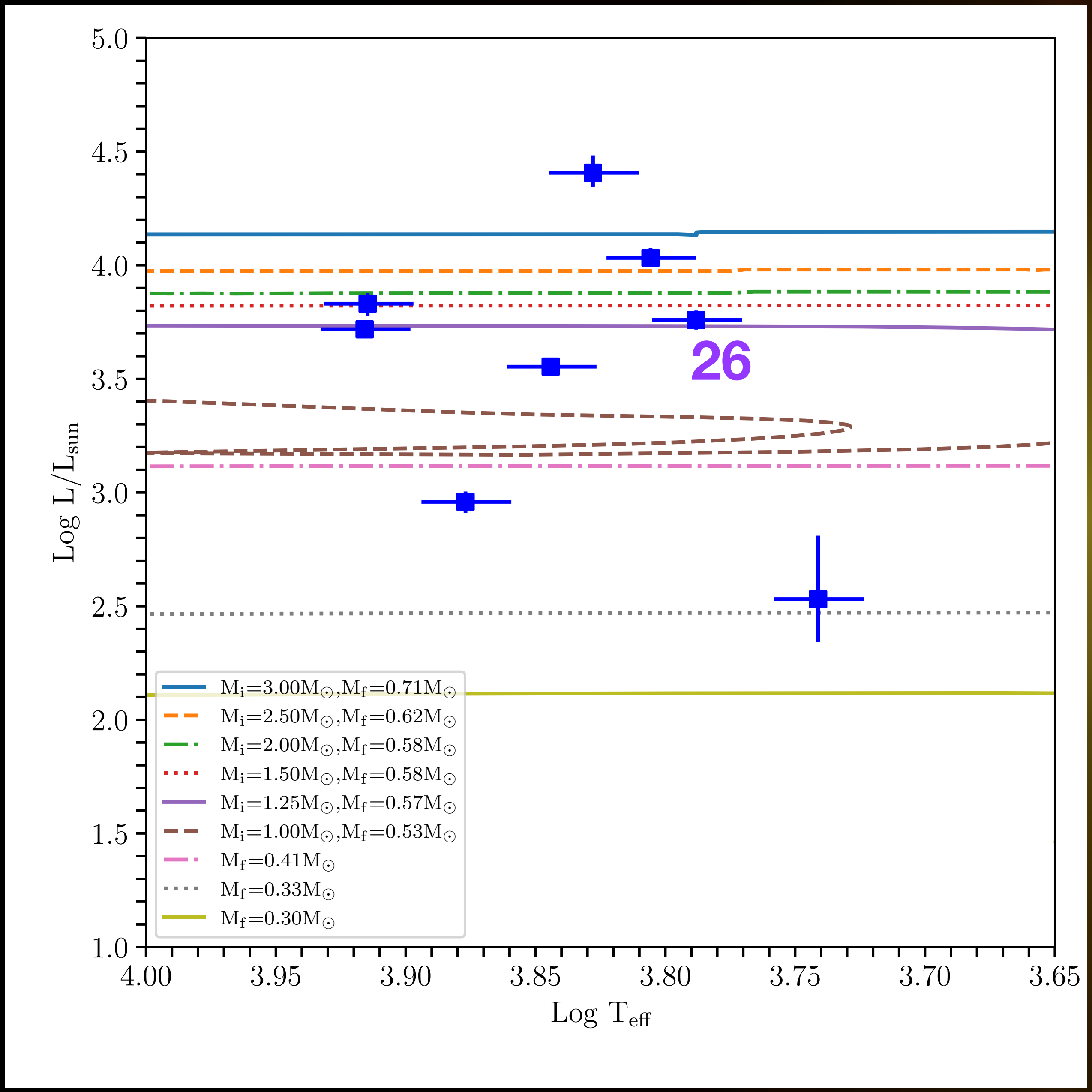

- No *s*-process enhancements
- luminosity: 5000–6300 Lsun
- Extremely large surface nitrogen, [N/Fe] = 1.1
- Possibility explored: extremely deep mixing during the RGB ascending
- e.g., D'Antona & Ventura 2007

Index	Object	T_{eff}	$L/L_{\odot}$	[C/Fe]	[N/Fe]	[O/Fe]	Flag	M_{init}	chemistry
26	HD 161796	6139 ± 250	5742	0.3 ± 0.2	1.1 ± 0.2	0.4 ± 0.2	Q1	$1 - 1.2\ M_{\odot}$	FDU

A Signature of Deep Mixing During the RGB?

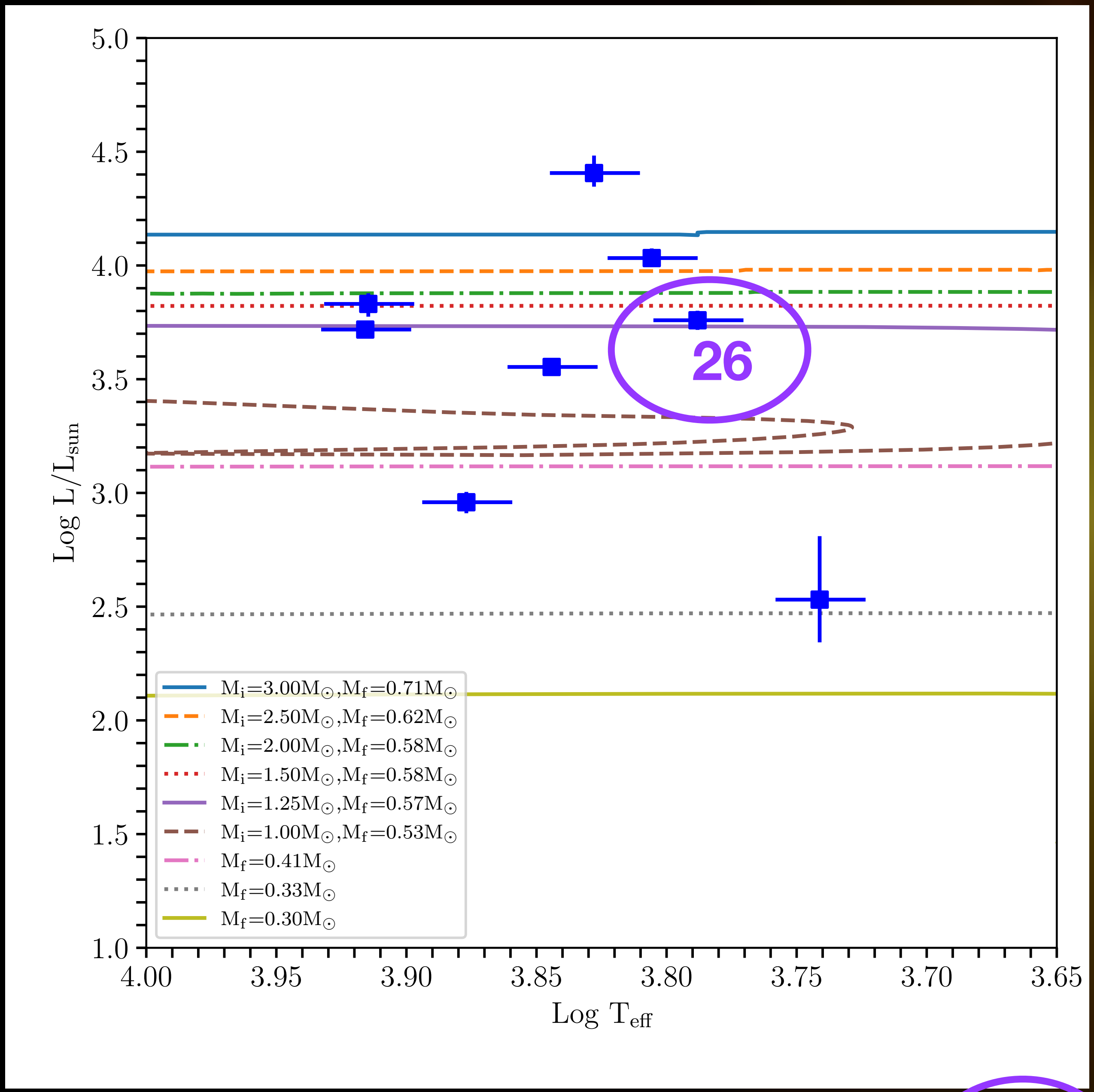

- No *s*-process enhancements
- luminosity: 5000–6300 Lsun
- Extremely large surface nitrogen, [N/Fe] = 1.1
- Possibility explored: extremely deep mixing during the RGB ascending
- e.g., D'Antona & Ventura 2007

Index	Object	T_{eff}	$L/L_\odot$	[C/Fe]	[N/Fe]	[O/Fe]	Flag	M_{init}	chemistry
26	HD 161796	6139 ± 250	5742	0.3 ± 0.2	1.1 ± 0.2	0.4 ± 0.2	Q1	$1 - 1.2\ M_\odot$	FDU

A Signature of Deep Mixing During the RGB?

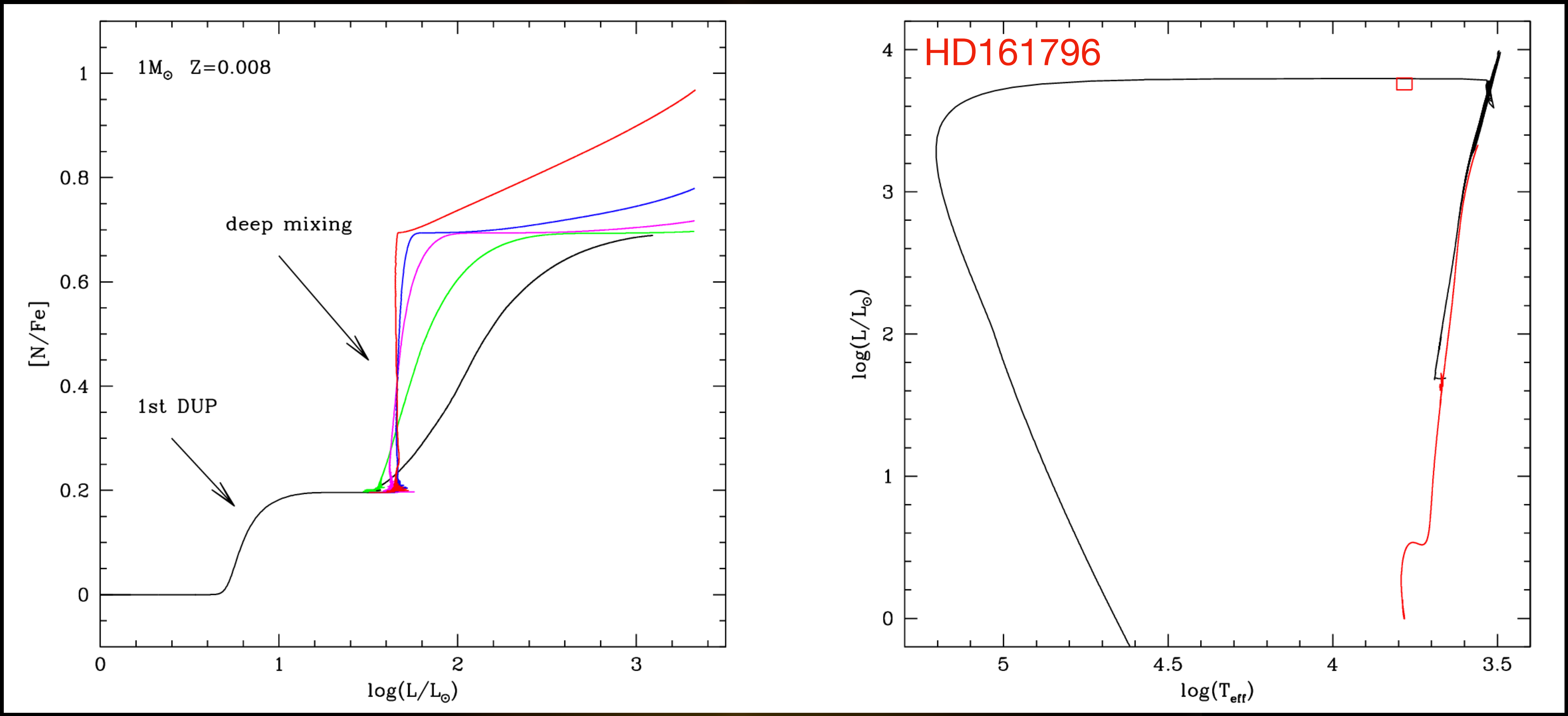

- AGB phase with a mass in the 1 – 1.1 M⊙ range
- Assuming a ~ 0.1 M⊙ mass loss during the RGB, this corresponds to age 4 – 5 Gyr
- Star must have experienced one or 2 TDU events before entering the post-AGB phase (observed value [N/Fe] = 1.1, [C/Fe] = 0.3 + lack of s-process enhancement)

Stars that Failed the Third Dredge-Up

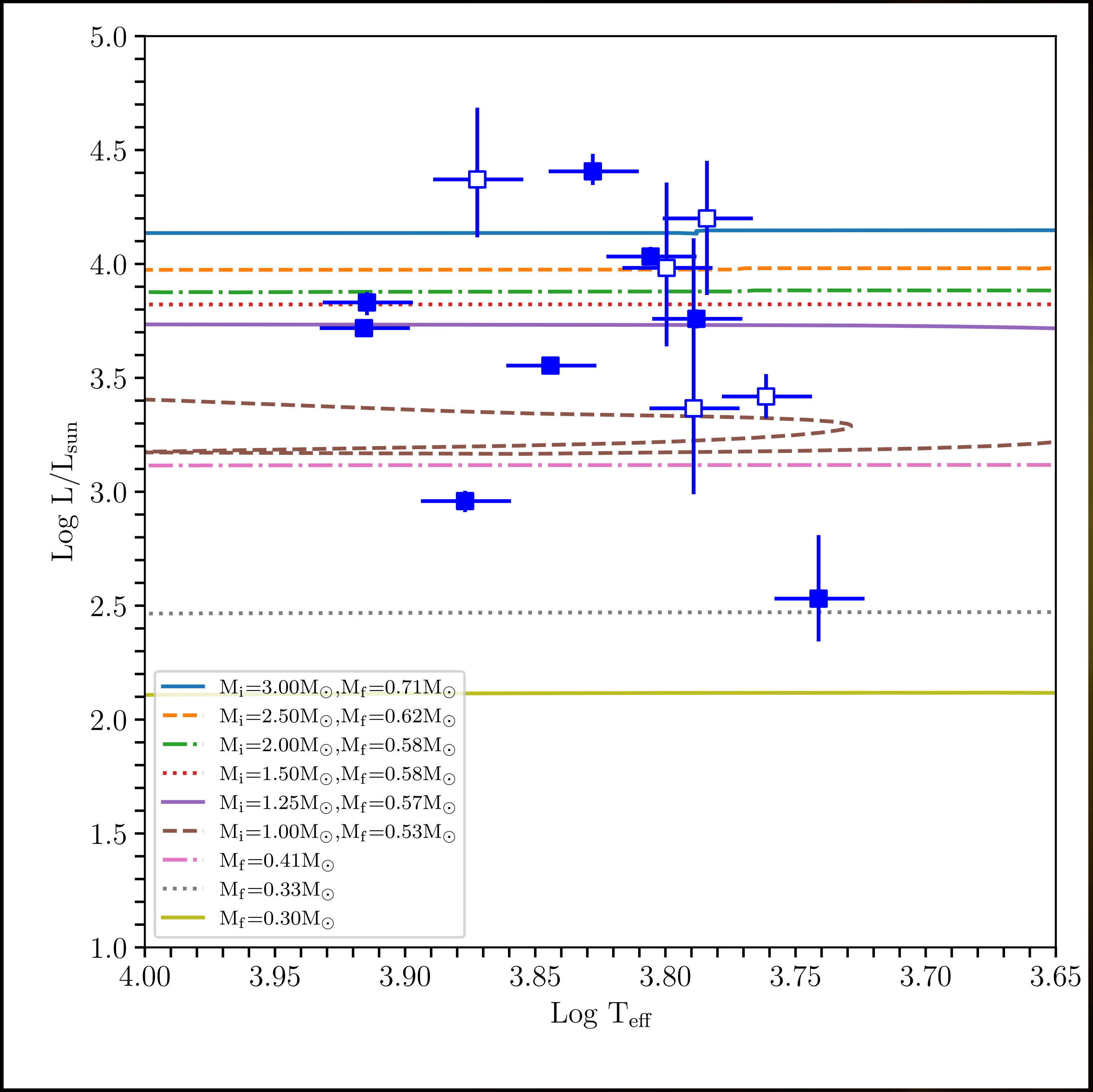

Index	Object	T_{eff}	$L/L_\odot$	[C/Fe]	[N/Fe]	[O/Fe]	Flag	M_{init}	chemistry
21	SAO 239853	7452 ± 250	23490	0.4 ± 0.15	0.6 ± 0.2	0.8 ± 0.2	Q2	$\sim 3\ M_\odot$	TDU
23	HD 112374	6393 ± 250	10777	0.1 ± 0.2	0.5 ± 0.2	0.8 ± 0.2	Q1	$2.5 - 3\ M_\odot$	TDU

STARS THAT FAILED THE THIRD DREDGE-UP

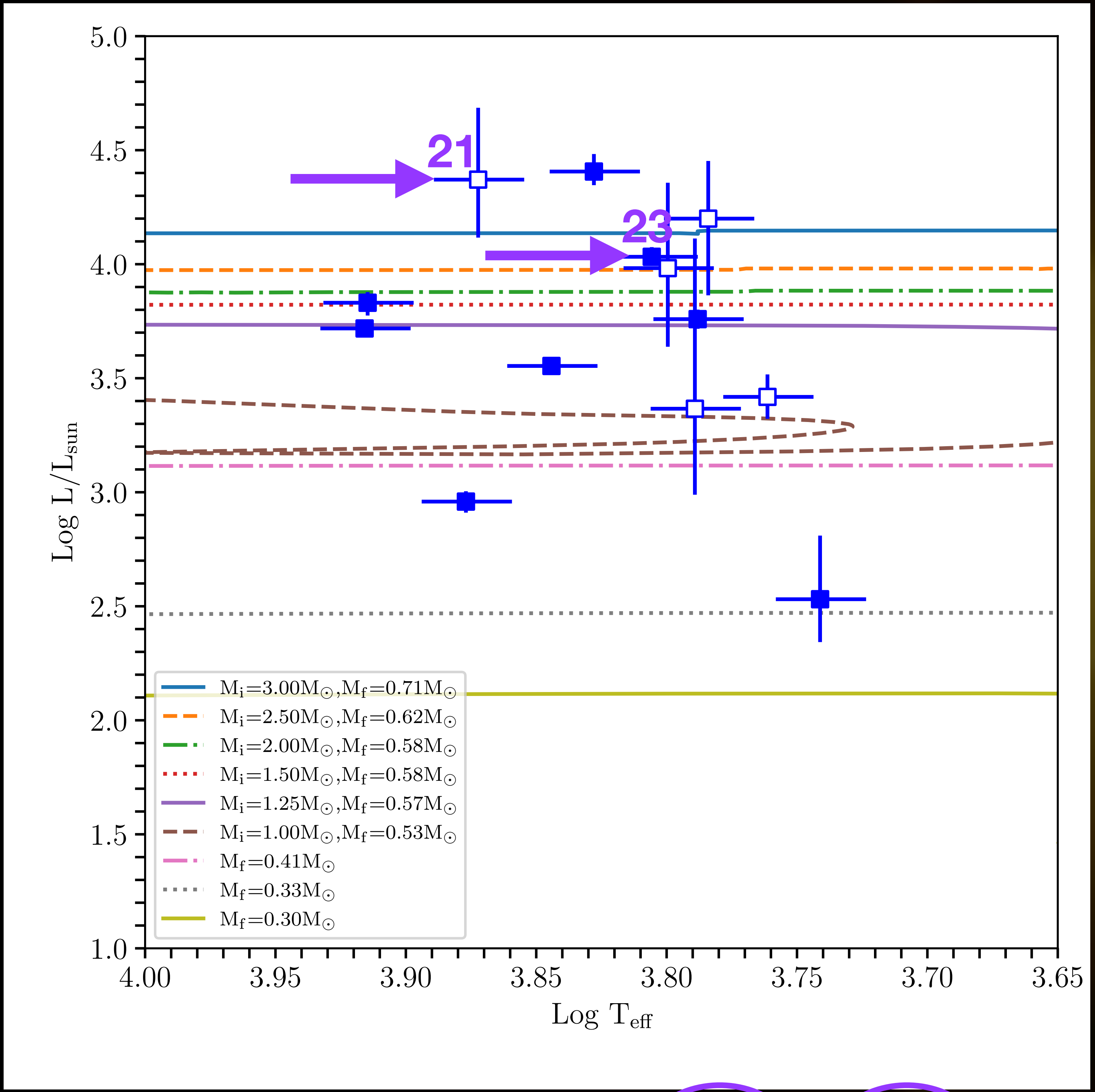

Index	Object	T_{eff}	$L/L_\odot$	[C/Fe]	[N/Fe]	[O/Fe]	Flag	M_{init}	chemistry
21	SAO 239853	7452 ± 250	23490	0.4 ± 0.15	0.6 ± 0.2	0.8 ± 0.2	Q2	$\sim 3\ M_\odot$	TDU
23	HD 112374	6393 ± 250	10777	0.1 ± 0.2	0.5 ± 0.2	0.8 ± 0.2	Q1	$2.5 - 3\ M_\odot$	TDU

STARS THAT FAILED THE THIRD DREDGE-UP

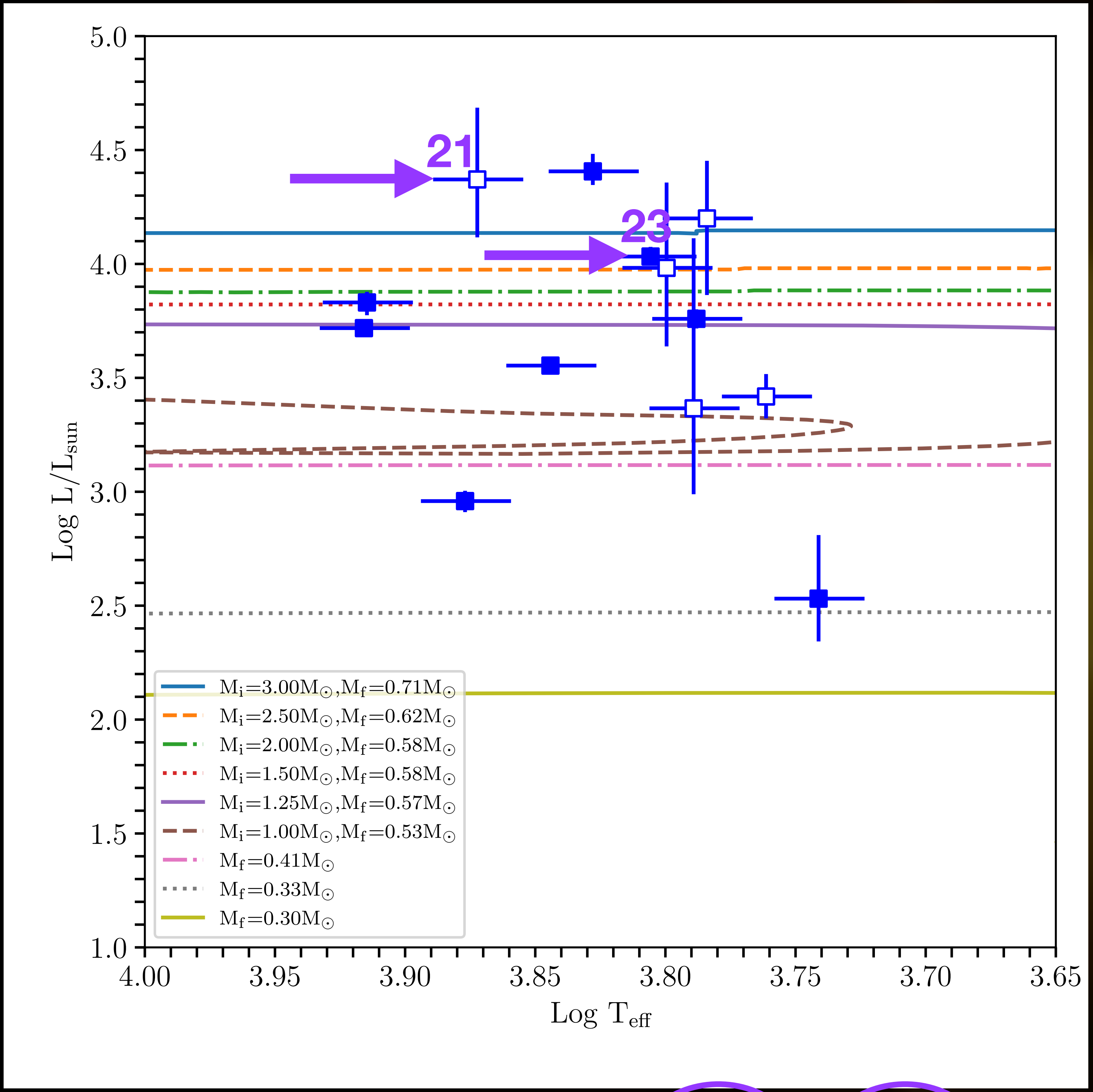

- ★ A fast loss of the external envelope halted further growth of the core mass and increase in the surface carbon and prevented *s*-process enrichment

Index	Object	T_{eff}	$L/L_{\odot}$	[C/Fe]	[N/Fe]	[O/Fe]	Flag	M_{init}	chemistry
21	SAO 239853	7452 ± 250	23490	0.4 ± 0.15	0.6 ± 0.2	0.8 ± 0.2	Q2	$\sim 3\ M_{\odot}$	TDU
23	HD 112374	6393 ± 250	10777	0.1 ± 0.2	0.5 ± 0.2	0.8 ± 0.2	Q1	$2.5 - 3\ M_{\odot}$	TDU

STARS THAT FAILED THE THIRD DREDGE-UP

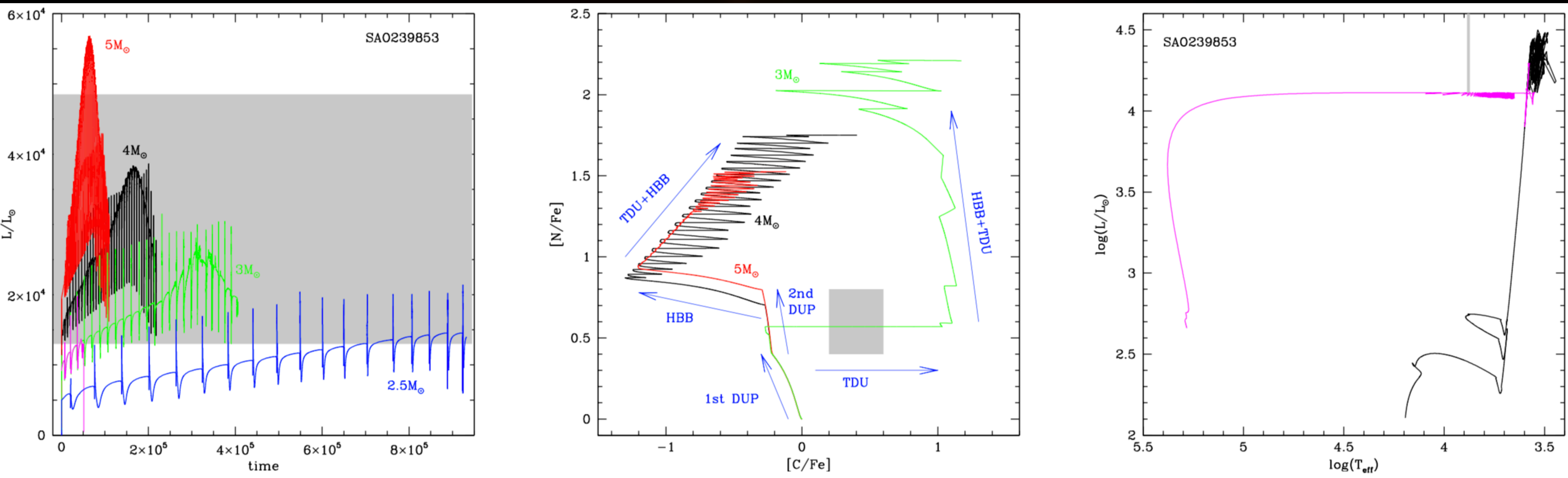

- ⋆ SAO239853: uncertain luminosity, given in the 13000 – 48500 L⊙ range.
- ⋆ The 3 Msun model star evolves to surface C and N abundances consistent with those observed during the first part of the AGB phase, after the star experienced a couple of TDU events
- ⋆ We artificially removed the envelope of the stars from this point on

THE LOW LUMINOSITY SAMPLE: POST-HB STARS

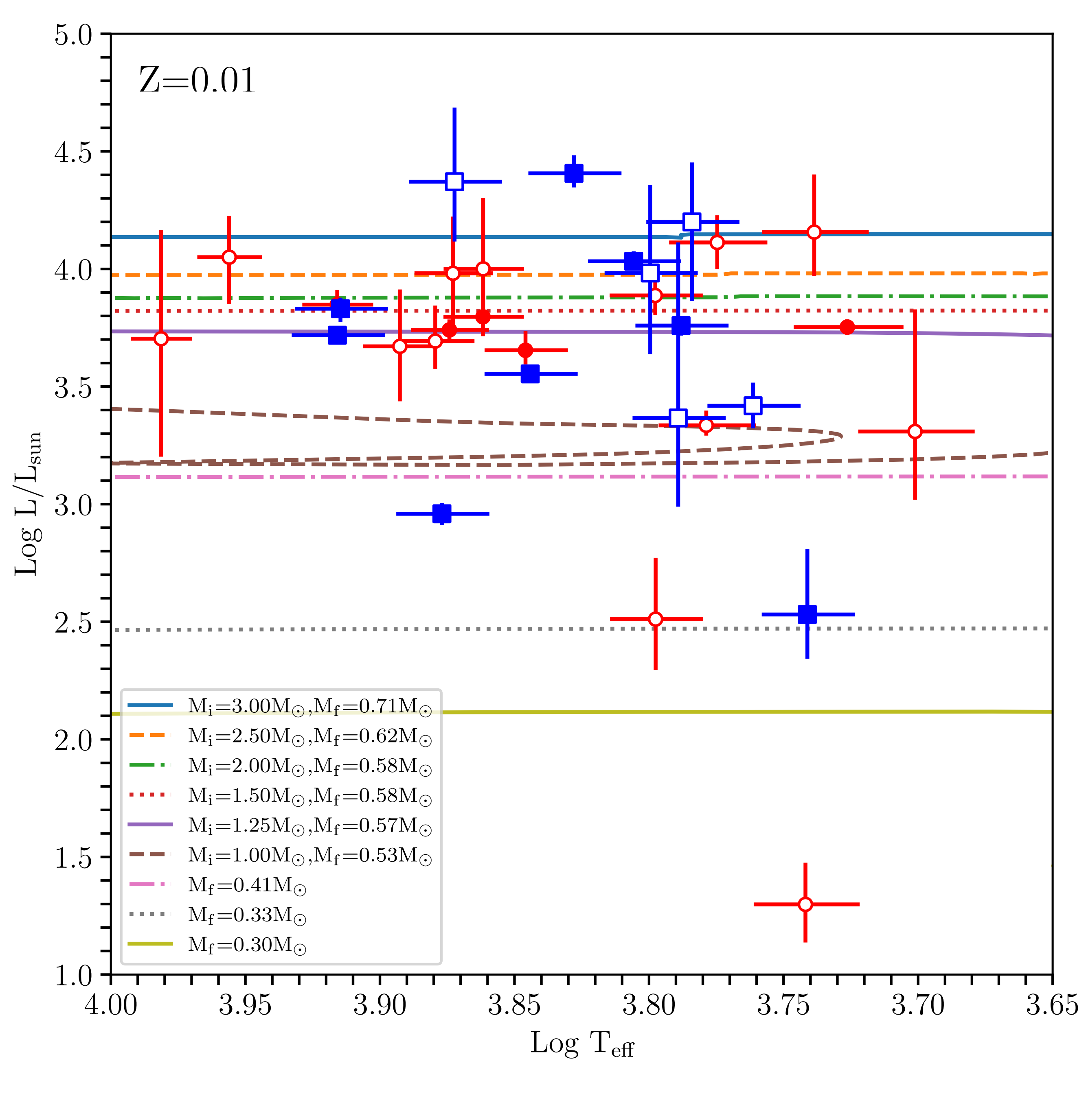

- ⋆ Descend from low-mass progenitors, that concluded the horizontal branch (hereafter HB) evolution, and are currently evolving through a post-HB phase
- ⋆ Likely to have formed 6 – 10 Gyr ago
- ⋆ We estimate of the mass at the beginning of the HB

THE LOW LUMINOSITY SAMPLE: POST-HB STARS

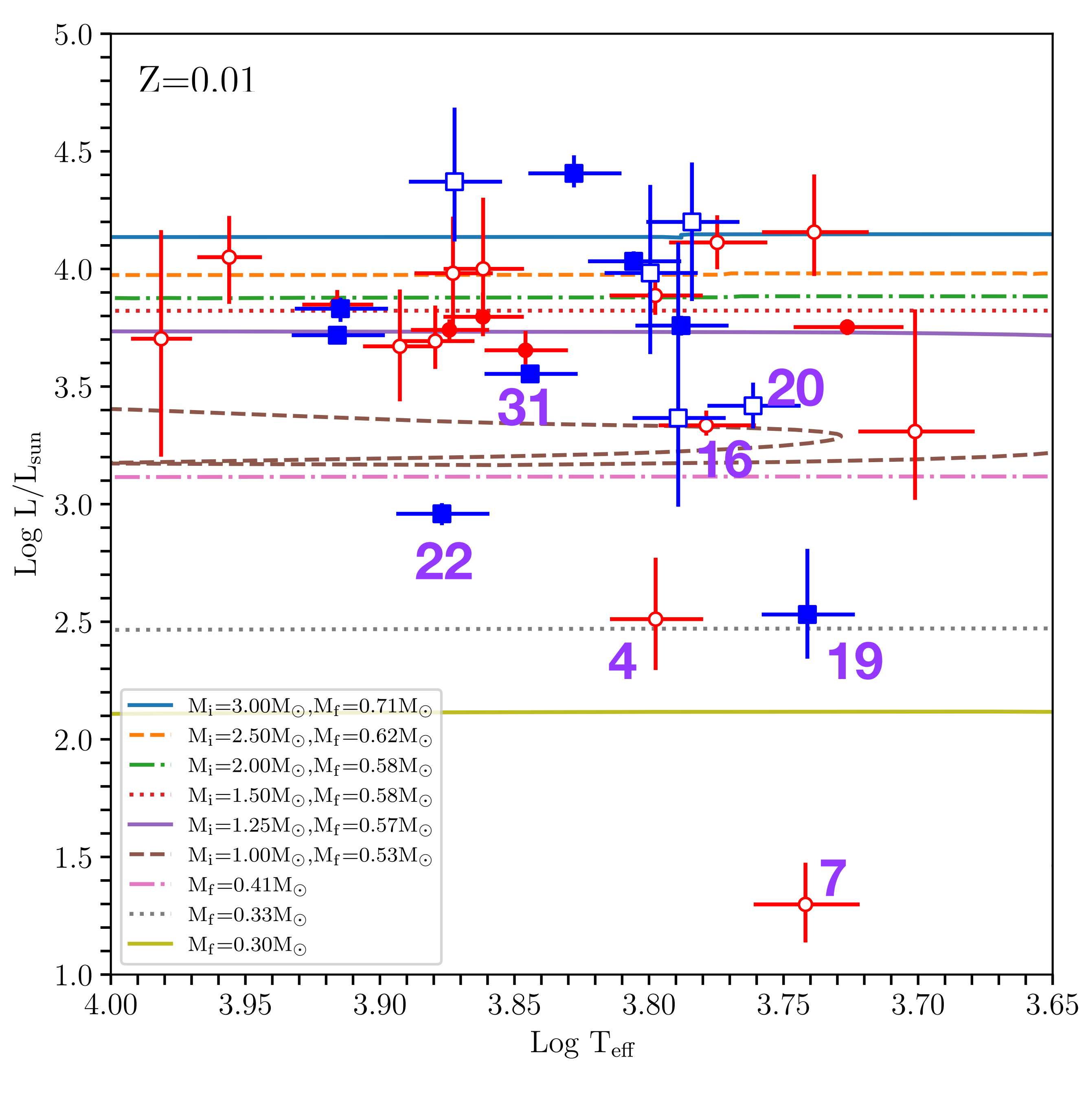

- ⋆ Descend from low-mass progenitors, that concluded the horizontal branch (hereafter HB) evolution, and are currently evolving through a post-HB phase
- ⋆ Likely to have formed 6 – 10 Gyr ago
- ⋆ We estimate of the mass at the beginning of the HB

THE LOW LUMINOSITY SAMPLE: POST-HB STARS

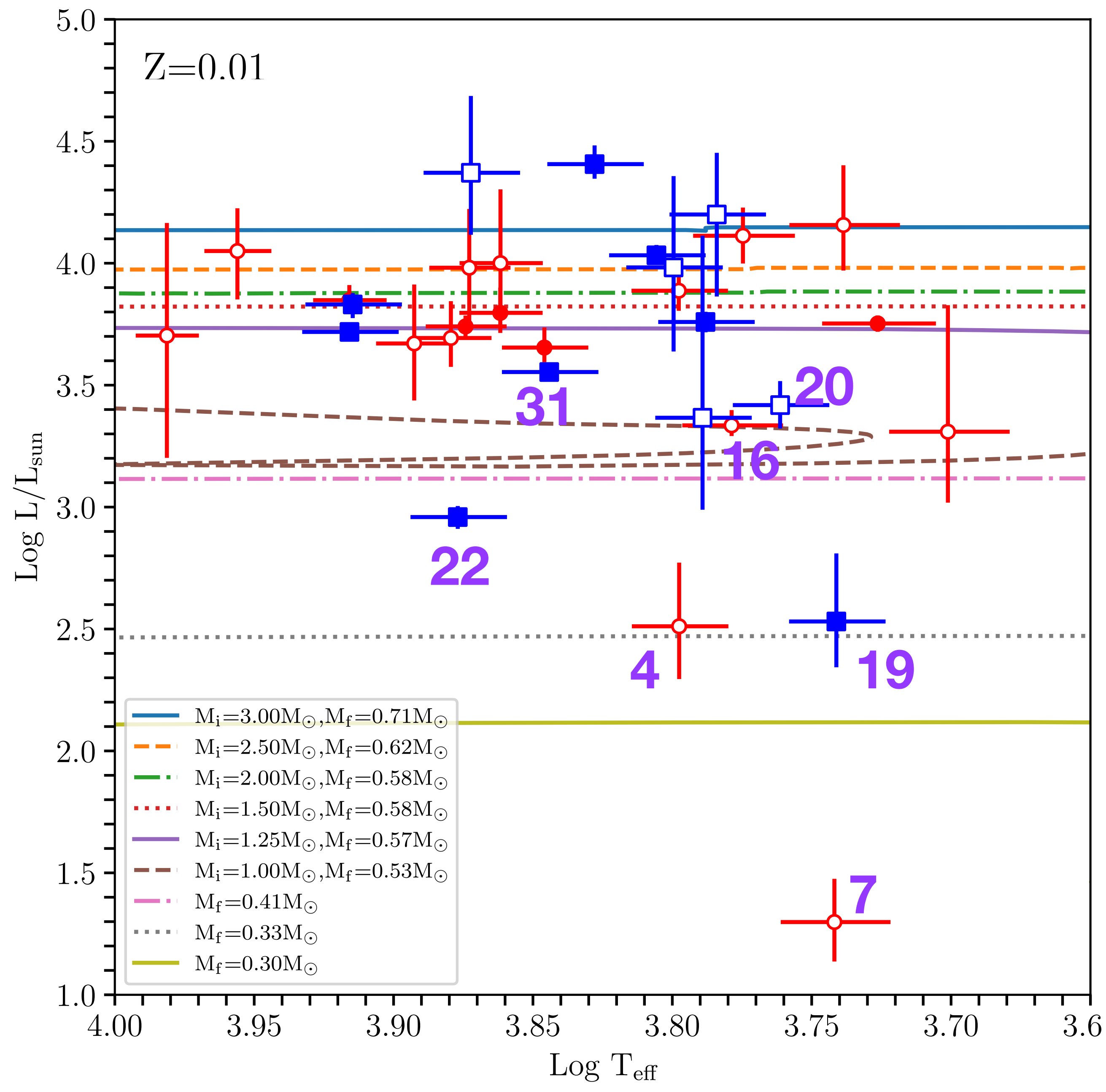

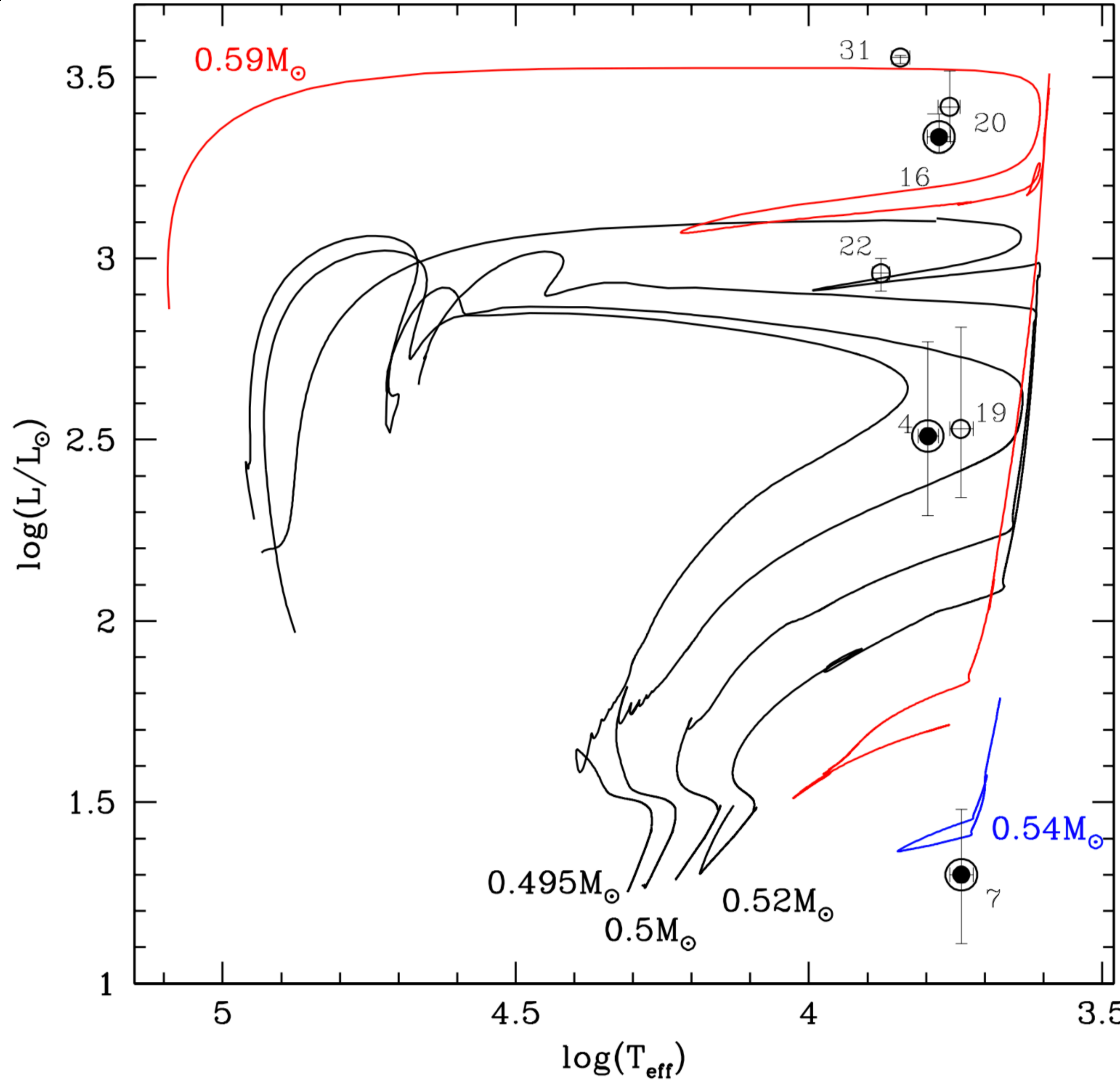

- ⋆ Descend from low-mass progenitors, that concluded the horizontal branch (hereafter HB) evolution, and are currently evolving through a post-HB phase
- ⋆ Likely to have formed 6 – 10 Gyr ago
- ⋆ We estimate of the mass at the beginning of the HB

The Low Luminosity Sample: Post-HB Stars

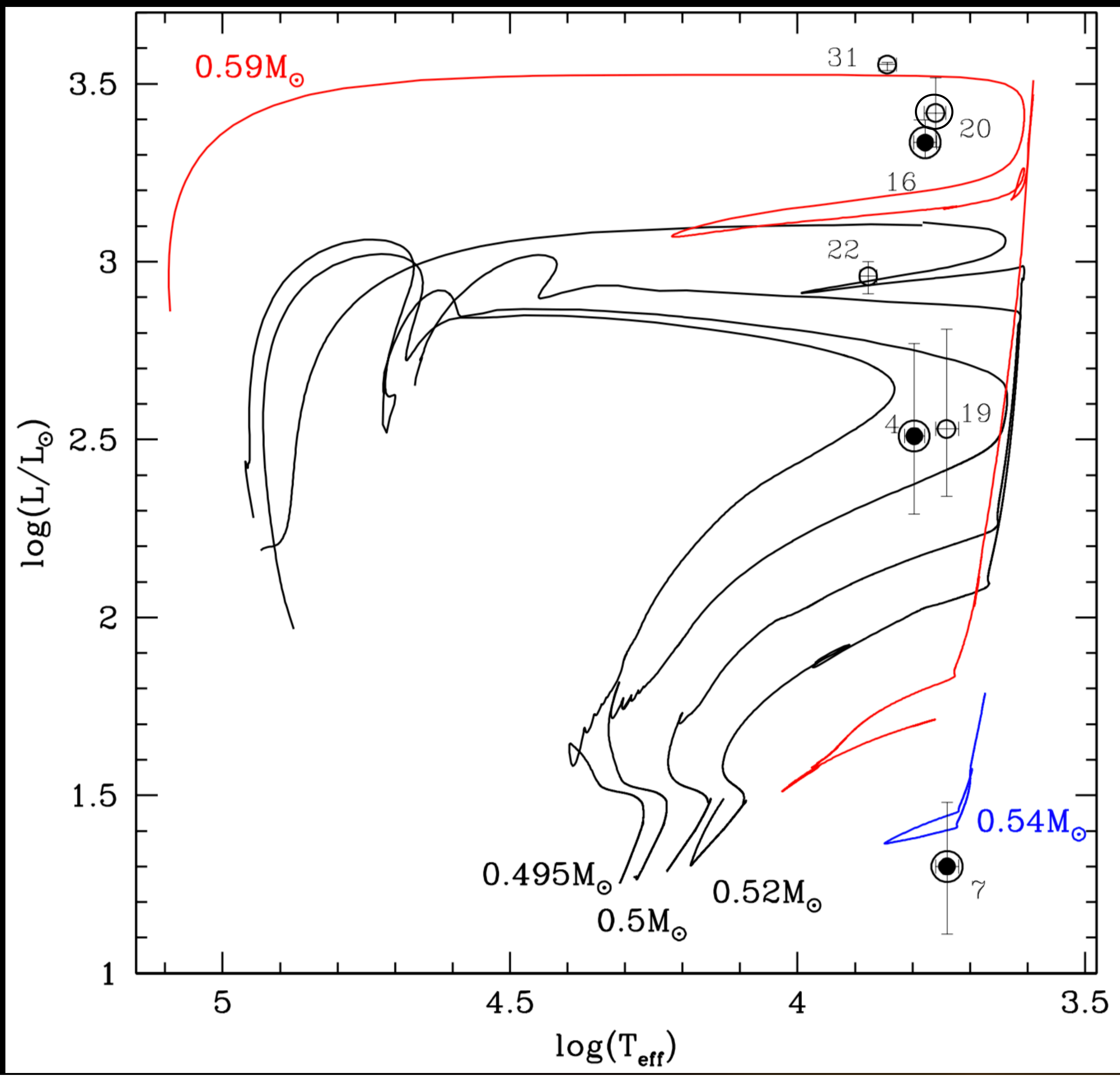

- AGB Manque stars
- An extremely Short AGB phase
- A core helium burning star
- *s*-process and carbon enrichment in faint stars

Index	Object	T_{eff}	$L/L_\odot$	[C/Fe]	[N/Fe]	[O/Fe]	Flag	M_{init}	chemistry
4	IRAS 05341+0852	6274 ± 250	324	1.03 ± 0.10	...	0.75 ± 0.11	Q2	$0.5 - 0.6\ M_\odot$	FLASH
7	IRAS 07430+1115	5519 ± 250	20	0.79 ± 0.13	...	0.30 ± 0.22	Q2	$0.5 - 0.6\ M_\odot$	FLASH
16	IRAS 22223+4327	6008 ± 250	2163	0.59 ± 0.06	0.15 ± 0.30	0.31 ± 0.06	Q2	$0.5 - 0.6\ M_\odot$	FLASH
19	IRAS 01259+6823	5510 ± 250	340	0.18 ± 0.15	...	0.31 ± 0.06	Q1	$0.5 - 0.6\ M_\odot$	FDU
20	IRAS 08187-1905	5772 ± 250	2619	0.62 ± 0.15	0.49 ± 0.3	0.26 ± 0.1	Q2	$0.5 - 0.6\ M_\odot$	FLASH
22	HD 107369	7533 ± 250	910	< -0.2	0.49 ± 0.3	0 ± 0.2	Q1	$0.5 - 0.6\ M_\odot$	FDU
31	HR 7671	6985 ± 250	3579	-0.57 ± 0.13	0.51 ± 0.16	0.46 ± 0.05	Q1	$0.5 - 0.6\ M_\odot$	FDU

THE LOW LUMINOSITY SAMPLE: POST-HB STARS

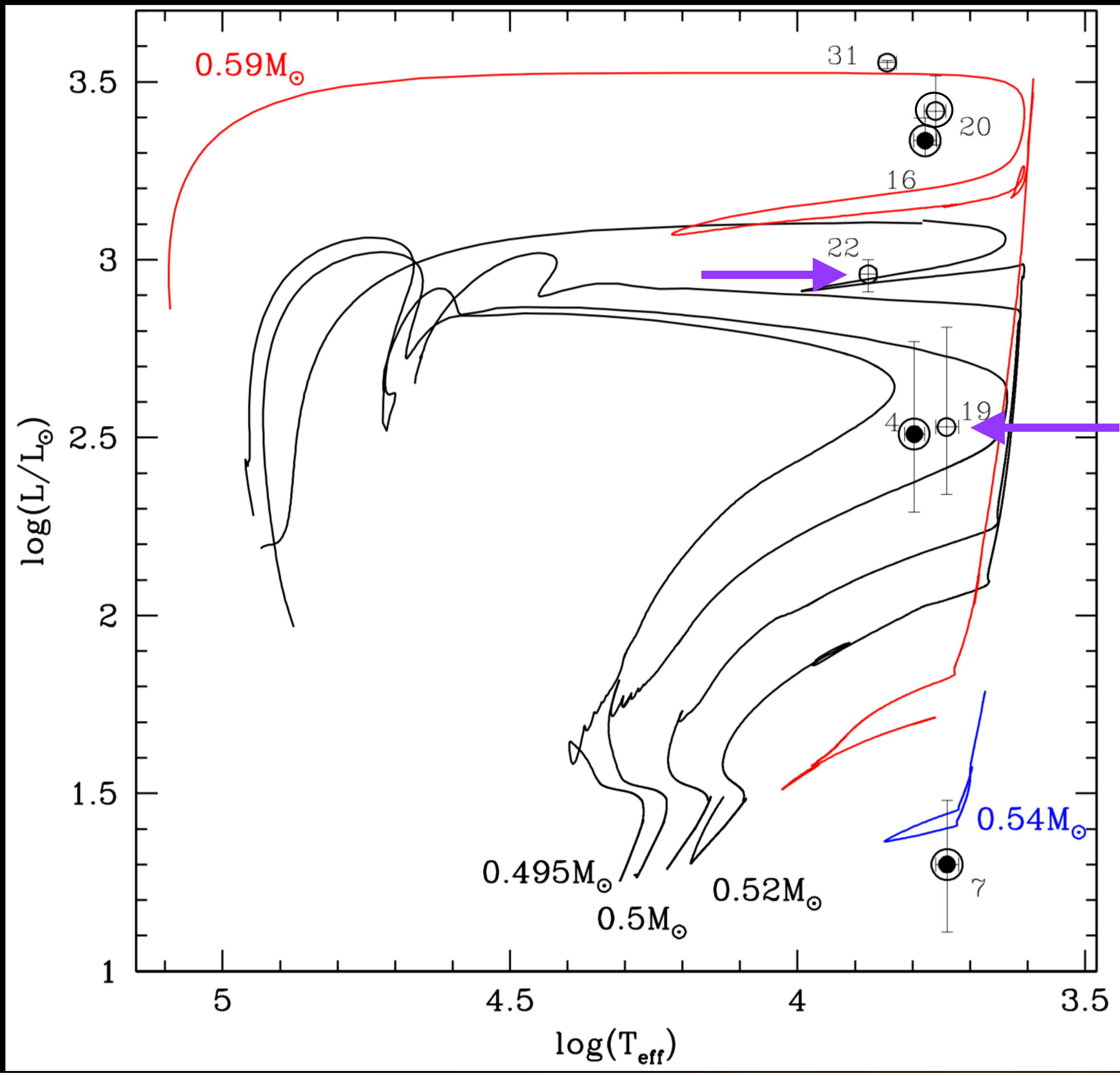

- AGB Manque stars
- An extremely Short AGB phase
- A core helium burning star
- *s*-process and carbon enrichment in faint stars

Index	Object	T_{eff}	$L/L_{\odot}$	[C/Fe]	[N/Fe]	[O/Fe]	Flag	M_{init}	chemistry
4	IRAS 05341+0852	6274 ± 250	324	1.03 ± 0.10	...	0.75 ± 0.11	Q2	$0.5 - 0.6\ M_{\odot}$	FLASH
7	IRAS 07430+1115	5519 ± 250	20	0.79 ± 0.13	...	0.30 ± 0.22	Q2	$0.5 - 0.6\ M_{\odot}$	FLASH
16	IRAS 22223+4327	6008 ± 250	2163	0.59 ± 0.06	0.15 ± 0.30	0.31 ± 0.06	Q2	$0.5 - 0.6\ M_{\odot}$	FLASH
19	IRAS 01259+6823	5510 ± 250	340	0.18 ± 0.15	...	0.31 ± 0.06	Q1	$0.5 - 0.6\ M_{\odot}$	FDU
20	IRAS 08187-1905	5772 ± 250	2619	0.62 ± 0.15	0.49 ± 0.3	0.26 ± 0.1	Q2	$0.5 - 0.6\ M_{\odot}$	FLASH
22	HD 107369	7533 ± 250	910	< -0.2	0.49 ± 0.3	0 ± 0.2	Q1	$0.5 - 0.6\ M_{\odot}$	FDU
31	HR 7671	6985 ± 250	3579	-0.57 ± 0.13	0.51 ± 0.16	0.46 ± 0.05	Q1	$0.5 - 0.6\ M_{\odot}$	FDU

THE LOW LUMINOSITY SAMPLE: POST-HB STARS

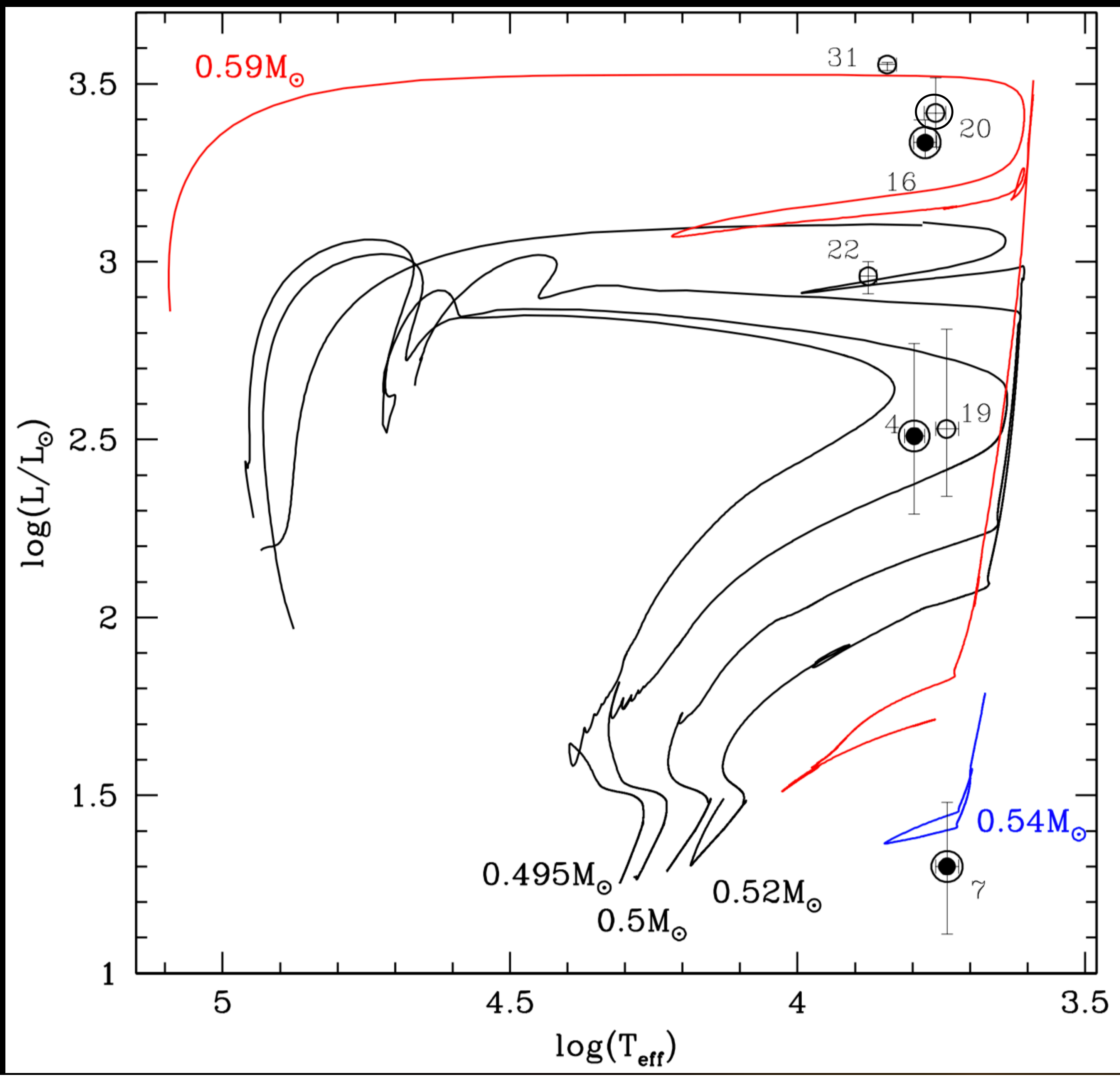

- AGB Manque stars
- An extremely Short AGB phase
- A core helium burning star
- *s*-process and carbon enrichment in faint stars

Index	Object	$T_{\rm eff}$	$L/L_\odot$	[C/Fe]	[N/Fe]	[O/Fe]	Flag	$M_{\rm init}$	chemistry
4	IRAS 05341+0852	6274 ± 250	324	1.03 ± 0.10	...	0.75 ± 0.11	Q2	$0.5 - 0.6\ M_\odot$	FLASH
7	IRAS 07430+1115	5519 ± 250	20	0.79 ± 0.13	...	0.30 ± 0.22	Q2	$0.5 - 0.6\ M_\odot$	FLASH
16	IRAS 22223+4327	6008 ± 250	2163	0.59 ± 0.06	0.15 ± 0.30	0.31 ± 0.06	Q2	$0.5 - 0.6\ M_\odot$	FLASH
19	IRAS 01259+6823	5510 ± 250	340	0.18 ± 0.15	...	0.31 ± 0.06	Q1	$0.5 - 0.6\ M_\odot$	FDU
20	IRAS 08187-1905	5772 ± 250	2619	0.62 ± 0.15	0.49 ± 0.3	0.26 ± 0.1	Q2	$0.5 - 0.6\ M_\odot$	FLASH
22	HD 107369	7533 ± 250	910	< -0.2	0.49 ± 0.3	0 ± 0.2	Q1	$0.5 - 0.6\ M_\odot$	FDU
31	HR 7671	6985 ± 250	3579	-0.57 ± 0.13	0.51 ± 0.16	0.46 ± 0.05	Q1	$0.5 - 0.6\ M_\odot$	FDU

THE LOW LUMINOSITY SAMPLE: POST-HB STARS

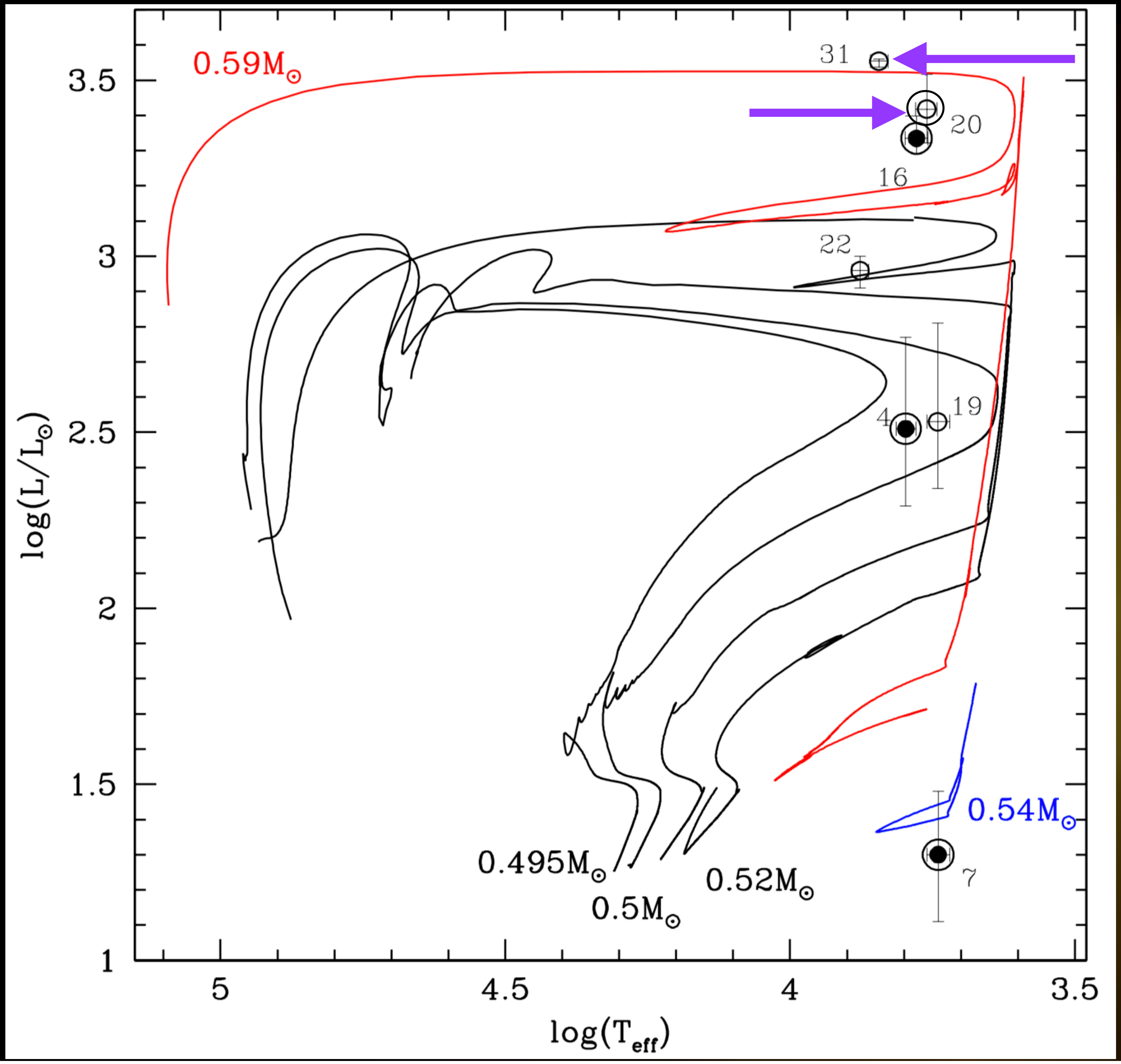

- ⋆ AGB Manque stars
- ⋆ An extremely Short AGB phase
- ⋆ A core helium burning star
- ⋆ *s*-process and carbon enrichment in faint stars

Index	Object	T_{eff}	$L/L_\odot$	[C/Fe]	[N/Fe]	[O/Fe]	Flag	M_{init}	chemistry
4	IRAS 05341+0852	6274 ± 250	324	1.03 ± 0.10	...	0.75 ± 0.11	Q2	$0.5 - 0.6\ M_\odot$	FLASH
7	IRAS 07430+1115	5519 ± 250	20	0.79 ± 0.13	...	0.30 ± 0.22	Q2	$0.5 - 0.6\ M_\odot$	FLASH
16	IRAS 22223+4327	6008 ± 250	2163	0.59 ± 0.06	0.15 ± 0.30	0.31 ± 0.06	Q2	$0.5 - 0.6\ M_\odot$	FLASH
19	IRAS 01259+6823	5510 ± 250	340	0.18 ± 0.15	...	0.31 ± 0.06	Q1	$0.5 - 0.6\ M_\odot$	FDU
20	IRAS 08187-1905	5772 ± 250	2619	0.62 ± 0.15	0.49 ± 0.3	0.26 ± 0.1	Q2	$0.5 - 0.6\ M_\odot$	FLASH
22	HD 107369	7533 ± 250	910	< -0.2	0.49 ± 0.3	0 ± 0.2	Q1	$0.5 - 0.6\ M_\odot$	FDU
31	HR 7671	6985 ± 250	3579	-0.57 ± 0.13	0.51 ± 0.16	0.46 ± 0.05	Q1	$0.5 - 0.6\ M_\odot$	FDU

THE LOW LUMINOSITY SAMPLE: POST-HB STARS

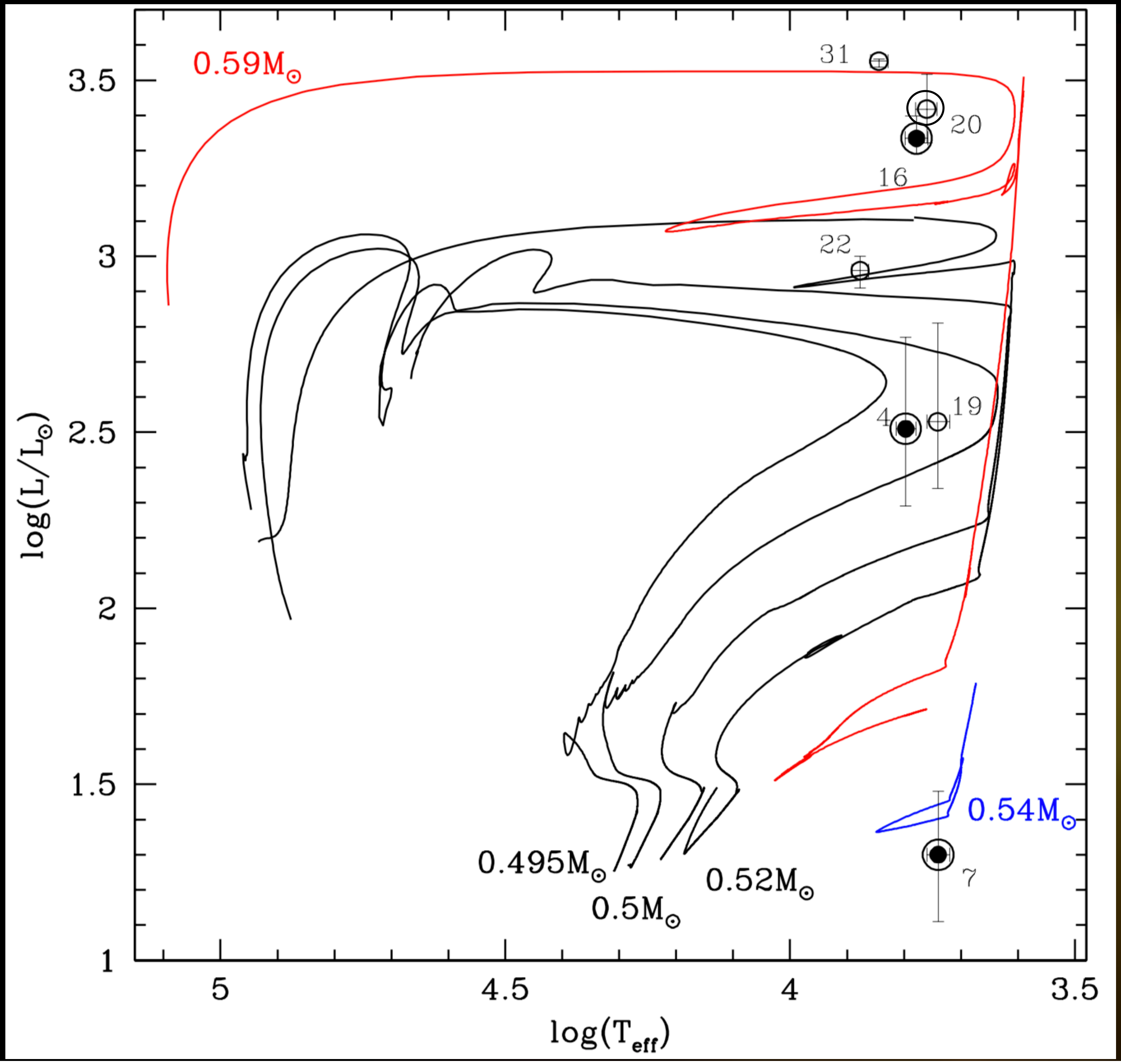

- AGB Manque stars
- An extremely Short AGB phase
- A core helium burning star
- *s*-process and carbon enrichment in faint stars

Index	Object	T_{eff}	$L/L_\odot$	[C/Fe]	[N/Fe]	[O/Fe]	Flag	M_{init}	chemistry
4	IRAS 05341+0852	6274 ± 250	324	1.03 ± 0.10	...	0.75 ± 0.11	Q2	$0.5 - 0.6\ M_\odot$	FLASH
7	IRAS 07430+1115	5519 ± 250	20	0.79 ± 0.13	...	0.30 ± 0.22	Q2	$0.5 - 0.6\ M_\odot$	FLASH
16	IRAS 22223+4327	6008 ± 250	2163	0.59 ± 0.06	0.15 ± 0.30	0.31 ± 0.06	Q2	$0.5 - 0.6\ M_\odot$	FLASH
19	IRAS 01259+6823	5510 ± 250	340	0.18 ± 0.15	...	0.31 ± 0.06	Q1	$0.5 - 0.6\ M_\odot$	FDU
20	IRAS 08187-1905	5772 ± 250	2619	0.62 ± 0.15	0.49 ± 0.3	0.26 ± 0.1	Q2	$0.5 - 0.6\ M_\odot$	FLASH
22	HD 107369	7533 ± 250	910	< -0.2	0.49 ± 0.3	0 ± 0.2	Q1	$0.5 - 0.6\ M_\odot$	FDU
31	HR 7671	6985 ± 250	3579	-0.57 ± 0.13	0.51 ± 0.16	0.46 ± 0.05	Q1	$0.5 - 0.6\ M_\odot$	FDU

THE LOW LUMINOSITY SAMPLE: POST-HB STARS

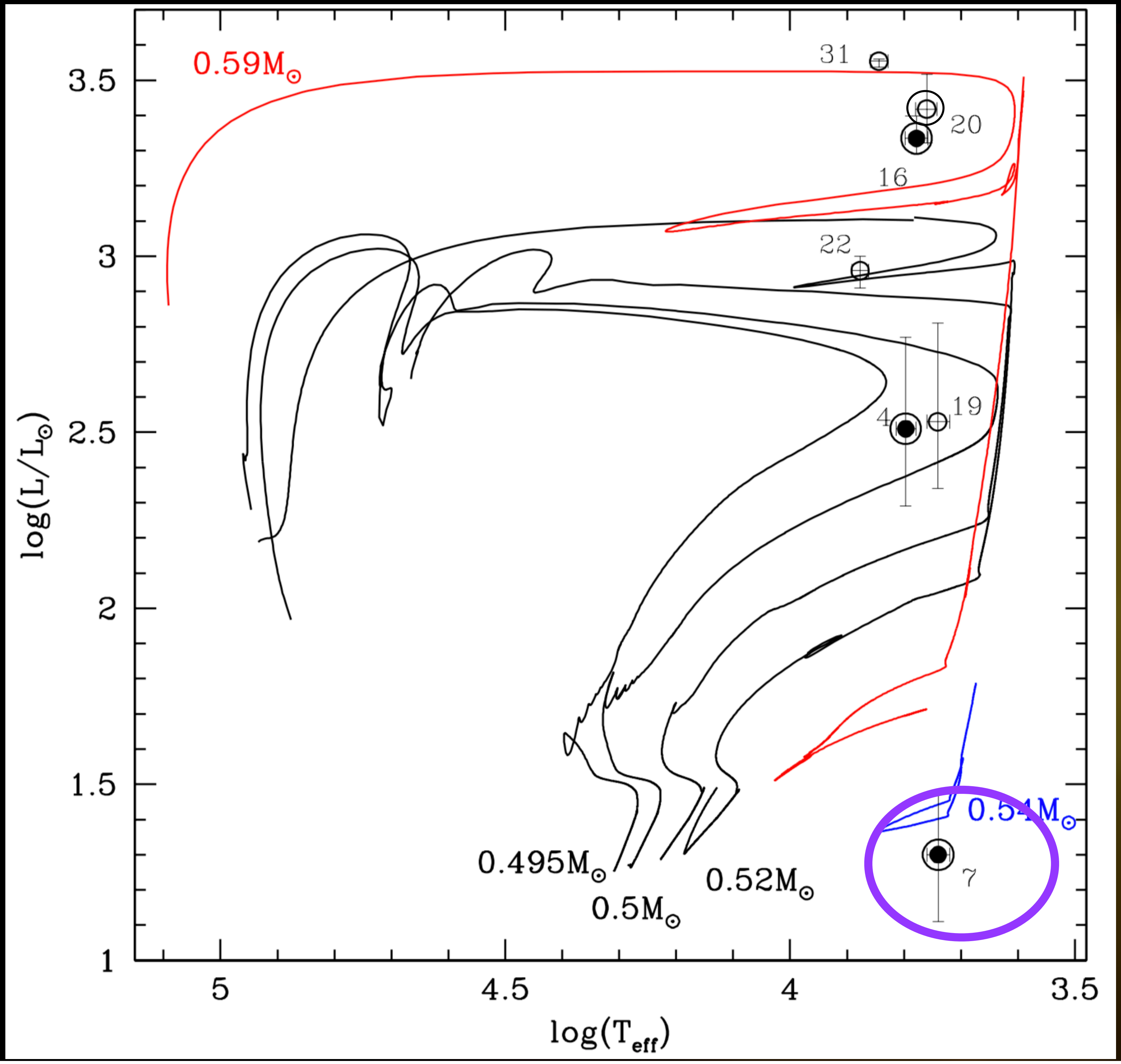

- AGB Manque stars
- An extremely Short AGB phase
- A core helium burning star
- *s*-process and carbon enrichment in faint stars

Index	Object	T_{eff}	$L/L_\odot$	[C/Fe]	[N/Fe]	[O/Fe]	Flag	M_{init}	chemistry
4	IRAS 05341+0852	6274 ± 250	324	1.03 ± 0.10	...	0.75 ± 0.11	Q2	$0.5 - 0.6\ M_\odot$	FLASH
7	IRAS 07430+1115	5519 ± 250	20	0.79 ± 0.13	...	0.30 ± 0.22	Q2	$0.5 - 0.6\ M_\odot$	FLASH
16	IRAS 22223+4327	6008 ± 250	2163	0.59 ± 0.06	0.15 ± 0.30	0.31 ± 0.06	Q2	$0.5 - 0.6\ M_\odot$	FLASH
19	IRAS 01259+6823	5510 ± 250	340	0.18 ± 0.15	...	0.31 ± 0.06	Q1	$0.5 - 0.6\ M_\odot$	FDU
20	IRAS 08187-1905	5772 ± 250	2619	0.62 ± 0.15	0.49 ± 0.3	0.26 ± 0.1	Q2	$0.5 - 0.6\ M_\odot$	FLASH
22	HD 107369	7533 ± 250	910	< -0.2	0.49 ± 0.3	0 ± 0.2	Q1	$0.5 - 0.6\ M_\odot$	FDU
31	HR 7671	6985 ± 250	3579	-0.57 ± 0.13	0.51 ± 0.16	0.46 ± 0.05	Q1	$0.5 - 0.6\ M_\odot$	FDU

The Low Luminosity Sample: Post-HB Stars

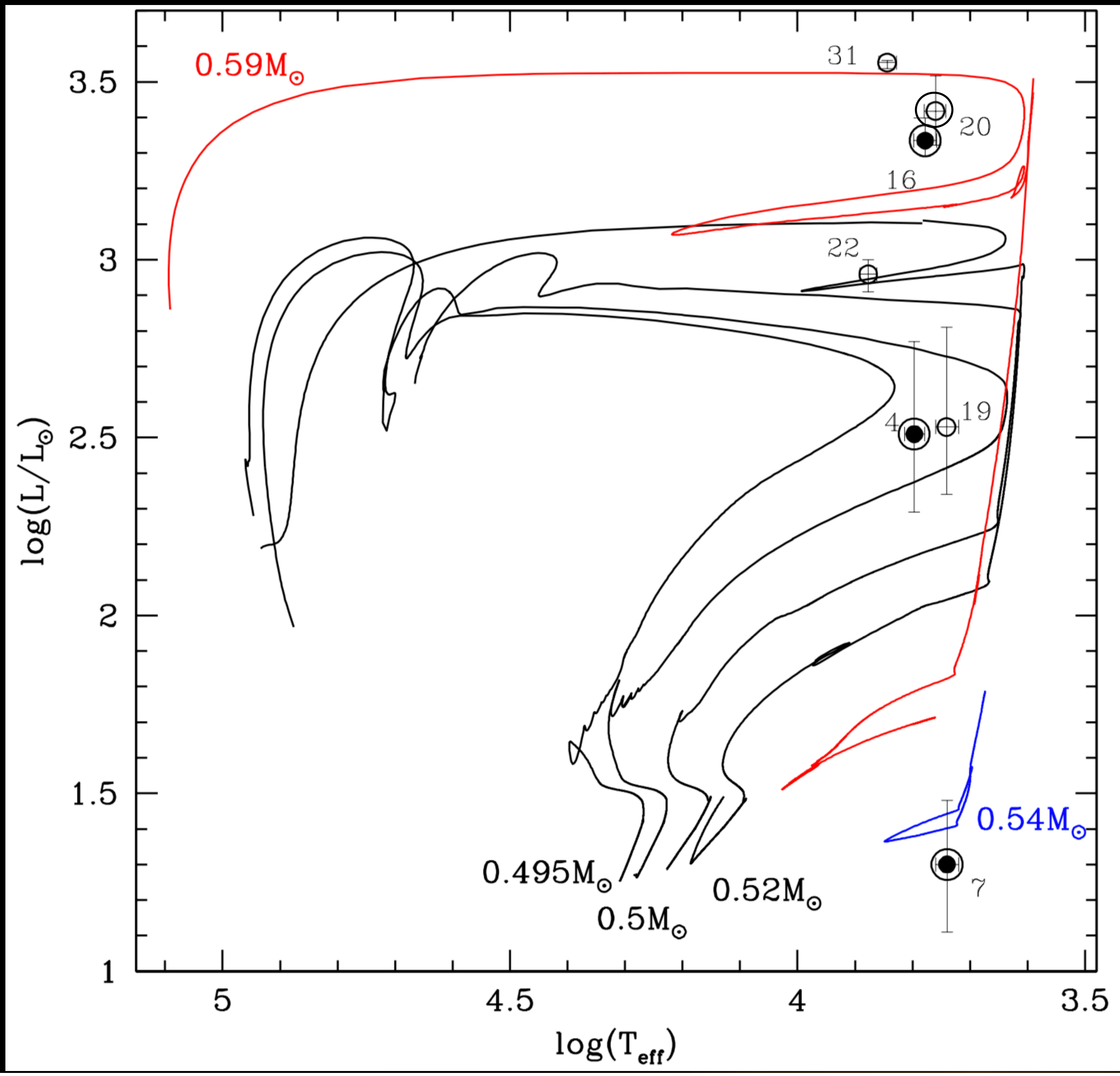

- AGB Manque stars
- An extremely Short AGB phase
- A core helium burning star
- *s*-process and carbon enrichment in faint stars

Index	Object	T_{eff}	$L/L_\odot$	[C/Fe]	[N/Fe]	[O/Fe]	Flag	M_{init}	chemistry
4	IRAS 05341+0852	6274 ± 250	324	1.03 ± 0.10	...	0.75 ± 0.11	Q2	$0.5 - 0.6$ $M_\odot$	FLASH
7	IRAS 07430+1115	5519 ± 250	20	0.79 ± 0.13	...	0.30 ± 0.22	Q2	$0.5 - 0.6$ $M_\odot$	FLASH
16	IRAS 22223+4327	6008 ± 250	2163	0.59 ± 0.06	0.15 ± 0.30	0.31 ± 0.06	Q2	$0.5 - 0.6$ $M_\odot$	FLASH
19	IRAS 01259+6823	5510 ± 250	340	0.18 ± 0.15	...	0.31 ± 0.06	Q1	$0.5 - 0.6$ $M_\odot$	FDU
20	IRAS 08187-1905	5772 ± 250	2619	0.62 ± 0.15	0.49 ± 0.3	0.26 ± 0.1	Q2	$0.5 - 0.6$ $M_\odot$	FLASH
22	HD 107369	7533 ± 250	910	< -0.2	0.49 ± 0.3	0 ± 0.2	Q1	$0.5 - 0.6$ $M_\odot$	FDU
31	HR 7671	6985 ± 250	3579	-0.57 ± 0.13	0.51 ± 0.16	0.46 ± 0.05	Q1	$0.5 - 0.6$ $M_\odot$	FDU

THE LOW LUMINOSITY SAMPLE: POST-HB STARS

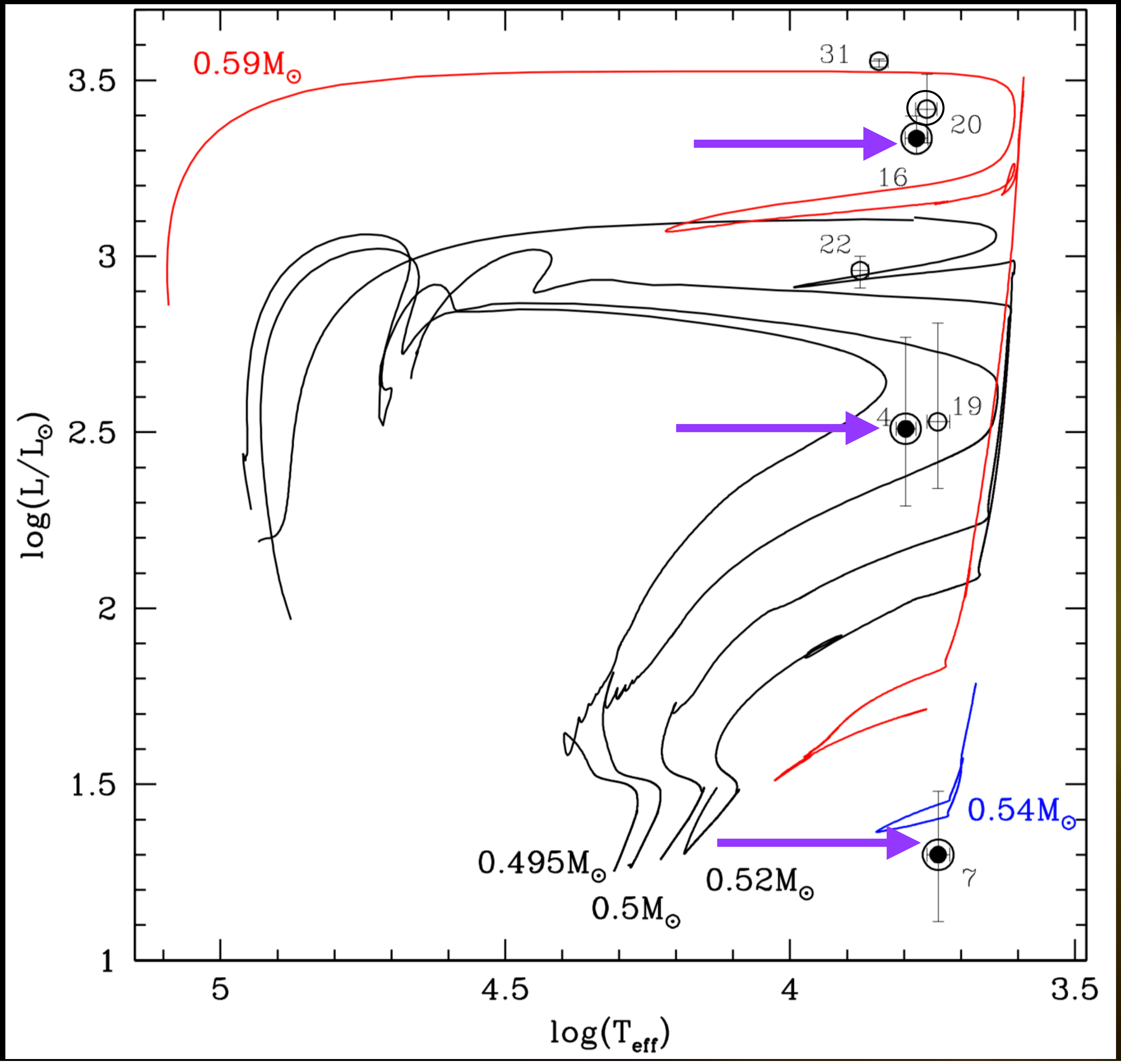

- AGB Manque stars
- An extremely Short AGB phase
- A core helium burning star
- *s*-process and carbon enrichment in faint stars

Index	Object	T_{eff}	$L/L_\odot$	[C/Fe]	[N/Fe]	[O/Fe]	Flag	M_{init}	chemistry
4	IRAS 05341+0852	6274 ± 250	324	1.03 ± 0.10	...	0.75 ± 0.11	Q2	$0.5 - 0.6\ M_\odot$	FLASH
7	IRAS 07430+1115	5519 ± 250	20	0.79 ± 0.13	...	0.30 ± 0.22	Q2	$0.5 - 0.6\ M_\odot$	FLASH
16	IRAS 22223+4327	6008 ± 250	2163	0.59 ± 0.06	0.15 ± 0.30	0.31 ± 0.06	Q2	$0.5 - 0.6\ M_\odot$	FLASH
19	IRAS 01259+6823	5510 ± 250	340	0.18 ± 0.15	...	0.31 ± 0.06	Q1	$0.5 - 0.6\ M_\odot$	FDU
20	IRAS 08187-1905	5772 ± 250	2619	0.62 ± 0.15	0.49 ± 0.3	0.26 ± 0.1	Q2	$0.5 - 0.6\ M_\odot$	FLASH
22	HD 107369	7533 ± 250	910	< -0.2	0.49 ± 0.3	0 ± 0.2	Q1	$0.5 - 0.6\ M_\odot$	FDU
31	HR 7671	6985 ± 250	3579	-0.57 ± 0.13	0.51 ± 0.16	0.46 ± 0.05	Q1	$0.5 - 0.6\ M_\odot$	FDU

THE LOW LUMINOSITY SAMPLE: POST-HB STARS

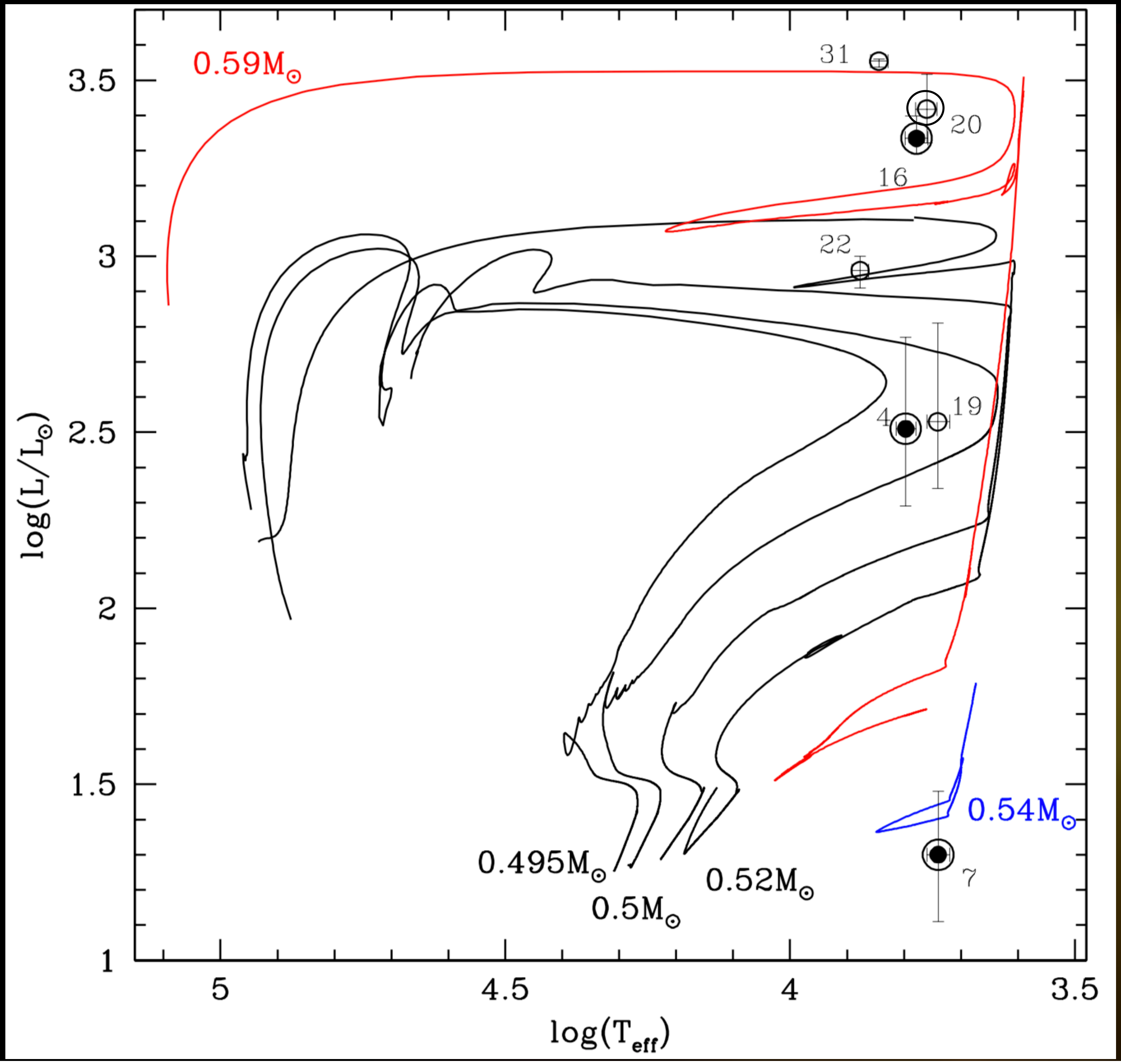

- ⋆ AGB Manque stars
- ⋆ An extremely Short AGB phase
- ⋆ A core helium burning star
- ⋆ *s*-process and carbon enrichment in faint stars

Index	Object	T_{eff}	$L/L_\odot$	[C/Fe]	[N/Fe]	[O/Fe]	Flag	M_{init}	chemistry
4	IRAS 05341+0852	6274 ± 250	324	1.03 ± 0.10	...	0.75 ± 0.11	Q2	$0.5 - 0.6\ M_\odot$	FLASH
7	IRAS 07430+1115	5519 ± 250	20	0.79 ± 0.13	...	0.30 ± 0.22	Q2	$0.5 - 0.6\ M_\odot$	FLASH
16	IRAS 22223+4327	6008 ± 250	2163	0.59 ± 0.06	0.15 ± 0.30	0.31 ± 0.06	Q2	$0.5 - 0.6\ M_\odot$	FLASH
19	IRAS 01259+6823	5510 ± 250	340	0.18 ± 0.15	...	0.31 ± 0.06	Q1	$0.5 - 0.6\ M_\odot$	FDU
20	IRAS 08187-1905	5772 ± 250	2619	0.62 ± 0.15	0.49 ± 0.3	0.26 ± 0.1	Q2	$0.5 - 0.6\ M_\odot$	FLASH
22	HD 107369	7533 ± 250	910	< -0.2	0.49 ± 0.3	0 ± 0.2	Q1	$0.5 - 0.6\ M_\odot$	FDU
31	HR 7671	6985 ± 250	3579	-0.57 ± 0.13	0.51 ± 0.16	0.46 ± 0.05	Q1	$0.5 - 0.6\ M_\odot$	FDU

THE POST-AGB PHASE FOR UNDERSTANDING AGB NUCLEOSYNTHESIS

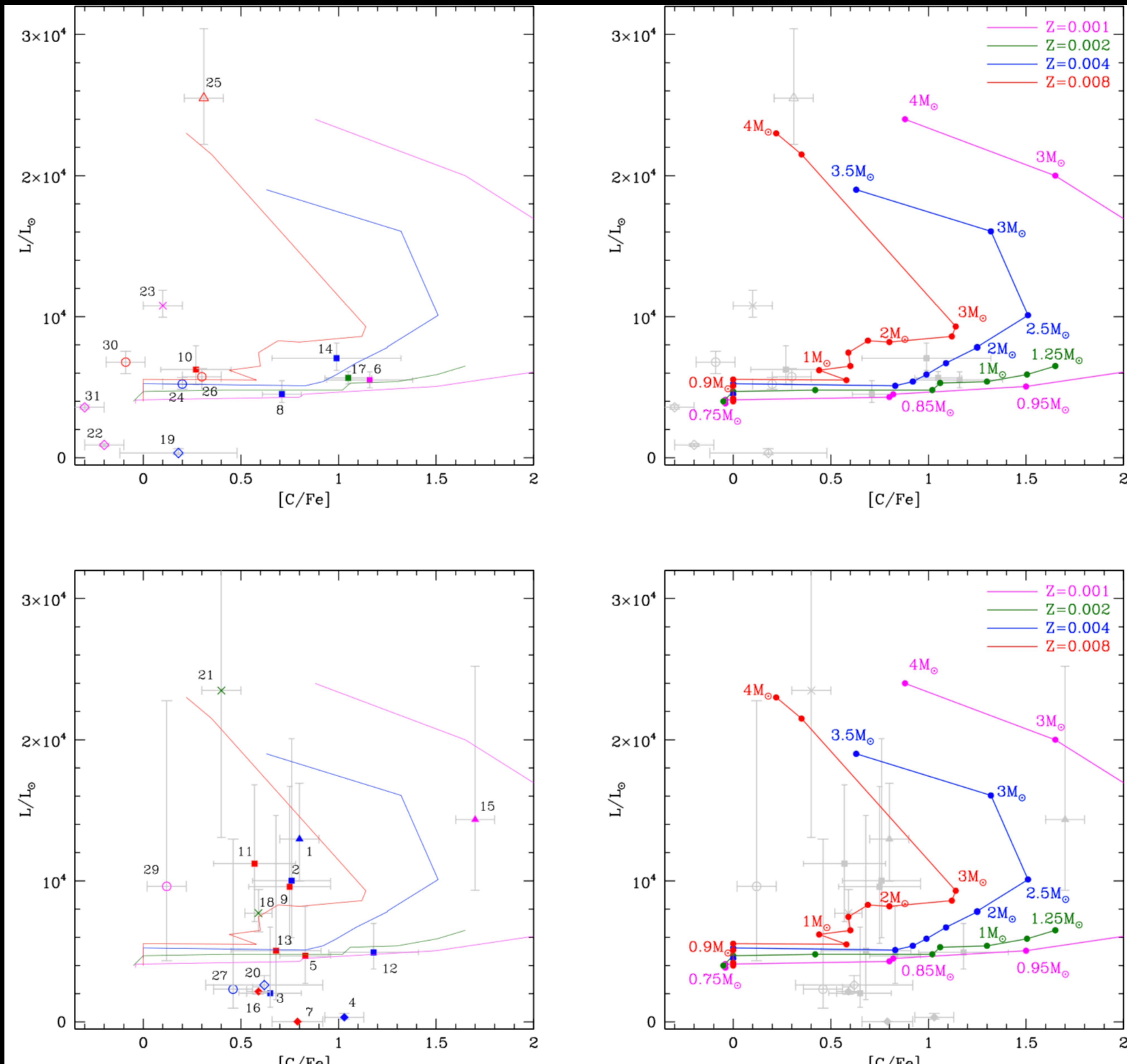

Kamath et al., 2022b, to-be-submitted

CONCLUSIONS

- **Post-AGB stars are exquisite tools** to reconstruct the evolution of the stars through the post-MS phases
- **~ 40%** of the single post-AGB stars in the sample **descend from 1 – 3 M⊙ progenitors**
- **5 sources are the progeny of low-mass stars,** that started the AGB phase with mass below ~ 1 M⊙
- **The three brightest stars,** whose surface chemical composition shows up the signature of proton-capture processing, are identified as the youngest stars in the sample, **descending from 3 – 4 M⊙ progenitors** that experienced both third dredge-up and hot bottom burning
- **A few low luminosity sources are tentatively identified as the progeny of low-mass (~ 0.5–0.7 M⊙),** post core helium burning stars, which after a short expansion phase lost the entire envelope and failed to reach the AGB
- **Surface carbon + luminosity** -> best indicator of the past history and nature of their progenitors

Current and Future Work

- Systematic surveys to identify low- and intermediate-mass stars in the Galaxy, LMC, SMC
- Exploring individual oxygen abundances as tracers of mixing, 12C+alpha reaction rate, overshooting…
- *s*-process nucleosynthesis, with a focus on Pb
- Isotopic abundance studies (PhD thesis of Maksym Mohorian)
- s-process in Post-AGBs and links to Ba stars and CEMPs (PhD thesis of Meghna Menon)
- Post-AGB stars as tracers of dust production and mass loss (PhD thesis of Silvia Tosi)
- AGB and post-AGB stars in star clusters (PhD thesis of Abhinna Sundar)

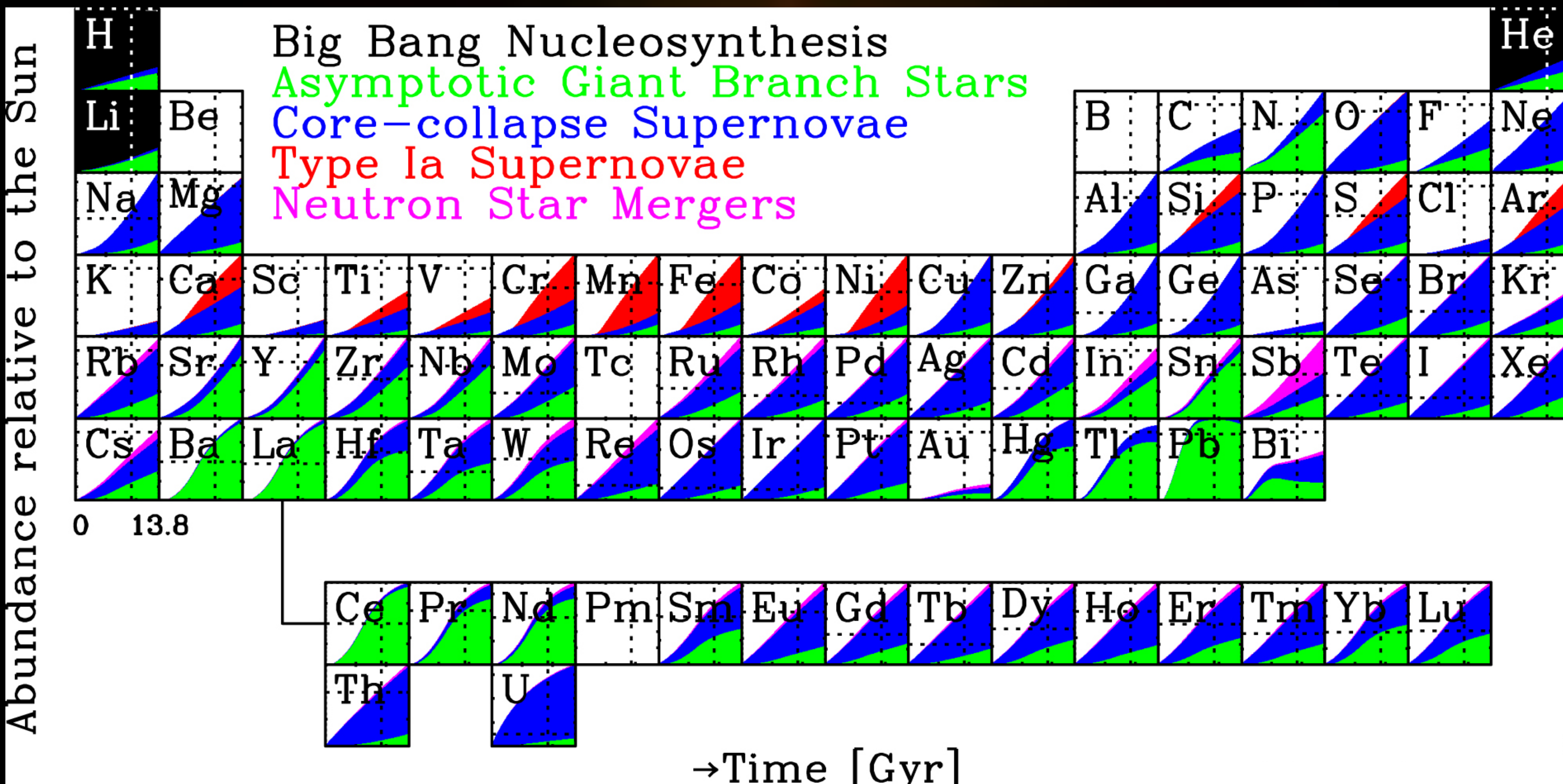

Kobayashi et al., 2020

AGB Nucleosynthesis

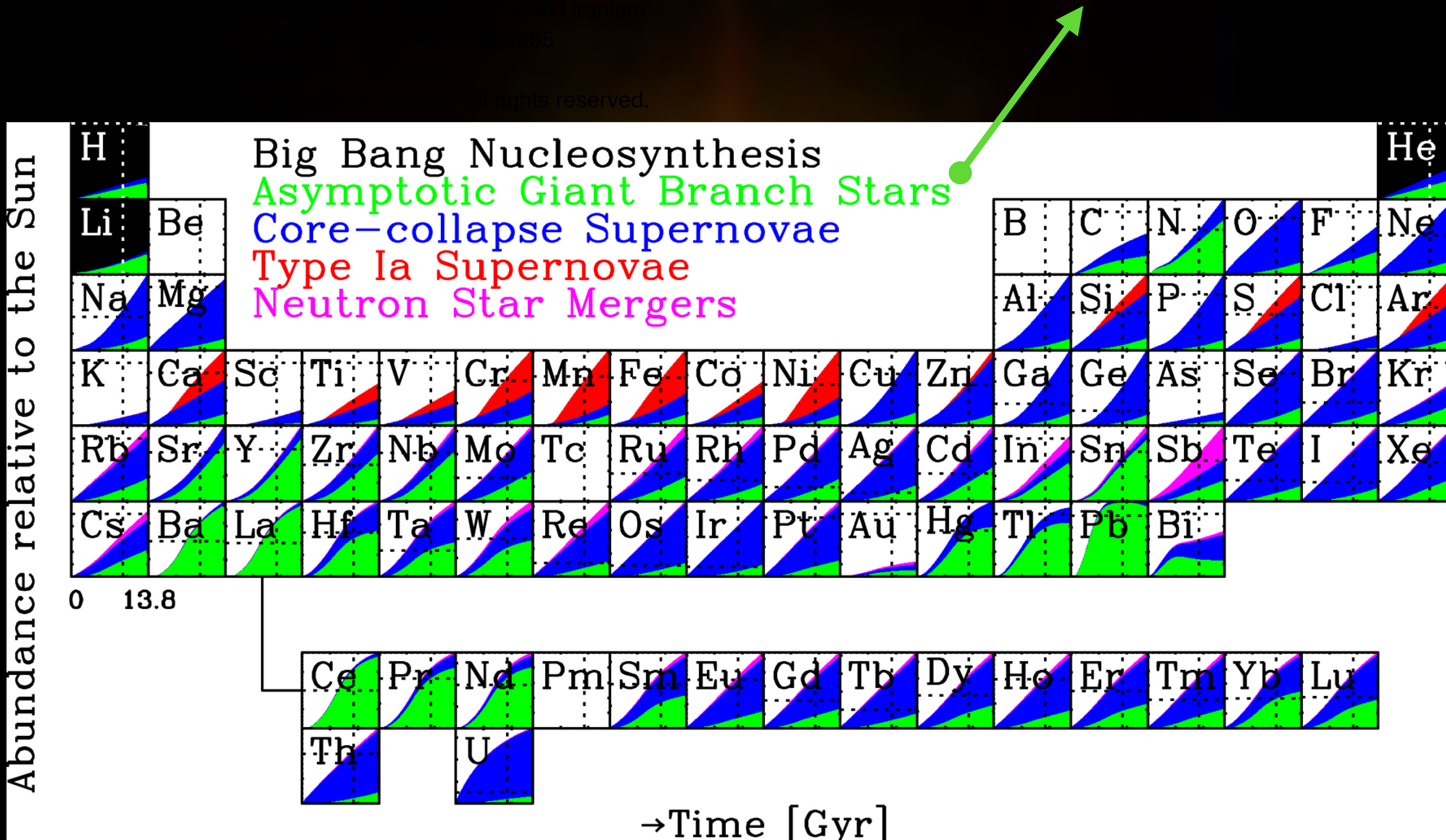

Kobayashi et al., 2020

AGB Nucleosynthesis

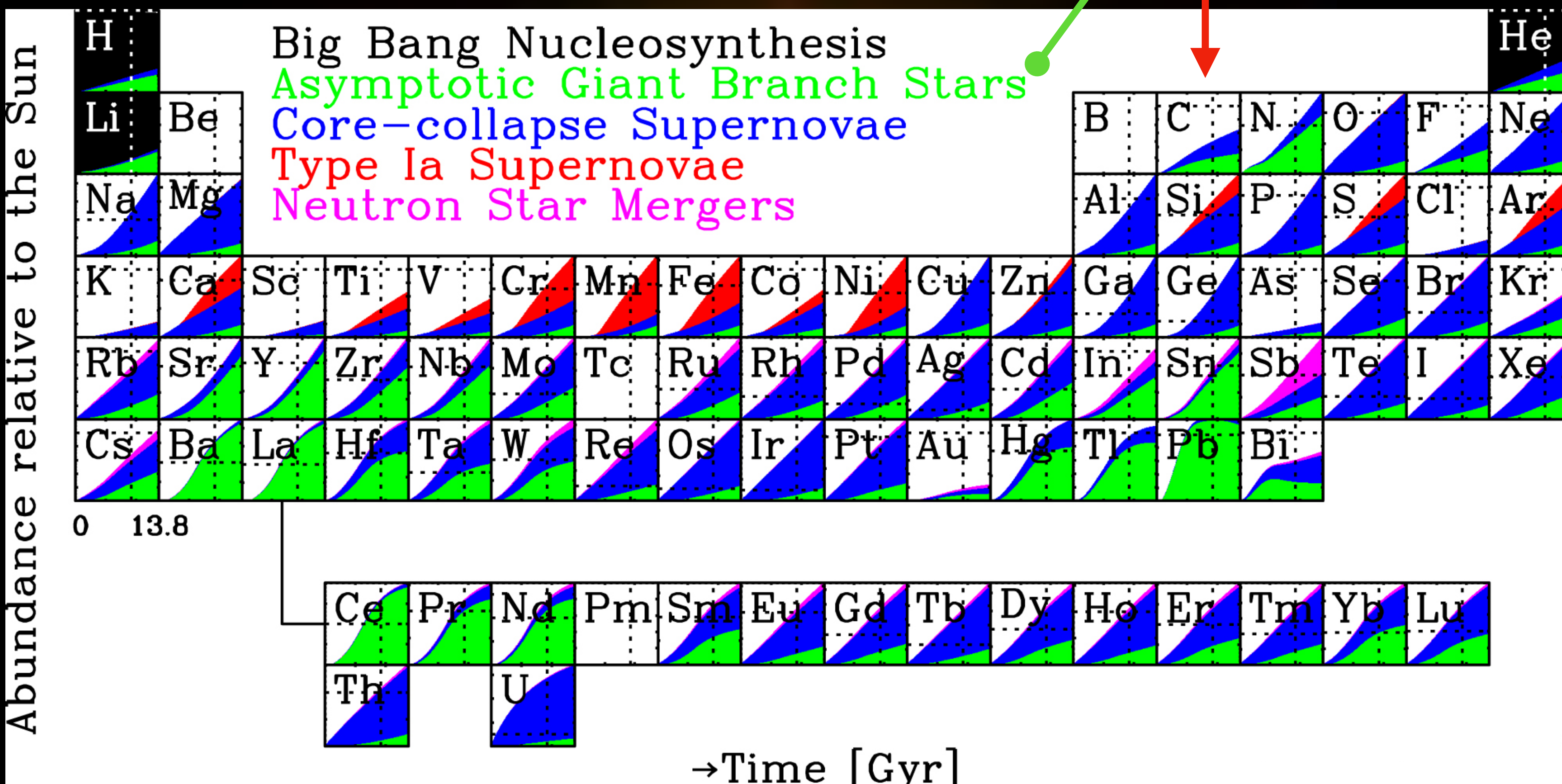

Kobayashi et al., 2020

AGB Nucleosynthesis

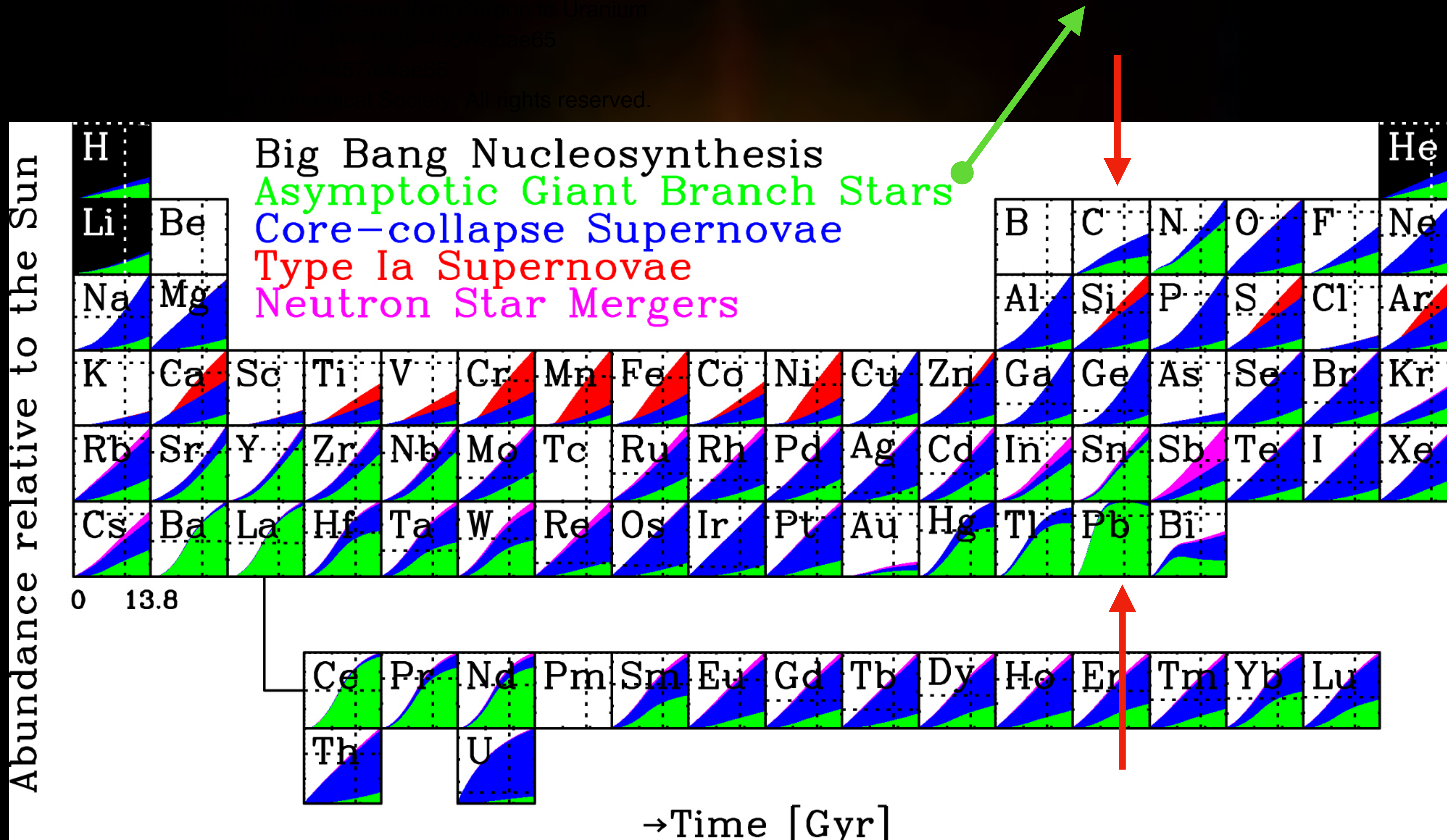

Kobayashi et al., 2020

ORIGINS: CNO, IRON-PEAK, *s*-PROCESS ELEMENTS

Present-day solar photospheric logarithmic abundances

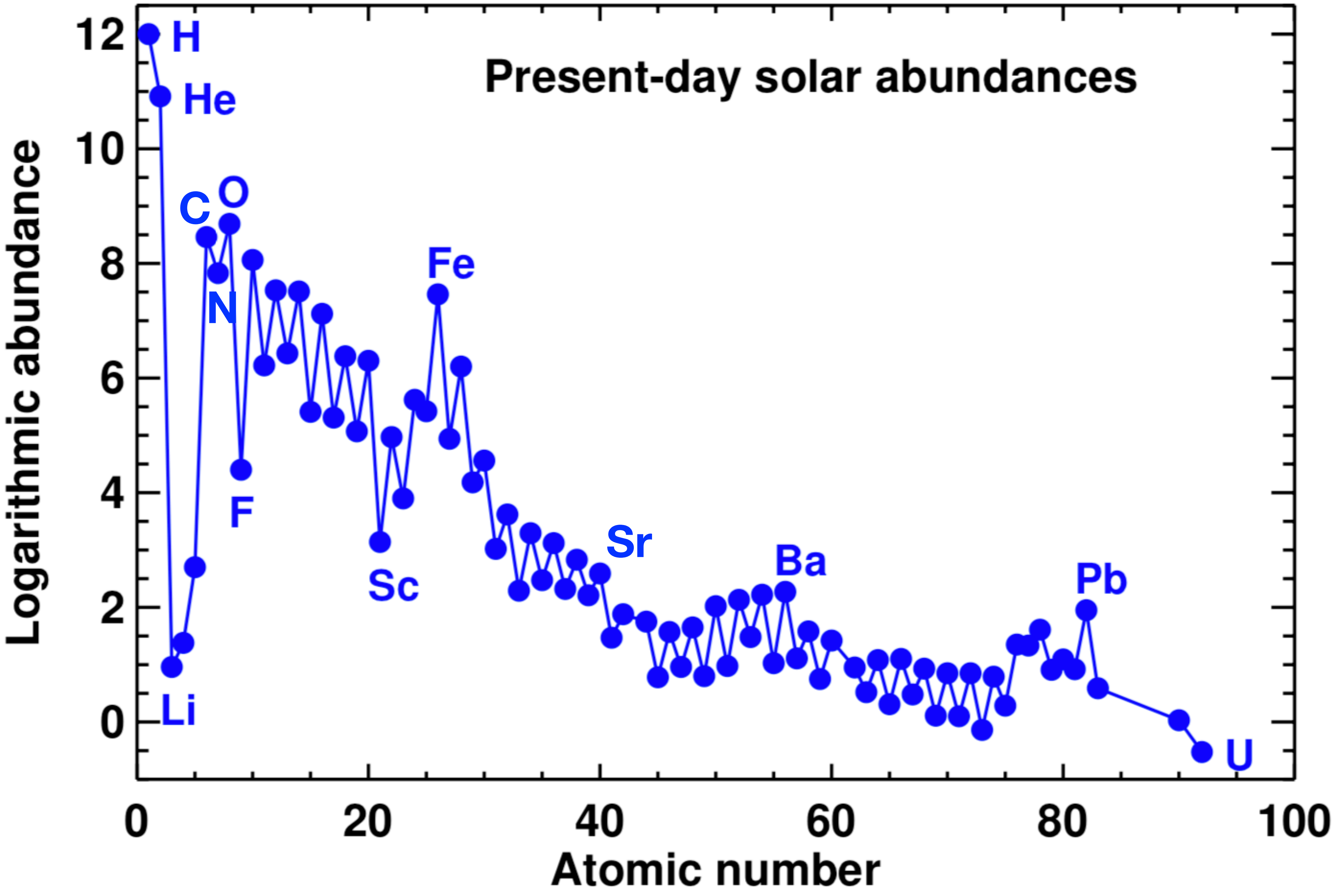

Asplund et al., 2021

Weak component from Fe to Sr

$\tau \approx 0.06$ mbarn−1

Massive stars

ORIGINS: CNO, IRON-PEAK, *s*-PROCESS ELEMENTS

Present-day solar photospheric logarithmic abundances

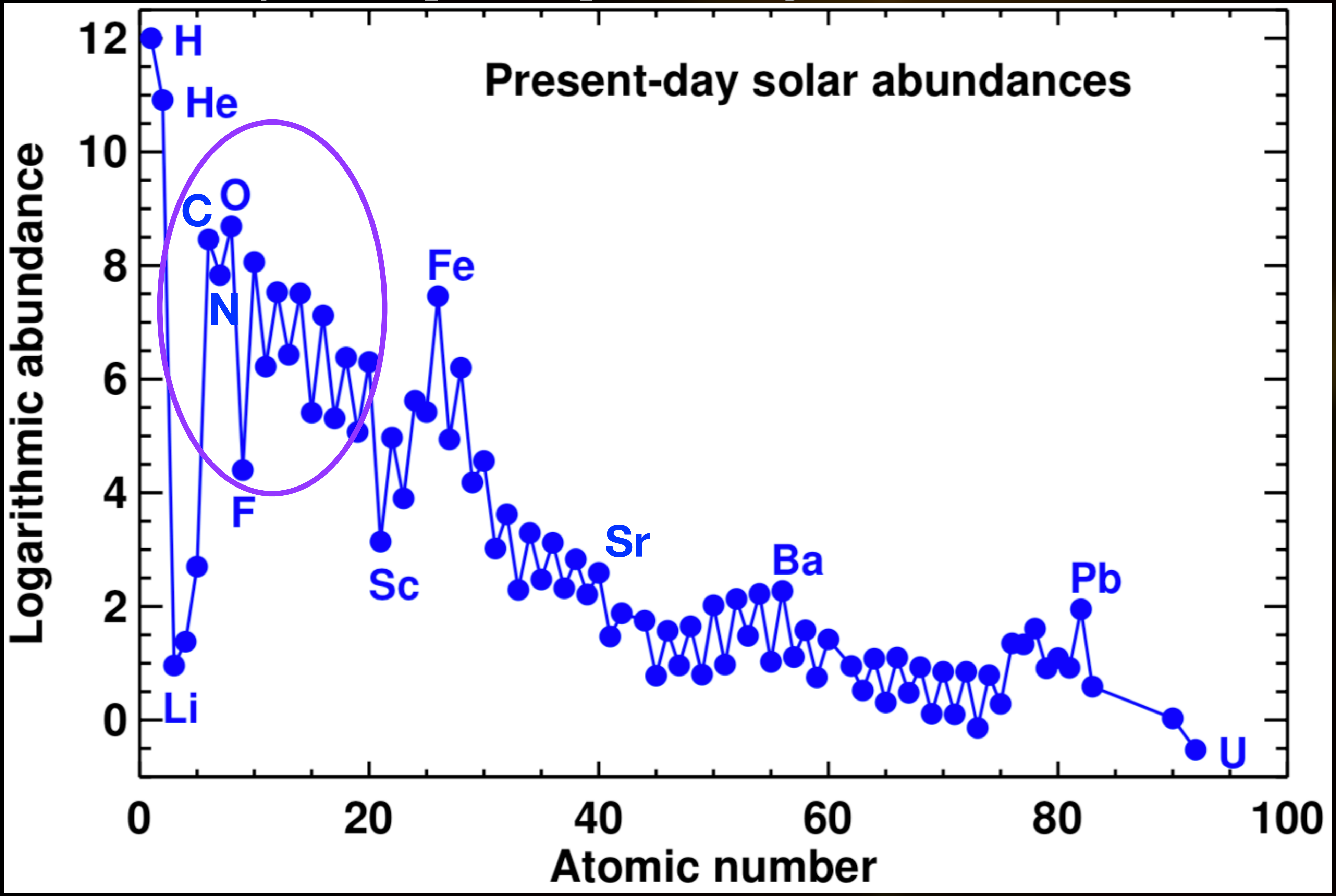

Weak component

from Fe to Sr

$\tau \approx 0.06$ mbarn−1

Massive stars

Asplund et al., 2021

ORIGINS: CNO, IRON-PEAK, *s*-PROCESS ELEMENTS

Present-day solar photospheric logarithmic abundances

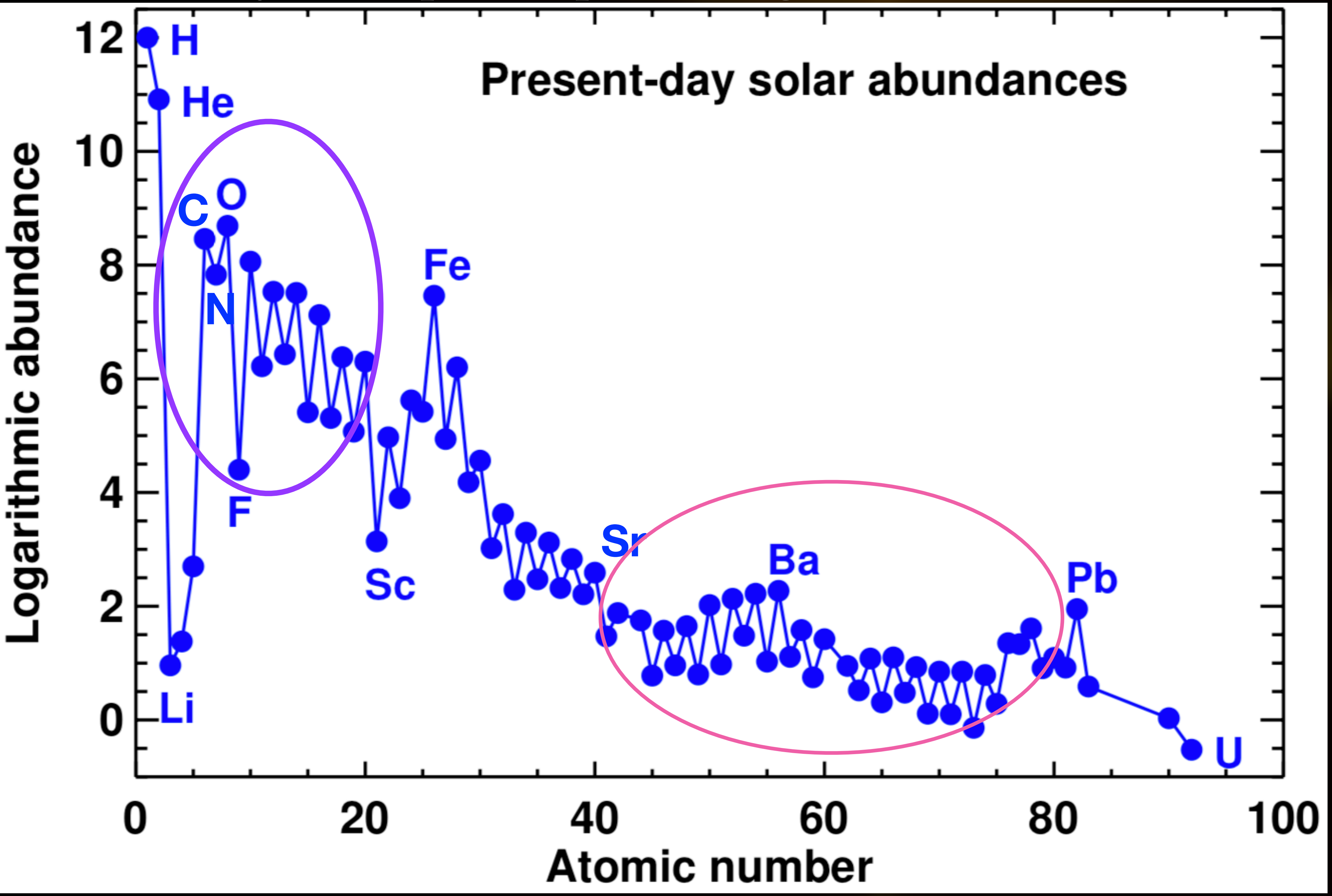

Asplund et al., 2021

Weak component

from Fe to Sr

τ ≈ 0.06 mbarn−1

Massive stars

Main component

from Sr to Pb

τ ≈ 0.3 mbarn−1

Low-mass AGBs

ORIGINS: CNO, IRON-PEAK, *s*-PROCESS ELEMENTS

Present-day solar photospheric logarithmic abundances

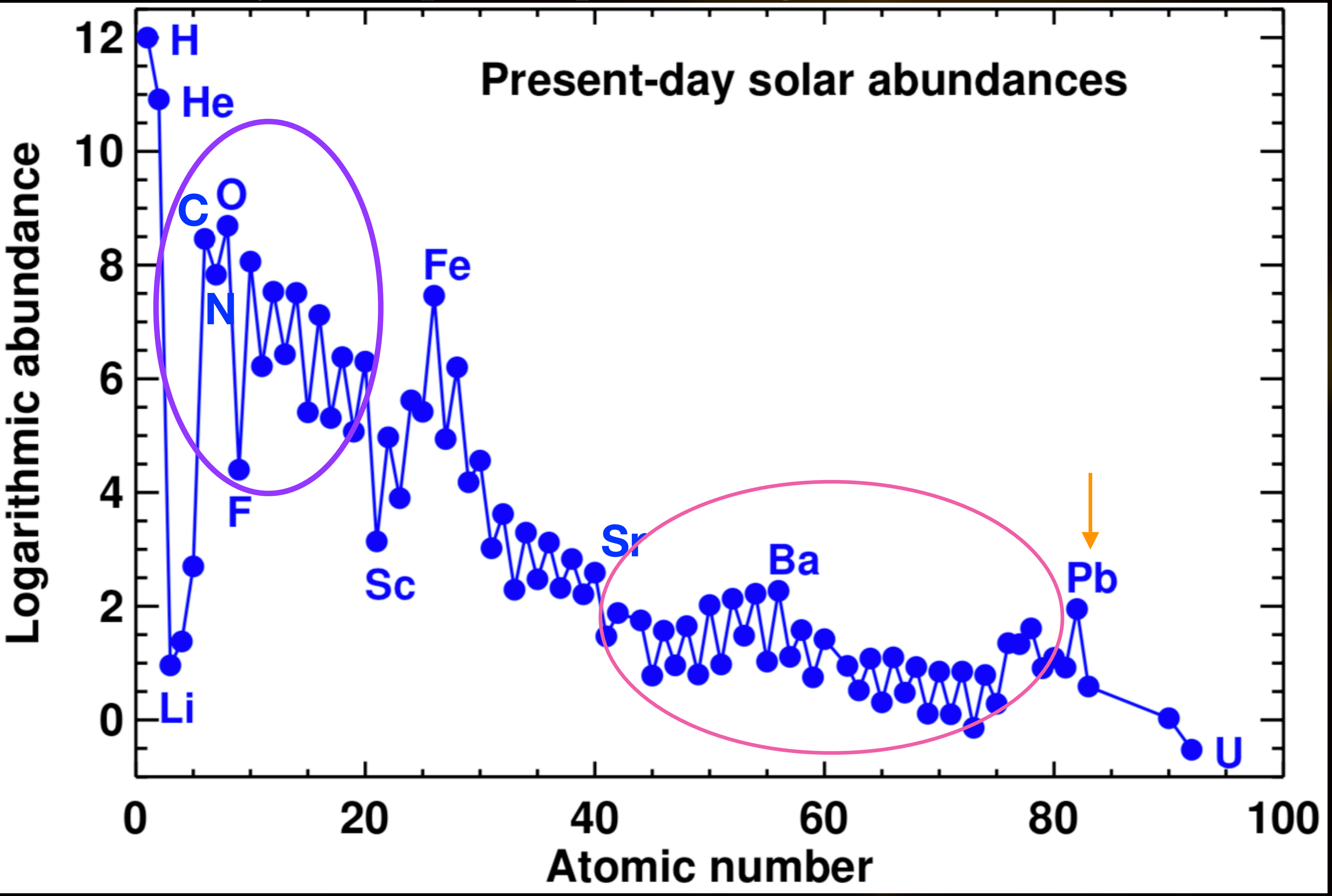

Asplund et al., 2021

Weak component

from Fe to Sr

τ ≈ 0.06 mbarn−1

Massive stars

Main component

from Sr to Pb

τ ≈ 0.3 mbarn−1

Low-mass AGBs

Strong component

Pb

τ ≈ 7.0 mbarn−1

Low-mass, Low-metallicity AGBs

AGB Nucleosynthesis - Observational Constraints

Over a wide range of initial masses and metallicities!

- **Third Dredge-Up:**
  ^{4}He; ^{12}C; ^{14}N; ^{16}O; ^{19}F; ^{22}Ne; $^{25,26}Mg$
  $^{12,13}C$; $^{14,15}N$; $^{16,17,18}O$

- **Hot Bottom Burning:**
  ^{7}Li; ^{13}C; ^{14}N; $^{25,26}Mg$; $^{26,27}Al$
  $^{12,13}C$; $^{14,15}N$; $^{16,17,18}O$, $^{24,25,26}Mgl$ $^{28,29,30}Si$; $^{32,33,34}S$…

- **Neutron Capture Nucleosynthesis:**
  s-process elements (light-*s* elements, heavy-*s* elements, Pb)

Table 1
Fundamental Properties of the *s*-process-rich and Non-enriched Single Galactic Post-AGB Stars

Index	Object	Parallax (mas)	Error (mas)	RUWE	$z_{(1/\mathrm{parallax})}$ (pc)	z_{BJ} (pc)	z_{BJL} (pc)	z_{BJU} (pc)	T_{eff} (K)	log g (dex)	E($B-V$)	$L/L_{\odot}$	$L_{\mathrm{Lower}}/L_{\odot}$	$L_{\mathrm{Upper}}/L_{\odot}$	Flag
							Post-AGB stars with *s*-process enrichment								
1	IRAS Z02229+6208	0.38	0.06	2.5	2627.53	2352.18	2063.48	2687.03	5952 ± 250	0.00	$1.90^{+0.08}_{-0.42}$	12959	9973	16911	Q2
2	IRAS 04296+3429	−0.38	0.17	5.8	−2635.11	5048.41	3899.38	7150.92	7272 ± 250	0.73	$2.03^{+0.06}_{-0.19}$	10009	5971	20082	Q2
3	IRAS 05113+1347	−0.01	0.15	6.7	−108371.7	4629.82	3312.65	8416.2	5025 ± 250	0.01	$0.75^{+0.35}_{-0.09}$	2037	1043	6731	Q2
4	IRAS 05341+0852	0.51	0.19	13.0	1960.07	2057.38	1603.89	2778.95	6274 ± 250	0.84	$1.18^{+0.19}_{-0.06}$	324	197	592	Q2
5	IRAS 06530−0213	0.24	0.07	3.7	4145.93	3777.67	2886.46	4990.04	7809 ± 250	1.70	$1.85^{+0.02}_{-0.18}$	4687	2736	8178	Q2
6	IRAS 07134+1005	0.45	0.02	0.9	2203.76	2099.09	1991.41	2209.25	7485 ± 250	0.50	$0.43^{+0.10}_{-0.22}$	5505	4955	6098	Q1
7	IRAS 07430+1115	3.06	0.5	21.8	327.04	360.93	299.59	442.65	5519 ± 250	1.43	$1.04^{+0.38}_{-0.12}$	20	14	30	Q2
8	IRAS 08143−4406	0.24	0.02	1.4	4198.54	4154.69	3877.12	4568.46	7013 ± 250	1.31	$1.53^{+0.95}_{-0.95}$	4509	3927	5452	Q1
9	IRAS 08281−4850	−0.14	0.07	6.0	−7300.68	11452.58	8728.27	15113.73	7462 ± 250	1.04	$1.23^{+0.11}_{-0.04}$	9584	5567	16692	Q2
10	IRAS 12360−5740	0.09	0.01	1.1	10970.73	9082.07	8261.41	10230.48	7273 ± 250	1.59	$1.01^{+0.35}_{-0.35}$	6258	5178	7940	Q1
11	IRAS 13245−5036	0.01	0.02	1.6	85919.8	14207.28	11305.73	17383.96	9037 ± 250	3.20	$0.64^{+0.14}_{-0.09}$	11221	7106	16800	Q2
12	IRAS 14325−6428	0.19	0.04	2.2	5220.46	4883.39	4261.63	5811.07	7256 ± 250	1.00	$1.07^{+0.22}_{-0.17}$	4935	3758	6988	Q2
13	IRAS 14429−4539	−0.11	0.51	2.8	−9372.15	3847.71	2160.1	6548.2	9579 ± 250	2.48	$2.63^{+0.36}_{-0.51}$	5049	1591	14624	Q2
14	IRAS 19500−1709	0.4	0.03	1.0	2504.9	2310.24	2164.96	2481.49	8239 ± 250	1.08	$0.56^{+0.03}_{-0.07}$	7053	6194	8138	Q1
15	IRAS 20000+3239	0.2	0.05	2.2	4880.07	4581.29	3695.53	6075.01	5478 ± 250	0.13	$1.76^{+0.09}_{-0.46}$	14342	9332	25218	Q2
16	IRAS 22223+4327	0.33	0.03	1.7	3007.27	2678.03	2546.9	2878.56	6008 ± 250	1.05	$0.43^{+0.28}_{-0.06}$	2163	1956	2499	Q2
17	IRAS 22272+5435	0.69	0.03	1.2	1457.75	1409.84	1355.87	1464.67	5325 ± 250	0.77	$0.88^{+0.34}_{-0.08}$	5659	5234	6108	Q1
18	IRAS 23304+6147	0.24	0.03	1.6	4226.42	3979.67	3620.05	4390.37	6276 ± 250	0.78	$1.83^{+0.17}_{-0.20}$	7712	6381	9386	Q2
							Post-AGB stars without *s*-process enrichment								
19	IRAS 01259+6823	0.62	0.14	1.3	1624.61	1781.38	1434.96	2456.33	5510 ± 250	2.50	$1.02^{+0.24}_{-0.07}$	340	220	646	Q1
20	IRAS 08187−1905	0.29	0.03	1.7	3473.16	3258.96	2917.24	3649.91	5772 ± 250	0.98	$0.07^{+0.31}_{-0.02}$	2619	2099	3286	Q2
21	SAO 239853	−0.01	0.07	3.7	−117255.41	8691.08	6485.52	12490.93	7452 ± 250	1.49	$0.30^{+0.08}_{-0.08}$	23490	13080	48520	Q2
22	HD 107369	0.37	0.02	1.1	2725.26	2568.38	2429.15	2705.92	7533 ± 250	2.45	$0.07^{+0.13}_{-0.05}$	910	814	1010	Q1
23	HD 112374	0.57	0.02	1.0	1763.78	1684.48	1619.4	1768.68	6393 ± 250	0.80	$0.30^{+0.10}_{-0.28}$	10777	9961	11882	Q1
24	HD 133656	0.56	0.03	0.9	1776.54	1707.63	1646.84	1781.63	8238 ± 250	1.38	$0.29^{+0.01}_{-0.08}$	5227	4861	5690	Q1
25	HR 6144	0.28	0.03	1.2	3561.19	3101.16	2894.87	3387.69	6728 ± 250	0.93	$0.11^{+0.15}_{-0.01}$	25491	22212	30419	Q1
26	HD 161796	0.5	0.02	1.2	1991.19	1920.96	1829.56	2015.66	6139 ± 250	0.99	$0.13^{+0.45}_{-0.13}$	5742	5209	6322	Q1
27	IRAS 18025−3906	0.54	0.19	8.6	1865.62	3046.67	1973.6	7194.98	6154 ± 250	1.18	$0.96^{+0.35}_{-0.17}$	2324	975	12963	Q2
28	HD 335675	0.03	0.18	13.7	30507.45	4888.53	3319.14	6540.55	6082 ± 250	1.58	$0.85^{+0.20}_{-0.04}$	15843	7303	28359	Q2
29	IRAS 19386+0155	0.32	0.16	11.6	3088.79	3631.35	2441.76	5588.81	6303 ± 250	1.00	$1.23^{+0.35}_{-0.14}$	9611	4345	22765	Q2
30	IRAS 19475+3119	0.32	0.02	1.4	3165.15	2971.43	2785.82	3135.57	8216 ± 250	1.01	$0.61^{+0.04}_{-0.16}$	6775	5955	7545	Q1
31	HR 7671	1.34	0.03	0.8	748.77	727.4	714.04	742.99	6985 ± 250	0.83	$0.40^{+0.11}_{-0.18}$	3579	3449	3734	Q1

Note. See Section 3 for more details.

Table 3
Chemical Abundances of the *s*-process Enriched and Non-*s*-process Enriched Single Galactic Post-AGB stars

Index	Object Name	[Fe/H]	[C/O]	[O/Fe]	[C/Fe]	[N/Fe]	[Zr/Fe]	[s/Fe]	[ls/Fe]	[hs/Fe]	[hs/ls]	Reference
Post-AGB stars with *s*-process enrichment												
1	IRAS Z02229+6208	-0.45 ± 0.14	…	…	0.78 ± 0.15	1.19 ± 0.30	2.22 ± 0.13	1.4 ± 0.15	2.03 ± 0.12	1.12 ± 0.03	-0.91 ± 0.12	1
2	IRAS 04296+3429	-0.62 ± 0.11	…	…	0.8 ± 0.2	0.39 ± 0.01	1.34 ± 0.23	1.5 ± 0.23	1.7 ± 0.23	1.5 ± 0.17	-0.2 ± 0.23	2
3	IRAS 05113+1347	-0.49 ± 0.15	2.42 ± 0.40	0.01 ± 0.27	0.65 ± 0.16	…	1.36 ± 0.15	1.54 ± 0.07	1.33 ± 0.13	1.65 ± 0.07	0.32 ± 0.15	3
4	IRAS 05341+0852	-0.54 ± 0.11	1.06 ± 0.30	0.75 ± 0.11	1.03 ± 0.10	…	1.76 ± 0.10	2.12 ± 0.05	1.87 ± 0.08	2.24 ± 0.06	0.37 ± 0.10	3
5	IRAS 06530–0213	-0.32 ± 0.11	1.66 ± 0.39	0.35 ± 0.11	0.83 ± 0.13	…	1.60 ± 0.10	1.94 ± 0.06	1.75 ± 0.09	2.04 ± 0.08	0.29 ± 0.13	3
6	IRAS 07134+1005	-0.91 ± 0.20	1.24 ± 0.29	0.81 ± 0.19	1.16 ± 0.22	0.57 ± 0.19	1.61 ± 0.09	1.63 ± 0.14	1.64 ± 0.13	1.63 ± 0.20	-0.01 ± 0.24	3
7	IRAS 07430+1115	-0.31 ± 0.15	1.71 ± 0.30	0.30 ± 0.22	0.79 ± 0.13	…	1.22 ± 0.15	1.47 ± 0.06	1.30 ± 0.14	1.55 ± 0.06	0.25 ± 0.15	3
8	IRAS 08143–4406	-0.43 ± 0.11	1.66 ± 0.39	0.19 ± 0.13	0.71 ± 0.10	0.01 ± 0.22	1.63 ± 0.11	1.65 ± 0.05	1.77 ± 0.08	1.58 ± 0.06	-0.19 ± 0.11	3
9	IRAS 08281–4850	-0.26 ± 0.11	2.34 ± 0.42	0.12 ± 0.11	0.75 ± 0.21	…	1.42 ± 0.11	1.58 ± 0.09	1.57 ± 0.11	1.58 ± 0.12	0.01 ± 0.17	3
10	IRAS 12360–5740	-0.40 ± 0.15	0.45 ± 0.20	0.31 ± 0.05	0.27 ± 0.18	0.22 ± 0.32	1.70 ± 0.17	1.88 ± 0.20	1.73 ± 0.20	2.02 ± 0.20	0.29 ± 0.20	4
11	IRAS 13245–5036	-0.30 ± 0.10	1.11 ± 0.30	0.26 ± 0.13	0.57 ± 0.21	…	1.72 ± 0.15	1.88 ± 0.09	1.56 ± 0.14	2.03 ± 0.11	0.47 ± 0.18	3
12	IRAS 14325–6428	-0.56 ± 0.10	2.27 ± 0.40	0.57 ± 0.09	1.18 ± 0.23	0.18 ± 0.20	1.16 ± 0.16	1.30 ± 0.14	1.25 ± 0.15	1.33 ± 0.19	0.08 ± 0.24	3
13	IRAS 14429–4539	-0.18 ± 0.11	1.29 ± 0.26	0.31 ± 0.12	0.68 ± 0.23	…	1.46 ± 0.17	1.41 ± 0.08	1.29 ± 0.15	1.47 ± 0.10	0.18 ± 0.08	3
14	IRAS 19500–1709	-0.59 ± 0.10	1.02 ± 0.17	0.72 ± 0.04	0.99 ± 0.06	0.41 ± 0.30	1.34 ± 0.10	1.35 ± 0.21	1.37 ± 0.29	1.34 ± 0.30	-0.03 ± 0.41	3
15	IRAS 20000+3239	-1.4 ± 0.2	…	…	1.7 ± 0.2	2.1 ± 0.2	1 ± 0.2	1.4 ± 0.2	1.1 ± 0.2	1.47 ± 0.10	0.34 ± 0.2	5
16	IRAS 22223+4327	-0.30 ± 0.11	1.04 ± 0.22	0.31 ± 0.06	0.59 ± 0.06	0.15 ± 0.30	1.35 ± 0.06	1.03 ± 0.05	1.34 ± 0.07	0.88 ± 0.07	-0.46 ± 0.10	3
17	IRAS 22272+5435	-0.77 ± 0.12	1.46 ± 0.26	0.63 ± 0.02	1.05 ± 0.07	…	1.54 ± 0.08	1.80 ± 0.05	1.61 ± 0.08	1.90 ± 0.07	0.28 ± 0.11	3
18	IRAS 23304+6147	-0.81 ± 0.2	2.8 ± 0.2	0.17 ± 0.03	0.91 ± 0.12	0.47 ± 0.15	1.26 ± 0.23	1.60 ± 0.25	1.55 ± 0.23	1.63 ± 0.21	0.09 ± 0.24	6
Post-AGB stars without *s*-process enrichment												
19	IRAS 01259+6823	-0.60 ± 0.1	0.4 ± 0.3	0.31 ± 0.06	0.18 ± 0.3	…	0.12 ± 0.1	0.3 ± 0.1	…	…	…	7
20	IRAS 08187–1905	-0.60 ± 0.1	…	0.26 ± 0.1	0.62 ± 0.3	0.49 ± 0.3	0.25 ± 0.1	…	…	…	…	7
21	SAO 239853	-0.81 ± 0.1	…	0.8 ± 0.2	0.4 ± 0.2	0.6 ± 0.2	…	-0.4 ± 0.2	…	…	…	8
22	HD 107369	-1.1 ± 0.1	…	0 ± 0.2	<-0.2	0.49 ± 0.3	…	-0.1 ± 0.2	…	…	…	8
23	HD 112374	-1.2 ± 0.1	…	0.8 ± 0.2	0.1 ± 0.2	0.5 ± 0.2	…	-0.3 ± 0.2	…	…	…	8
24	HD 133656	-0.7 ± 0.1	…	0.6 ± 0.2	0.3 ± 0.2	0.5 ± 0.2	…	-0.4 ± 0.2	…	…	…	8
25	HR 6144	-0.4 ± 0.1	…	0.3 ± 0.2	0.3 ± 0.2	0.9 ± 0.2	…	0.2 ± 0.2	…	…	…	8
26	HD 161796	-0.3 ± 0.1	…	0.4 ± 0.2	0.3 ± 0.2	1.1 ± 0.2	…	0 ± 0.2	…	…	…	8
27	IRAS 18025-3906	-0.51 ± 0.15	0.43	0.56 ± 0.2	0.46 ± 0.2	0.74 ± 0.2	-0.84 ± 0.04	…	…	…	…	9
28	HD 335675	-0.9 ± 0.2	0.25	0.77–0.19	0.4–0.35	<0.27	-0.36 ± 0.1	…	…	…	…	10
29	IRAS 19386+0155	-1.1 ± 0.14	…	…	0.1 ± 0.2	…	…	-0.3 ± 0.2	…	…	…	11
30	IRAS 19475+3119	-0.24 ± 0.15	0.19	0.30 ± 0.02	-0.09 ± 0.30	…	…	-0.30 ± 0.1	…	…	…	12
31	HR 7671	-1.6 ± 0.1	0.05	0.46 ± 0.05	-0.57 ± 0.13	0.51 ± 0.16	0.44 ± 0.15	…	…	…	…	13

Note. The index [s/Fe] is the mean of the relative abundances of the elements for the "ls" and "hs" indices. Typically, 'ls' refers to the light *s*-process elements, which in this case is represented by the relative abundances of Y and Zr, and 'hs' refers to the heavy s-process elements, which in this case is represented by the relative abundances of La, Ce, Nd, and Sm. [hs/ls] = [hs/Fe] − [ls/Fe]. More details on the derived abundances and abundance ratios can be found in the individual studies mentioned in column "Ref". The column "Ref." indicates the individual chemical abundance study: (1) Reddy et al. (1999), (2) Van Winckel & Reyniers (2000), (3) De Smedt et al. (2016), (4) Pereira et al. (2011), (5) Klochkova & Kipper (2006), (6) Reyneirs (2000), (7) Rao et al. (2012), (8) Van Winckel (1997), (9) Molina et al. (2019), (10) Şahin et al. (2011), (11) Pereira et al. (2004), (12) Arellano Ferro et al. (2001), (13) Reyniers & Cuypers (2005).

Index	Object	T_{eff}	$L/L_\odot$	[C/Fe]	[N/Fe]	[O/Fe]	Flag	M_{init}	chemistry
				s-process enriched stars					
1	IRAS Z02229+6208	5952 ± 250	12959	0.78 ± 0.15	1.19 ± 0.15	...	Q2	$3 - 3.5\ M_\odot$	TDU+HBB
2	IRAS 04296+3429	7252 ± 250	10009	0.8 ± 0.2	0.39 ± 0.2	...	Q2	$1 - 1.5\ M_\odot$	TDU
3	IRAS 05113+1347	5025 ± 250	2037	0.65 ± 0.16	...	0.01 ± 0.27	Q2	$1 - 1.3\ M_\odot$	TDU
4	IRAS 05341+0852	6274 ± 250	324	1.03 ± 0.10	...	0.75 ± 0.11	Q2	$0.5 - 0.6\ M_\odot$	FLASH
5	IRAS 06530-0213	7809 ± 250	4687	0.83 ± 0.13	...	0.35 ± 0.11	Q2	$1.5 - 2\ M_\odot$	TDU
6	IRAS 07134+1005	7485 ± 250	5505	1.16 ± 0.22	0.57 ± 0.19	0.81 ± 0.19	Q1	$0.9 - 1.2\ M_\odot$	TDU
7	IRAS 07430+1115	5519 ± 250	20	0.79 ± 0.13	...	0.30 ± 0.22	Q2	$0.5 - 0.6\ M_\odot$	FLASH
8	IRAS 08143-4406	7013 ± 250	4509	0.71 ± 0.10	0.01 ± 0.22	0.19 ± 0.13	Q1	$1 - 1.5\ M_\odot$	TDU
9	IRAS 08281-4850	7462 ± 250	9584	0.75 ± 0.21	...	0.12 ± 0.11	Q2	$1.5 - 2\ M_\odot$	TDU
10	IRAS 12360-5740	7273 ± 250	6258	0.27 ± 0.18	0.22 ± 0.32	0.31 ± 0.05	Q1	$1 - 1.5\ M_\odot$	TDU
11	IRAS 13245-5036	9037 ± 250	11221	0.57 ± 0.21	...	0.26 ± 0.13	Q2	$1.5 - 2\ M_\odot$	TDU
12	IRAS 14325-6428	7256 ± 250	4935	1.18 ± 0.23	0.18 ± 0.20	0.57 ± 0.09	Q2	$1.5 - 2\ M_\odot$	TDU
13	IRAS 14429-4539	9579 ± 250	5049	0.68 ± 0.23	...	0.31 ± 0.12	Q2	$1.5 - 2\ M_\odot$	TDU
14	IRAS 19500-1709	8239 ± 250	7053	0.99 ± 0.06	0.41 ± 0.30	0.72 ± 0.04	Q1	$1.5 - 2\ M_\odot$	TDU
15	IRAS 20000+3239	5478 ± 250	14342	1.7 ± 0.2	2.1 ± 0.2	...	Q2	$3 - 3.5\ M_\odot$	TDU+HBB
16	IRAS 22223+4327	6008 ± 250	2163	0.59 ± 0.06	0.15 ± 0.30	0.31 ± 0.06	Q2	$0.5 - 0.6\ M_\odot$	FLASH
17	IRAS 22272+5435	5325 ± 250	5659	1.05 ± 0.07	...	0.63 ± 0.02	Q1	$1 - 1.3\ M_\odot$	TDU
18	IRAS 23304+6147	6276 ± 250	7712	0.91 ± 0.47	0.15 ± 0.12	0.17 ± 0.03	Q2	$2 - 2.5\ M_\odot$	TDU
				non *s*-process enriched stars					
19	IRAS 01259+6823	5510 ± 250	340	0.18 ± 0.15	...	0.31 ± 0.06	Q1	$0.5 - 0.6\ M_\odot$	FDU
20	IRAS 08187-1905	5772 ± 250	2619	0.62 ± 0.15	0.49 ± 0.3	0.26 ± 0.1	Q2	$0.5 - 0.6\ M_\odot$	FLASH
21	SAO 239853	7452 ± 250	23490	0.4 ± 0.15	0.6 ± 0.2	0.8 ± 0.2	Q2	$\sim 3\ M_\odot$	TDU
22	HD 107369	7533 ± 250	910	< -0.2	0.49 ± 0.3	0 ± 0.2	Q1	$0.5 - 0.6\ M_\odot$	FDU
23	HD 112374	6393 ± 250	10777	0.1 ± 0.2	0.5 ± 0.2	0.8 ± 0.2	Q1	$2.5 - 3\ M_\odot$	TDU
24	HD 133656	8238 ± 250	5227	0.3 ± 0.2	0.5 ± 0.2	0.6 ± 0.2	Q1	$0.8 - 1\ M_\odot$	FDU
25	HR 6144	6728 ± 250	25491	0.3 ± 0.2	0.9 ± 0.2	0.3 ± 0.2	Q1	$4 - 5\ M_\odot$	HBB
26	HD 161796	6139 ± 250	5742	0.3 ± 0.2	1.1 ± 0.2	0.4 ± 0.2	Q1	$1 - 1.2\ M_\odot$	FDU
27	IRAS 18025-3906	6154 ± 250	2324	0.46 ± 0.2	0.74 ± 0.2	0.56 ± 0.2	Q2	$0.8 - 1\ M_\odot$	FDU, TDU
28	HD 335675	6082 ± 250	15843	0.4 ± 0.35	< 0.27	0.77 ± 0.19	Q2		
29	IRAS 19386+0155	6303 ± 250	9611	0.1 ± 0.2	...	...	Q2	$0.7 - 0.8\ M_\odot$	FDU
30	IRAS 19475+3119	8216 ± 250	6775	-0.09 ± 0.30	...	0.30 ± 0.02	Q1	$0.8 - 1\ M_\odot$	FDU
31	HR 7671	6985 ± 250	3579	-0.57 ± 0.13	0.51 ± 0.16	0.46 ± 0.05	Q1	$0.5 - 0.6\ M_\odot$	FDU

Post-AGB stars as tracers of the origin of elements and isotopes in the Universe

Luminosities and masses of single Galactic Post-Asymptotic Giant Branch (Post-AGB) stars with distances from *Gaia* EDR3: The revelation of an *s*-process diversity

Devika Kamath[1,2], Hans Van Winckel[3], Paolo Ventura[4], Maksym Mohorian[1,2], Bruce.J.Hrivnak[5], Flavia Dell'Agli[4] and Amanda Karakas[6,7]

[1] *Department of Physics and Astronomy, Macquarie University, Sydney, NSW, Australia*
[2] *Astronomy, Astrophysics and Astrophotonics Research Centre, Macquarie University, Sydney, NSW, Australia*
[3] *Instituut voor Sterrenkunde, K.U.Leuven, Celestijnenlaan 200D bus 2401, B-3001, Leuven, Belgium*
[4] *INAF, Observatory of Rome, Via Frascati 33, 00077 Monte Porzio Catone (RM), Italy*
[5] *Department of Physics and Astronomy, Valparaiso University, Valparaiso, IN 46383, USA*
[6] *School of Physics & Astronomy, Monash University, Clayton VIC 3800, Australia*
[7] *ARC Centre of Excellence for All Sky Astrophysics in 3 Dimensions (ASTRO 3D)*

New Post-AGB star models as tools to understand AGB evolution and nucleosynthesis.

D. Kamath[1⋆], F. Dell'Agli[2], P. Ventura[2], H. Van Winckel[3], S. Tosi[4] et al.
[1] *Department of Physics and Astronomy, Macquarie University, Sydney, NSW 2109, Australia*
[2] *INAF, Osservatorio Astronomico di Roma, Via Frascati 33, 00077, Monte Porzio Catone, Italy*
[4] *Dipartimento di Matematica e Fisica, Universitá degli Studi Roma Tre, via della Vasca Navale 84, 00100, Roma, Italy*

COMPLEXITIES IN SINGLE STAR AGB NUCLEOSYNTHESIS

- Under-abundance of lead (Pb)
  De Smedt et al., 2014, 2015; Kamath et al., 2021
  ***s*-process nucleosynthesis**

LEAD (Pb): A TRACER OF S-PROCESS AND I-PROCESS IN AGB STARS

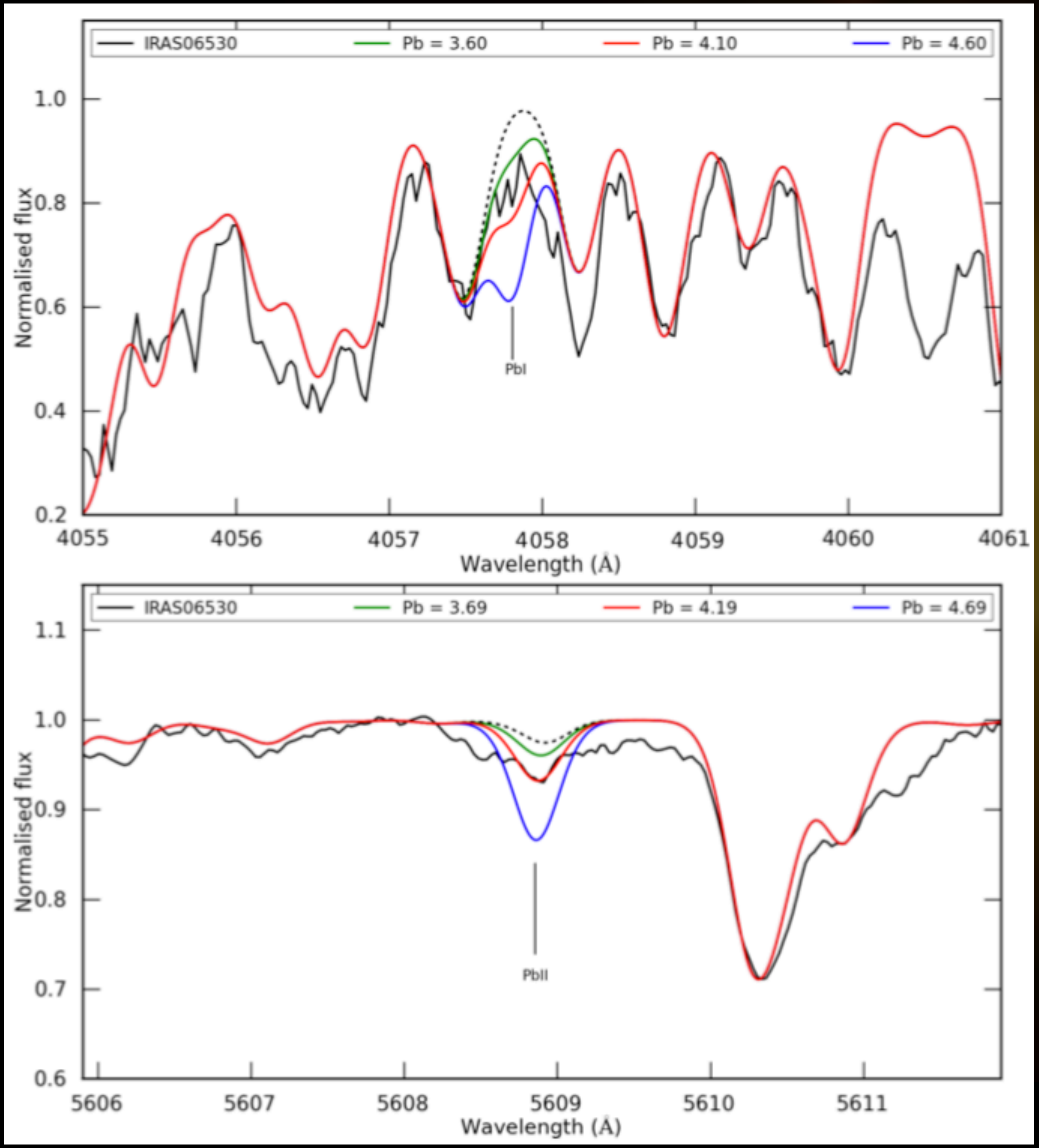

Strong component

Pb

τ ≈ 7.0 mbarn−1

Low-mass, Low-metallicity AGBs

Lead (Pb): A tracer of s-process and i-process in AGB stars

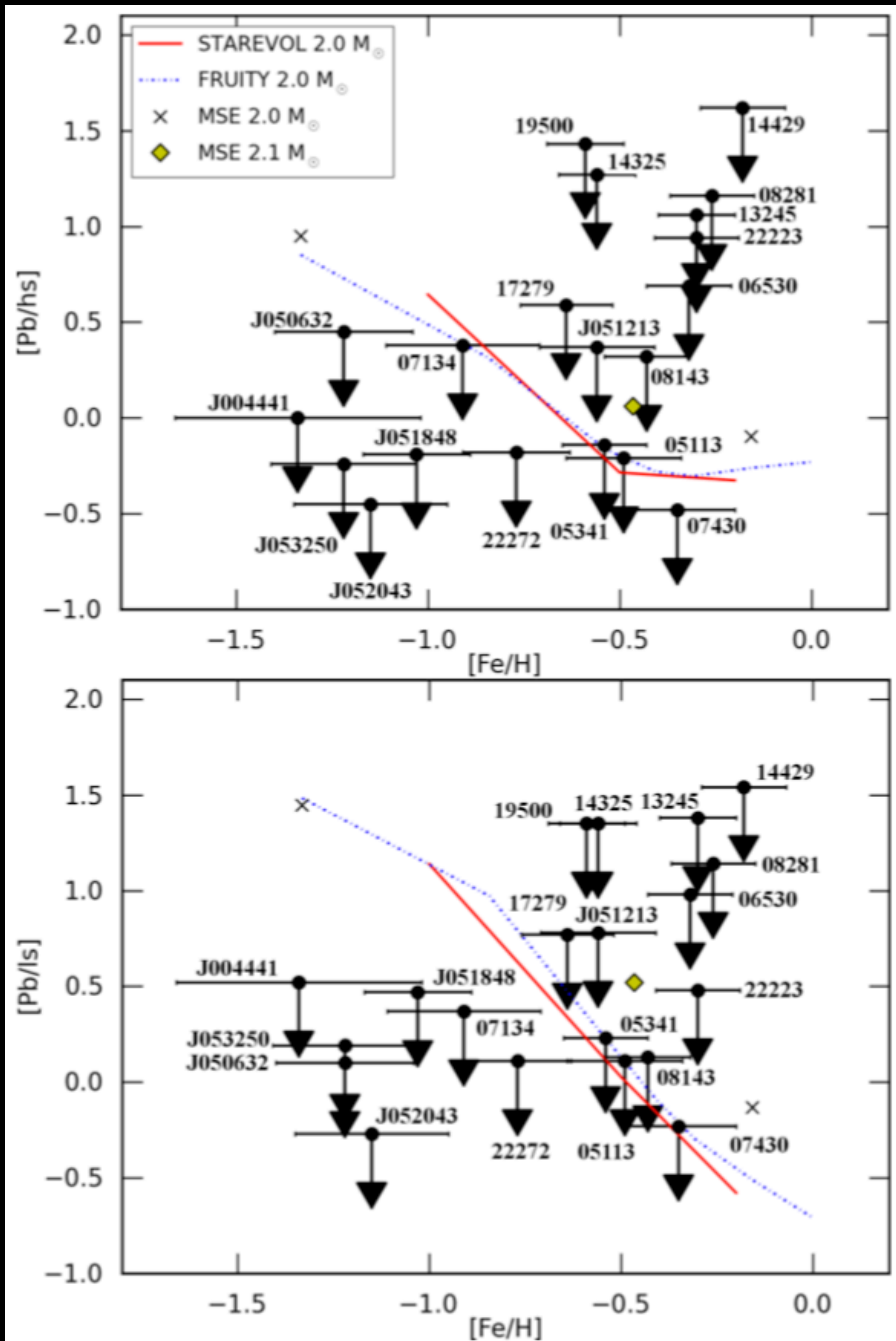

De Smedt et al., 2016

Kamath & Van Winckel 2021

LEAD (PB): A TRACER OF S-PROCESS AND I-PROCESS IN AGB STARS

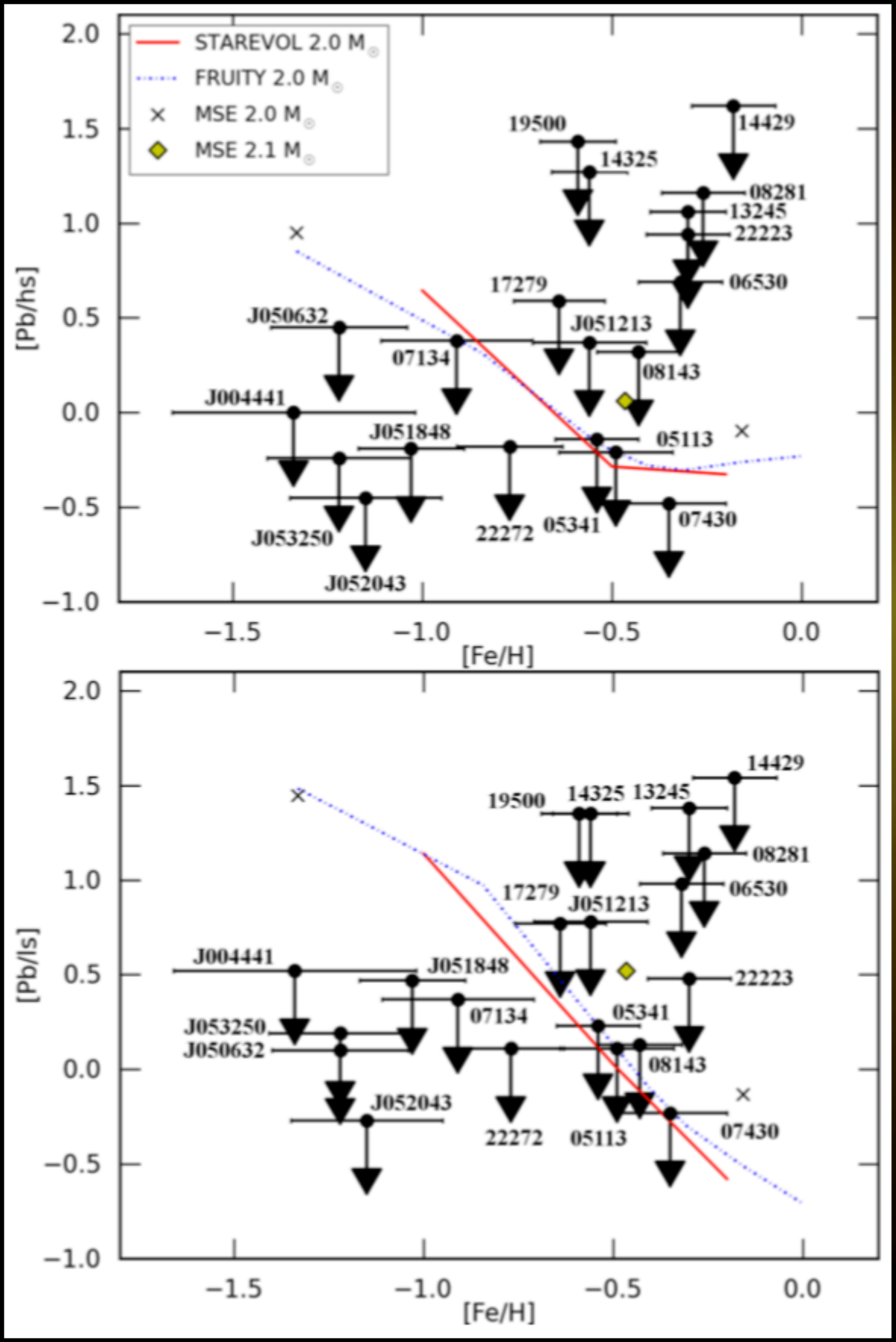

De Smedt et al., 2016

Discrepancy between the observed and predicted Pb over-abundances in single, low-metallicity ([Fe/H]<– 0.7 dex) post-AGBs

Kamath & Van Winckel 2021

Lead (Pb): A tracer of s-process and i-process in AGB stars

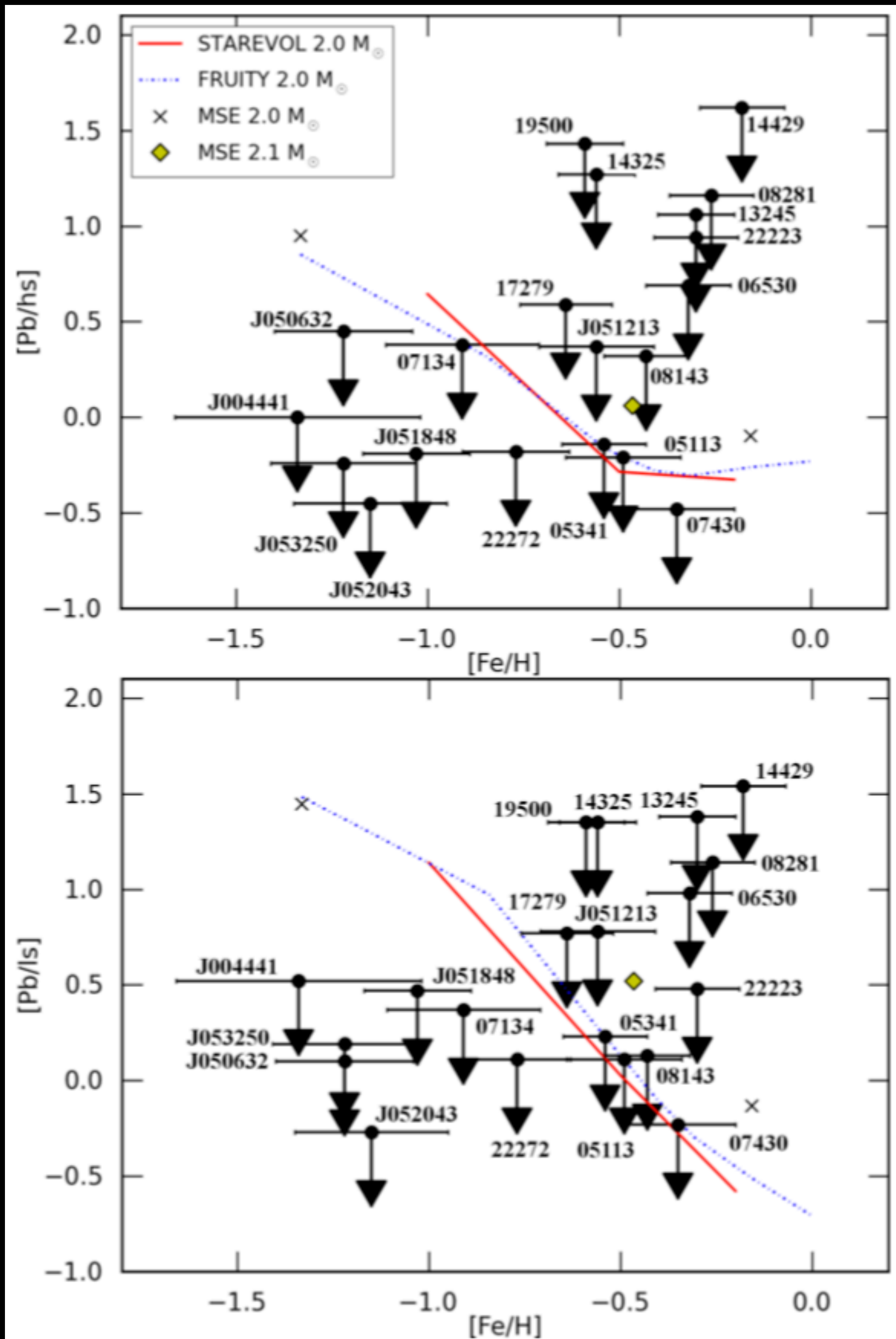

De Smedt et al., 2016

Discrepancy between the observed and predicted Pb over-abundances in single, low-metallicity ([Fe/H]<– 0.7 dex) post-AGBs

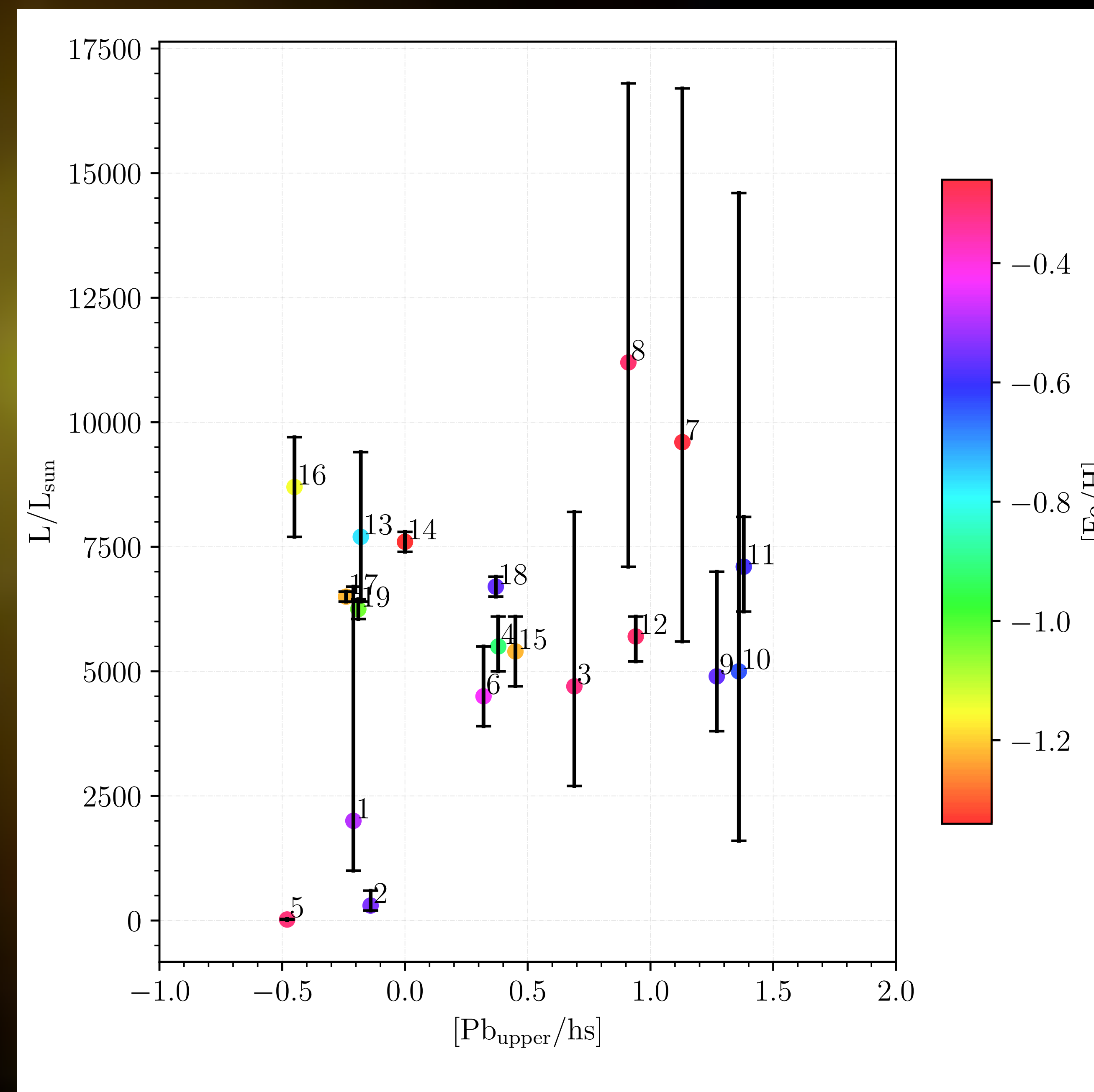

Kamath & Van Winckel 2021

THE ADVENT OF THE *i*-PROCESS:

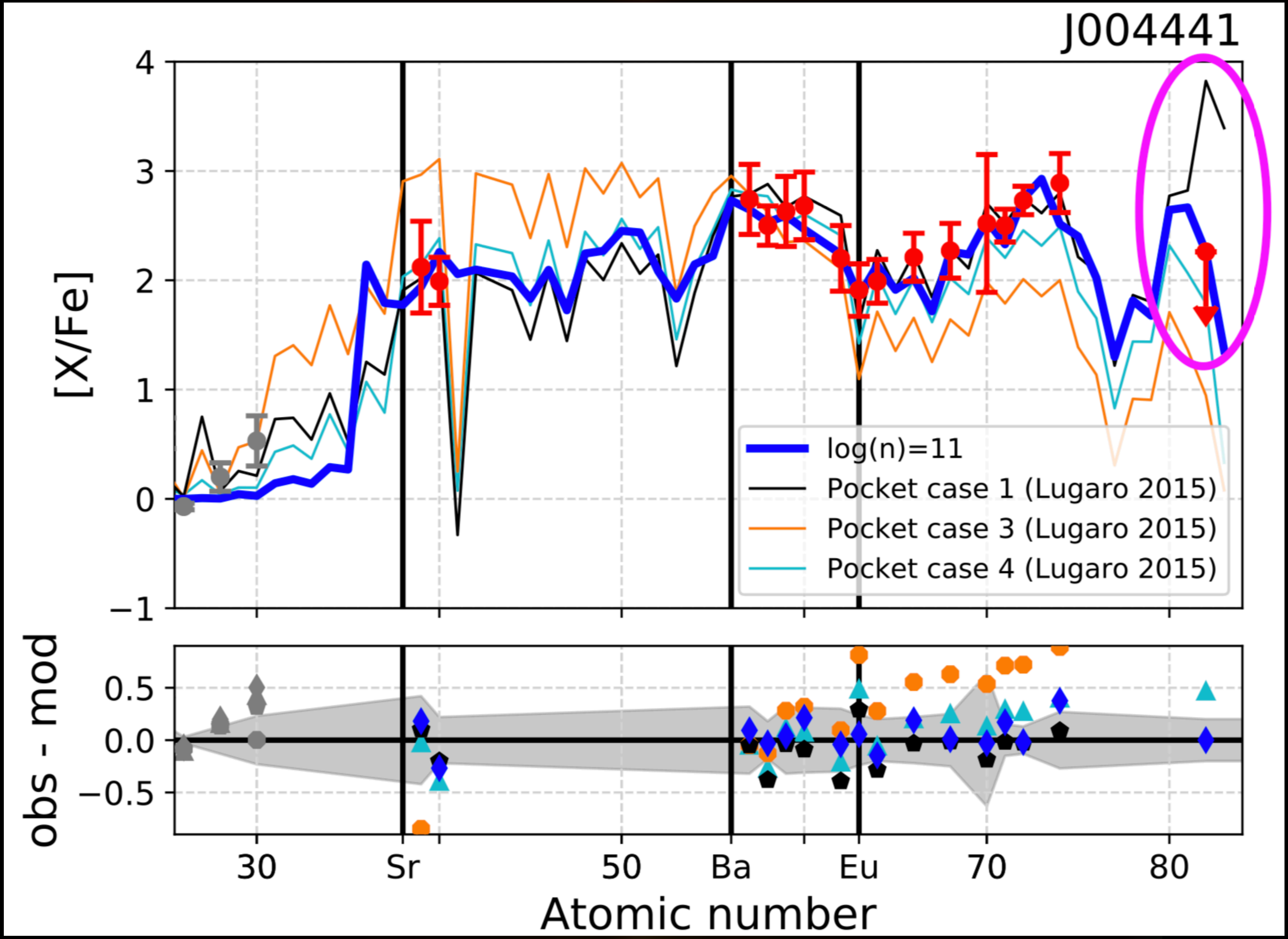

Hampel et al., 2019

A neutron density of ~10^{11} n/cm3 could produce a pattern that matches…

LEAD (Pb): A TRACER OF S-PROCESS AND I-PROCESS IN AGB STARS

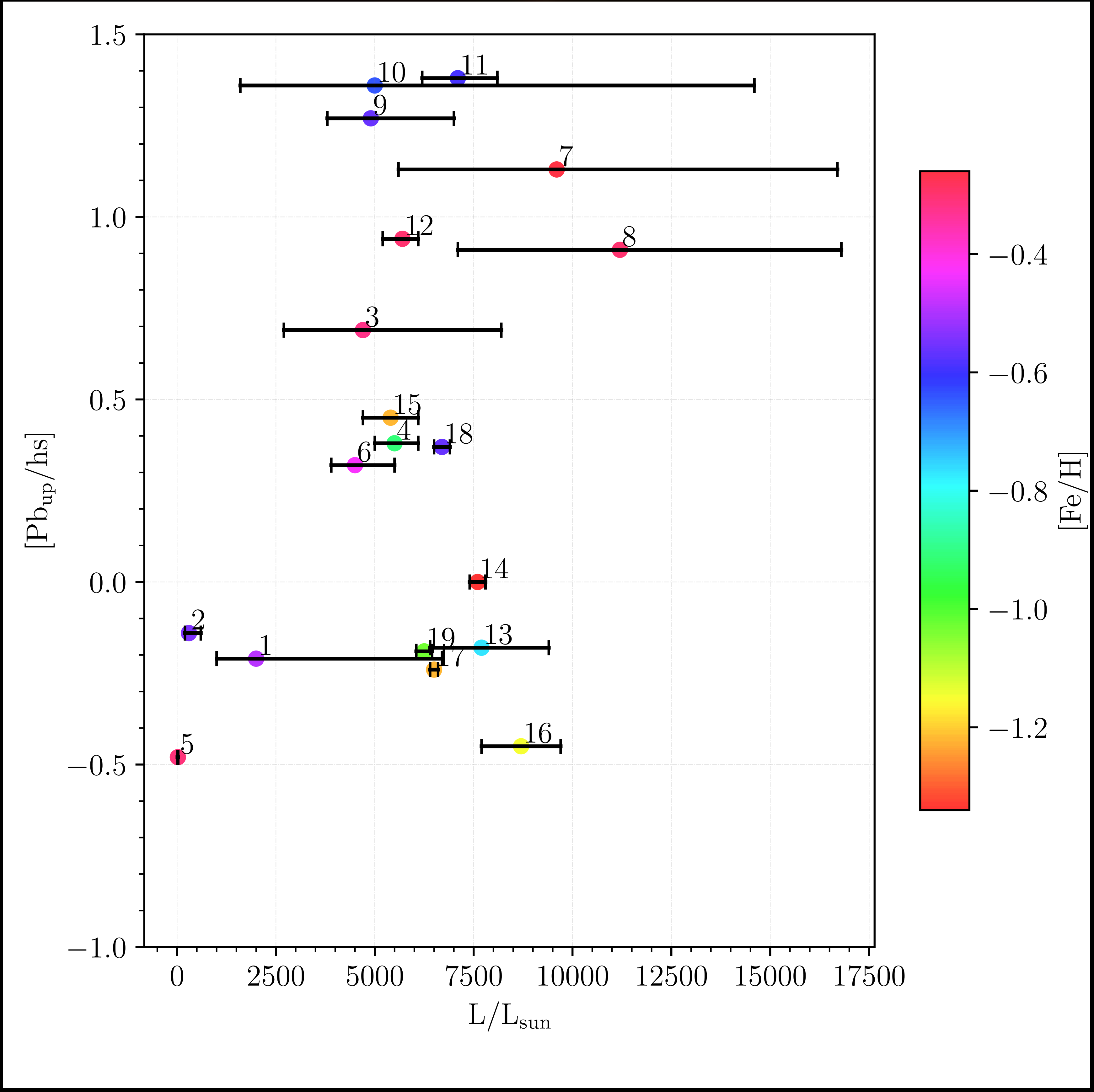

THE STATE-OF-THE-ART: SINGLE STAR AGB NUCLEOSYNTHESIS

- A subset of post-AGB stars reflect a lack of carbon production during the AGB phase
  Kamath et al.,2018
  efficiency of the third dredge-up

- **Non-uniform *s*-process production**
  Van Winckel 2003; Kamath et al.,2022; Kamath et al., 2022b to-be-submitted
  AGB nucleosynthesis

- Under-abundance of lead (b)
  De Smedt et al., 2014, 2015; Kamath et al., 2021
  ***s*-process nucleosynthesis**

- Observed C/O and 12C/13C ratios significantly lower than predictions
  De Smedt et al., 2012; Van Aarle et al., 2014; Kamath et al., 2014; 2015
  convection, mixing, and mass-loss

Position of the Galactic Post-AGBs in the HR-Diagram

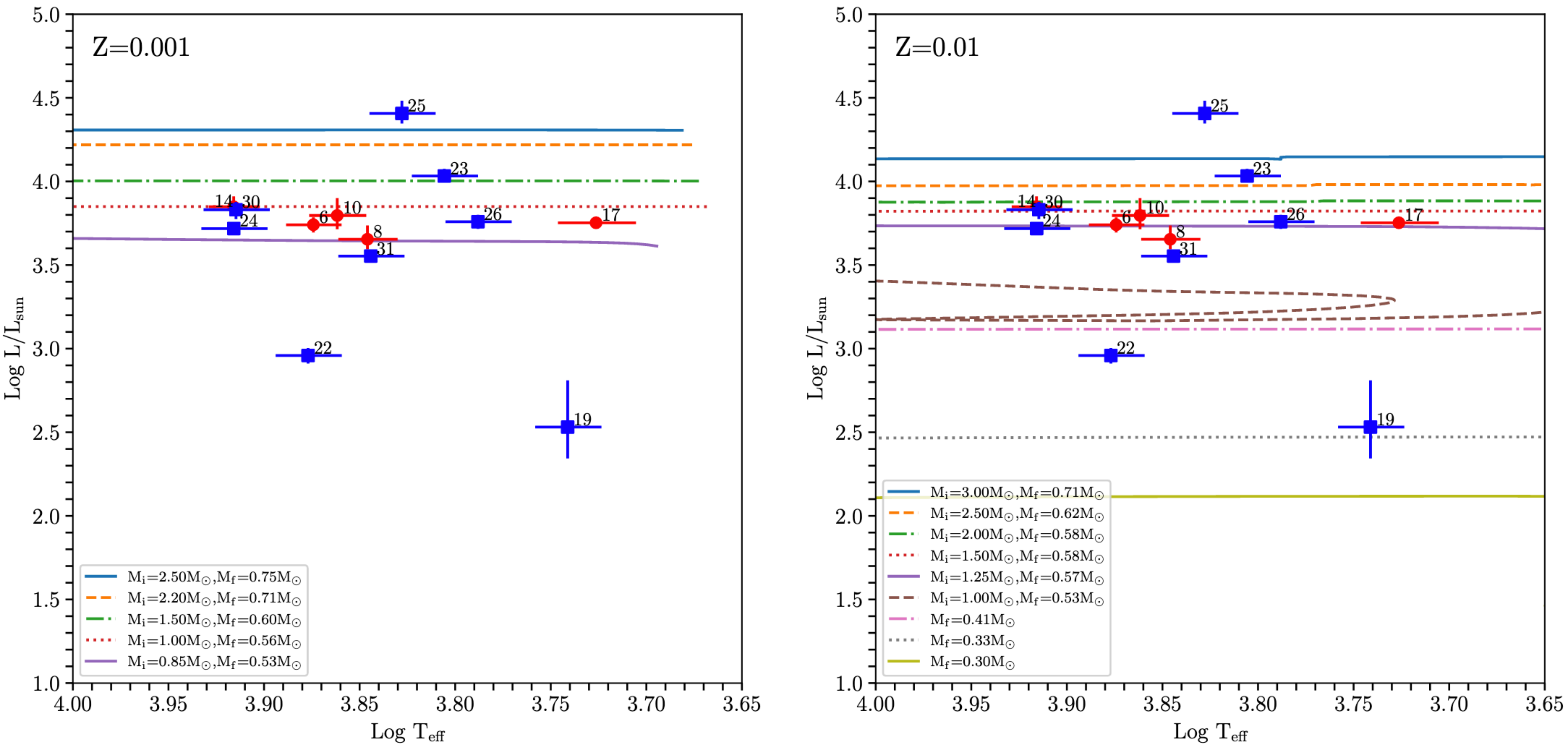

Filled: Quality 1 - Filled (based on GAIA astrometric data)

Red circles: s-process enriched Blue squares: non s-process rich

Chemical diversity NOT entirely a mass or initial metallicity effect!

THEORETICAL PREDICTIONS FOR TDU AND HBB FOR A RANGE OF METALLICITIES

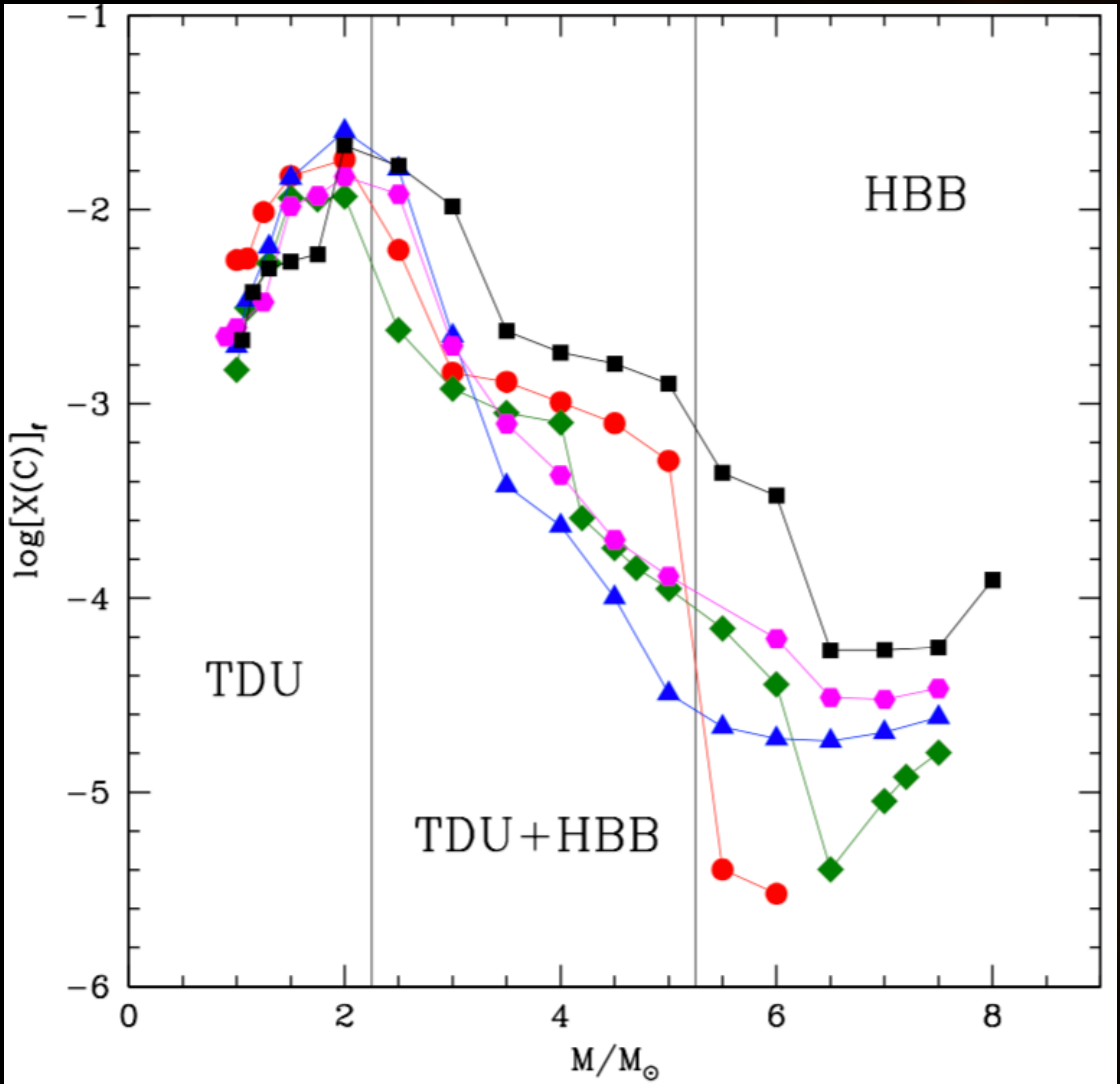

- Models with $M_{initial}$ = 1. 5 to 2.5 M_{sun} show strong C-enhancement
- Onset of HBB roughly at 2.5 to 3M_{sun} (depending on metallicity)

Dell' Agli et al., 2019

HEAVY-ELEMENT YIELDS AND ABUNDANCES OF AGB STARS WITH $Z = 0.0028$, $[Fe/H] \approx -0.7$

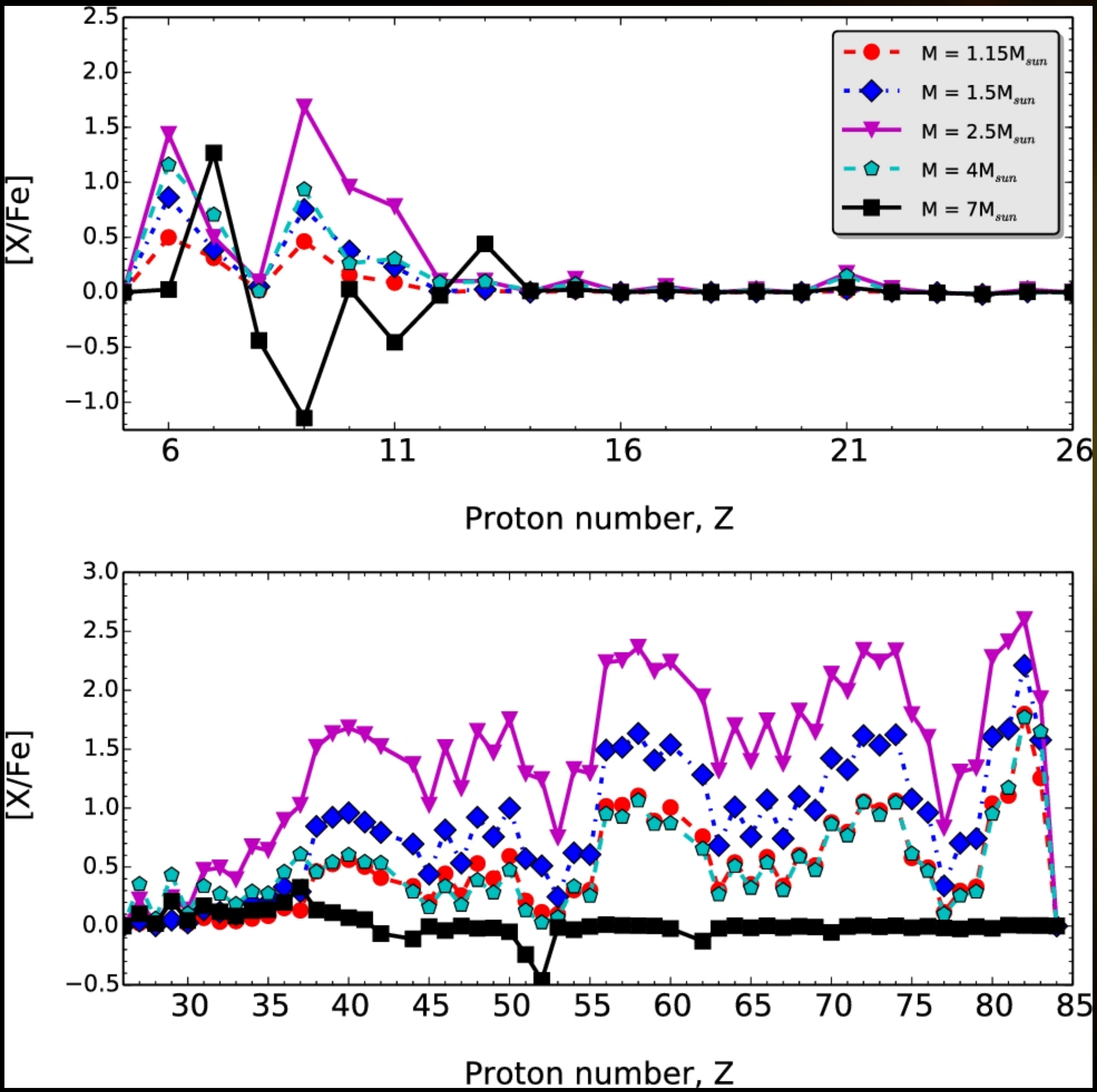

- Models with $M_{initial} = 1.15$ to 4 M_{sun} show strong C-enhancement
- Models with $M_{initial} = 1.15$ to 3.75 M_{sun} show mild to strong s-process enrichment

Karakas et al., 2018

Post-AGB stars as Exquisite tracers for CNO, Fe-peak, and *s*-process elements

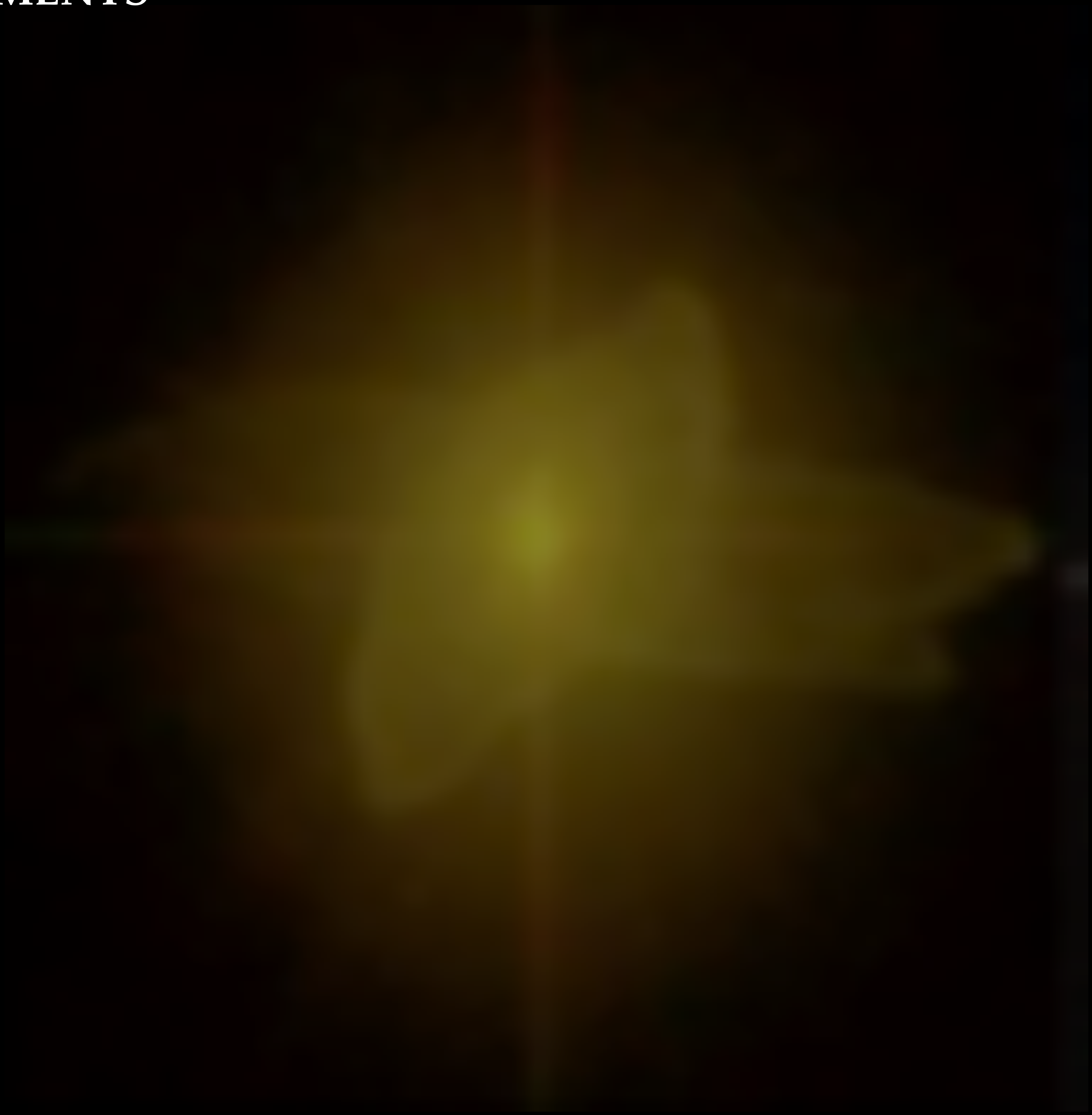

De Smedt PhD Thesis

POST-AGB STARS AS EXQUISITE TRACERS FOR CNO, FE-PEAK, AND *S*-PROCESS ELEMENTS

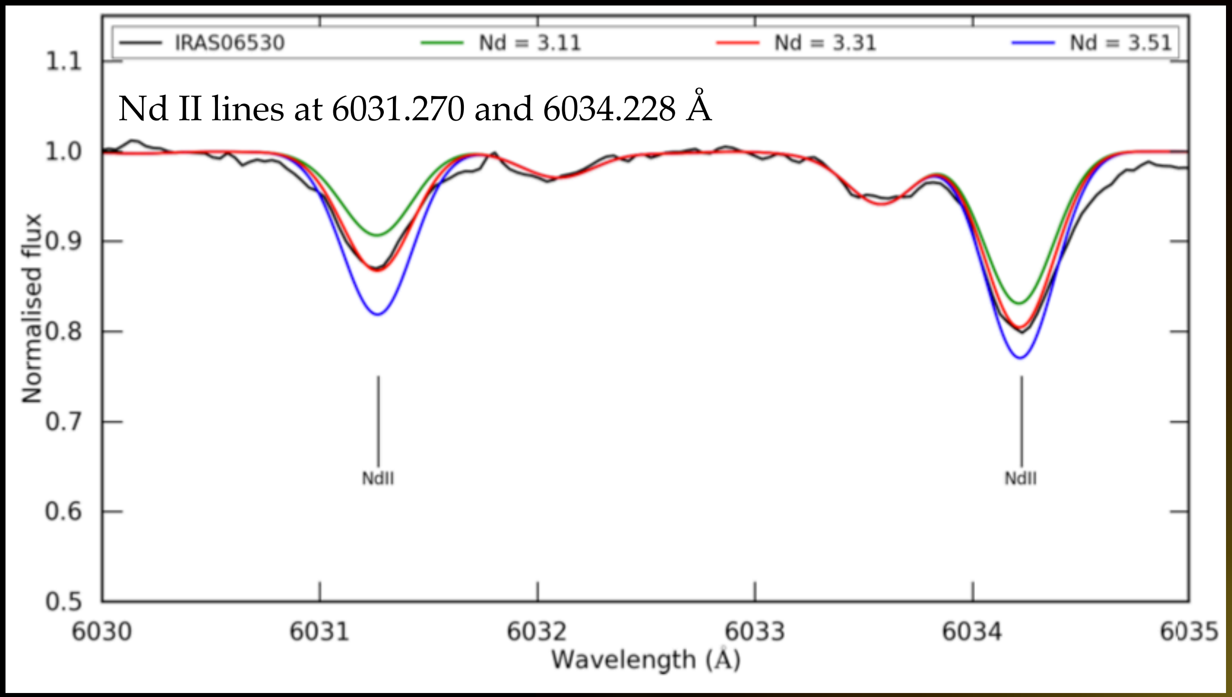

POST-AGB STARS AS EXQUISITE TRACERS FOR CNO, FE-PEAK, AND *S*-PROCESS ELEMENTS

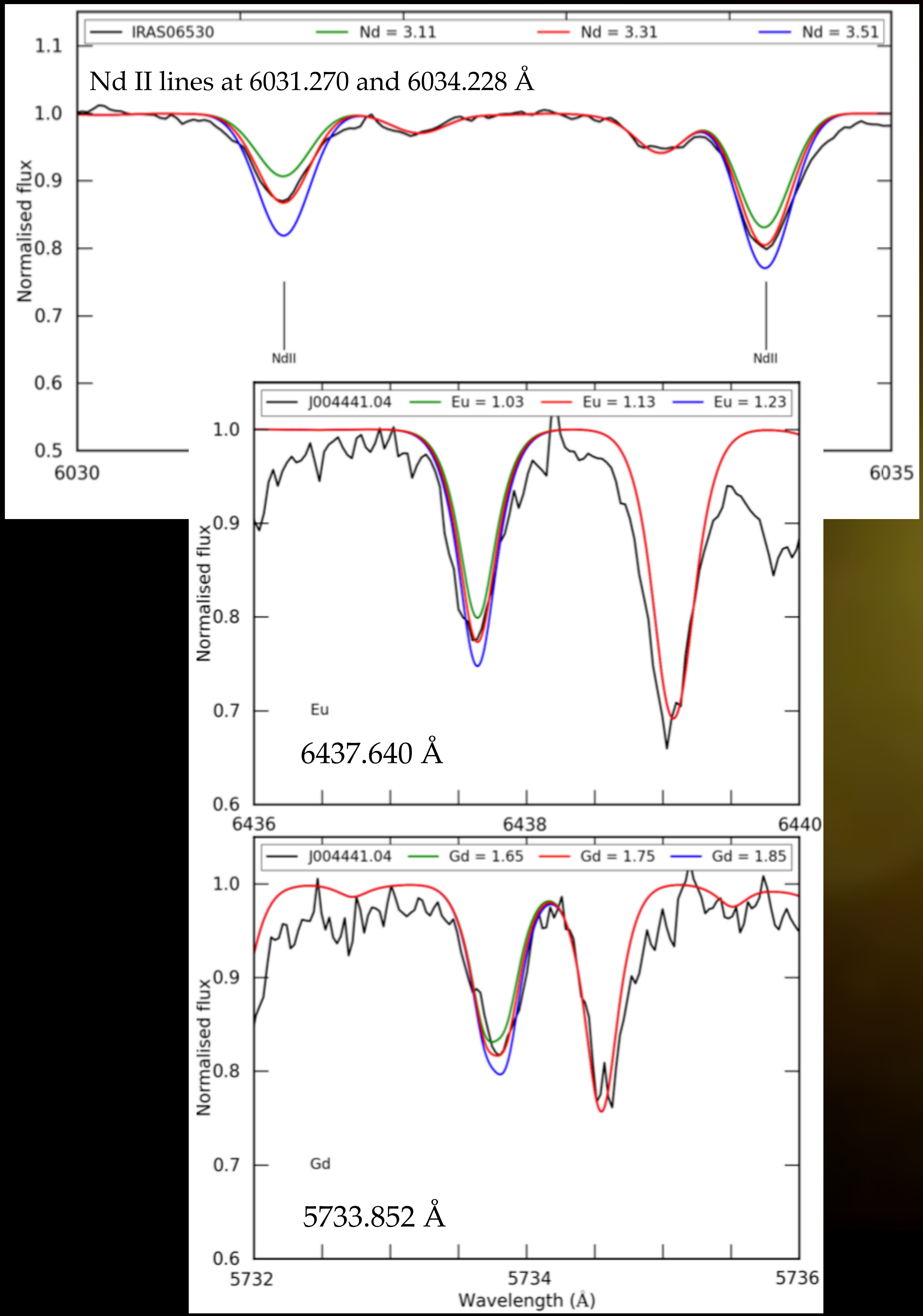

De Smedt PhD Thesis

Post-AGB stars as Exquisite tracers for CNO, Fe-peak, and *s*-process elements

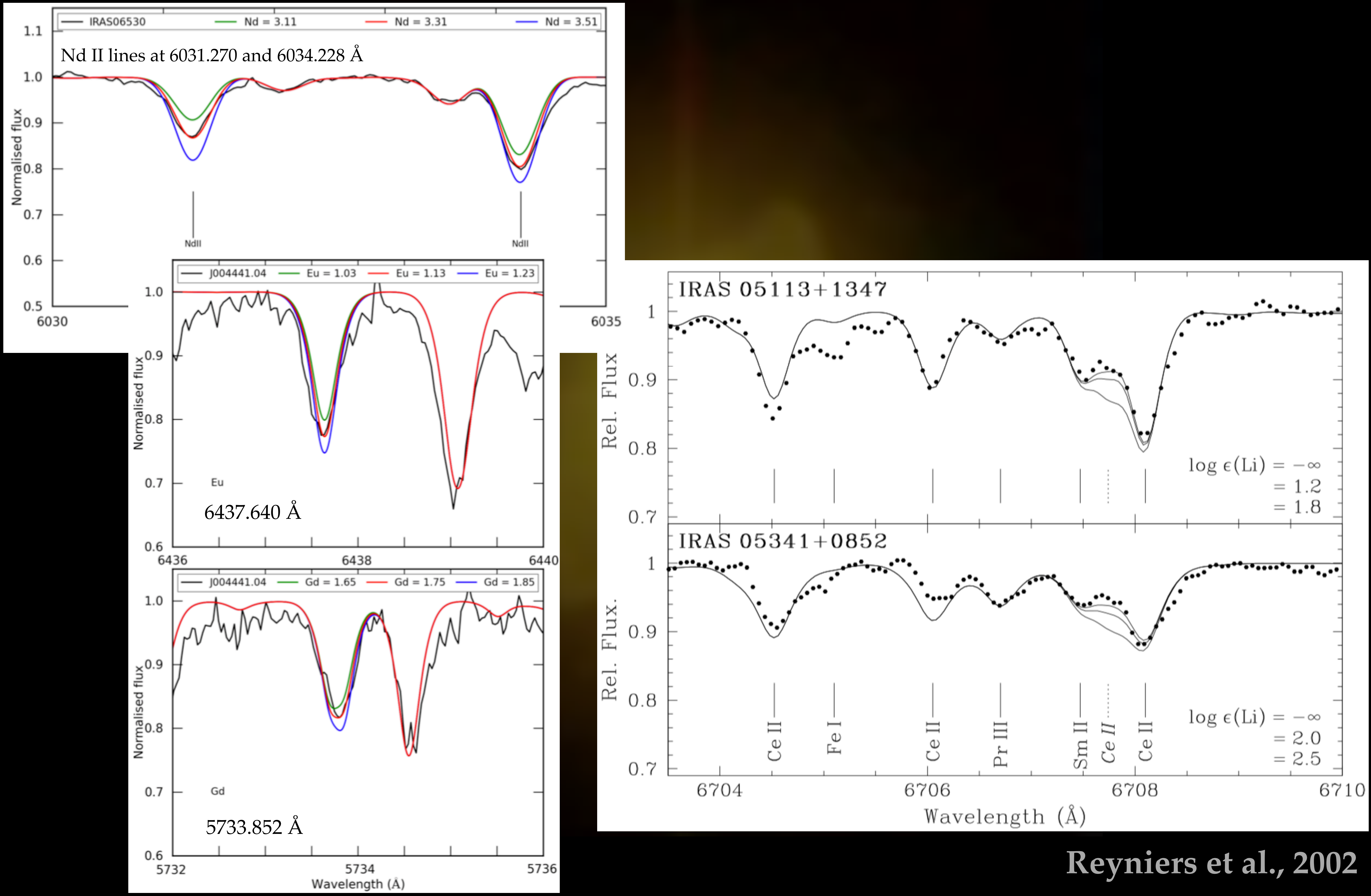

Reyniers et al., 2002

De Smedt PhD Thesis

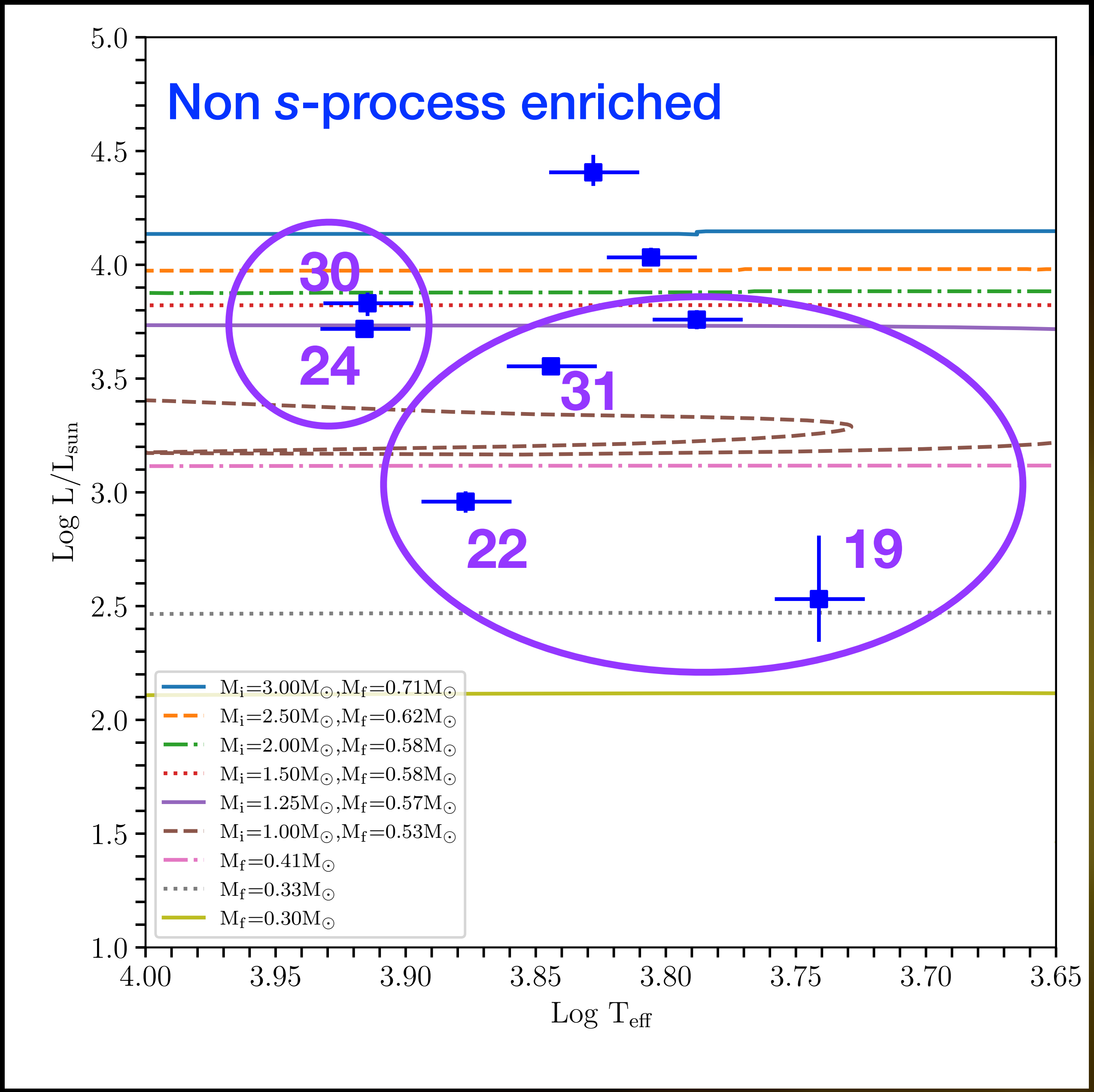

- **Case 1: First Dredge-Up (FDU)**
- **Progenitor mass below ~1 Msun**
  - Few thermal pulses before envelope is lost
  - Evolve as M-stars
  - Little to no C and *s*-process
  - Some N (~0.5 dex) from FDU

Index	Object	T_{eff}	$L/L_\odot$	[C/Fe]	[N/Fe]	[O/Fe]	Flag	M_{init}	chemistry
19	IRAS 01259+6823	5510 ± 250	340	0.18 ± 0.15	...	0.31 ± 0.06	Q1	$0.5 - 0.6\ M_\odot$	FDU
22	HD 107369	7533 ± 250	910	< -0.2	0.49 ± 0.3	0 ± 0.2	Q1	$0.5 - 0.6\ M_\odot$	FDU
24	HD 133656	8238 ± 250	5227	0.3 ± 0.2	0.5 ± 0.2	0.6 ± 0.2	Q1	$0.8 - 1\ M_\odot$	FDU
29	IRAS 19386+0155	6303 ± 250	9611	0.1 ± 0.2	...	...	Q2	$0.7 - 0.8\ M_\odot$	FDU
30	IRAS 19475+3119	8216 ± 250	6775	-0.09 ± 0.30	...	0.30 ± 0.02	Q1	$0.8 - 1\ M_\odot$	FDU
31	HR 7671	6985 ± 250	3579	-0.57 ± 0.13	0.51 ± 0.16	0.46 ± 0.05	Q1	$0.5 - 0.6\ M_\odot$	FDU

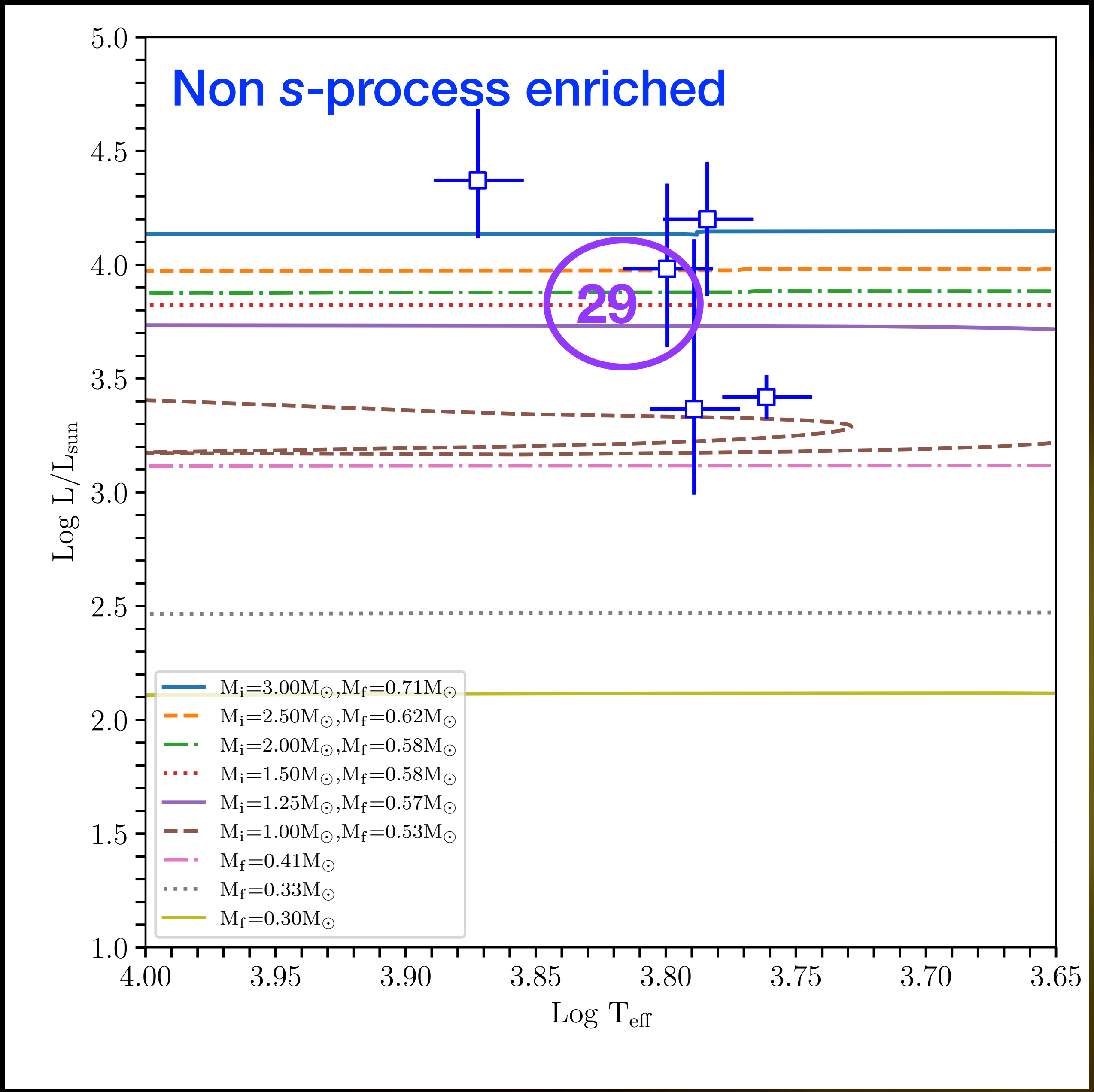

- **Case 1: First Dredge-Up (FDU)**
- **Progenitor mass below ~1 Msun**
  - Few thermal pulses before envelope is lost
  - Evolve as M-stars
  - Little to no C and *s*-process
  - Some N (~0.5 dex) from FDU

Index	Object	T_{eff}	$L/L_{\odot}$	[C/Fe]	[N/Fe]	[O/Fe]	Flag	M_{init}	chemistry
19	IRAS 01259+6823	5510 ± 250	340	0.18 ± 0.15	...	0.31 ± 0.06	Q1	$0.5 - 0.6\ M_{\odot}$	FDU
22	HD 107369	7533 ± 250	910	< -0.2	0.49 ± 0.3	0 ± 0.2	Q1	$0.5 - 0.6\ M_{\odot}$	FDU
24	HD 133656	8238 ± 250	5227	0.3 ± 0.2	0.5 ± 0.2	0.6 ± 0.2	Q1	$0.8 - 1\ M_{\odot}$	FDU
29	IRAS 19386+0155	6303 ± 250	9611	0.1 ± 0.2	...	...	Q2	$0.7 - 0.8\ M_{\odot}$	FDU
30	IRAS 19475+3119	8216 ± 250	6775	-0.09 ± 0.30	...	0.30 ± 0.02	Q1	$0.8 - 1\ M_{\odot}$	FDU
31	HR 7671	6985 ± 250	3579	-0.57 ± 0.13	0.51 ± 0.16	0.46 ± 0.05	Q1	$0.5 - 0.6\ M_{\odot}$	FDU

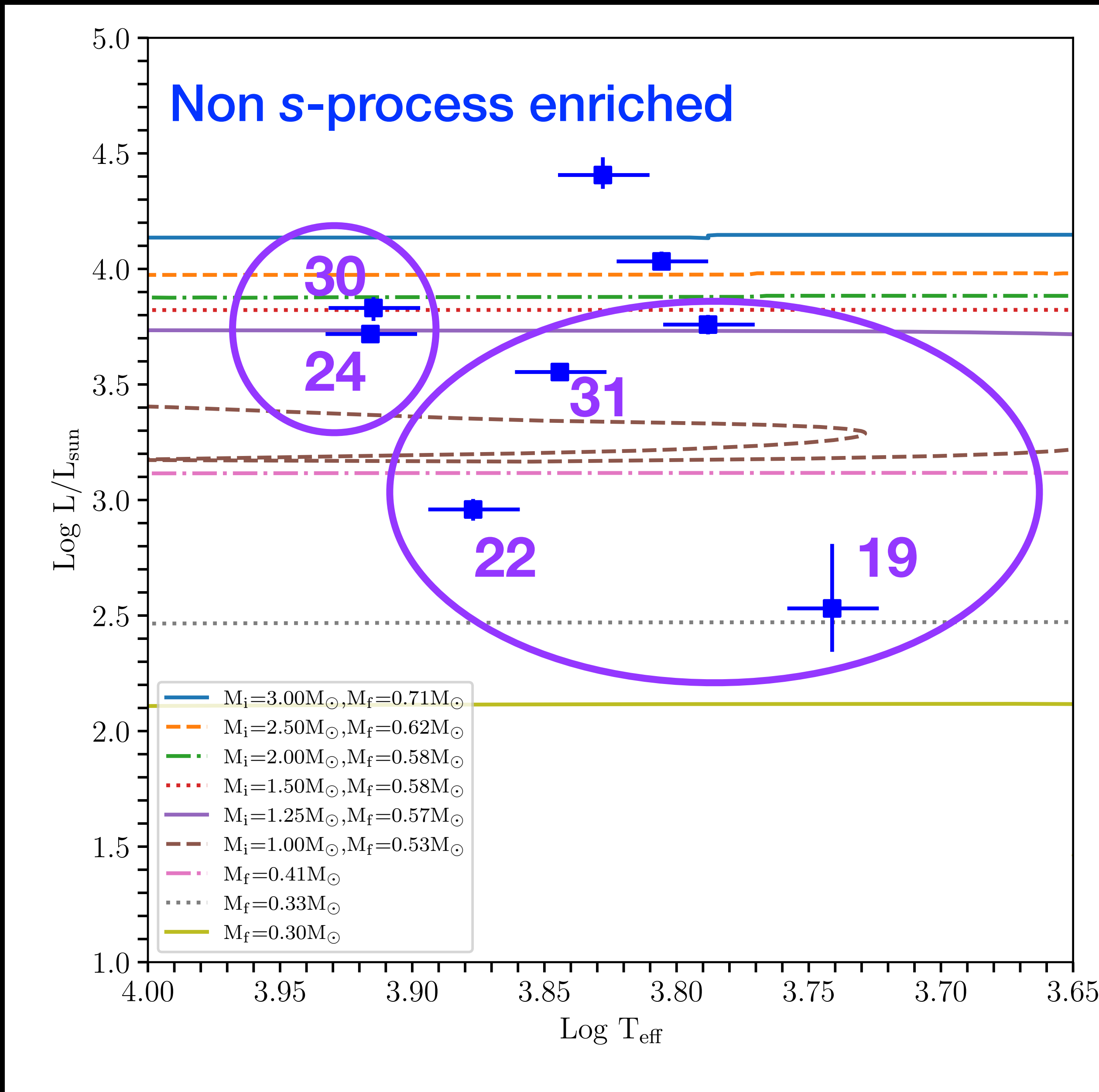

- **Case 1: First Dredge-Up (FDU)**
- **Progenitor mass below ~1 Msun**
  - Few thermal pulses before envelope is lost
  - Evolve as M-stars
  - Little to no C and *s*-process
  - Some N (~0.5 dex) from FDU

Index	Object	T_{eff}	$L/L_\odot$	[C/Fe]	[N/Fe]	[O/Fe]	Flag	M_{init}	chemistry
19	IRAS 01259+6823	5510 ± 250	340	0.18 ± 0.15	...	0.31 ± 0.06	Q1	$0.5 - 0.6\ M_\odot$	FDU
22	HD 107369	7533 ± 250	910	< -0.2	0.49 ± 0.3	0 ± 0.2	Q1	$0.5 - 0.6\ M_\odot$	FDU
24	HD 133656	8238 ± 250	5227	0.3 ± 0.2	0.5 ± 0.2	0.6 ± 0.2	Q1	$0.8 - 1\ M_\odot$	FDU
29	IRAS 19386+0155	6303 ± 250	9611	0.1 ± 0.2	...	...	Q2	$0.7 - 0.8\ M_\odot$	FDU
30	IRAS 19475+3119	8216 ± 250	6775	-0.09 ± 0.30	...	0.30 ± 0.02	Q1	$0.8 - 1\ M_\odot$	FDU
31	HR 7671	6985 ± 250	3579	-0.57 ± 0.13	0.51 ± 0.16	0.46 ± 0.05	Q1	$0.5 - 0.6\ M_\odot$	FDU

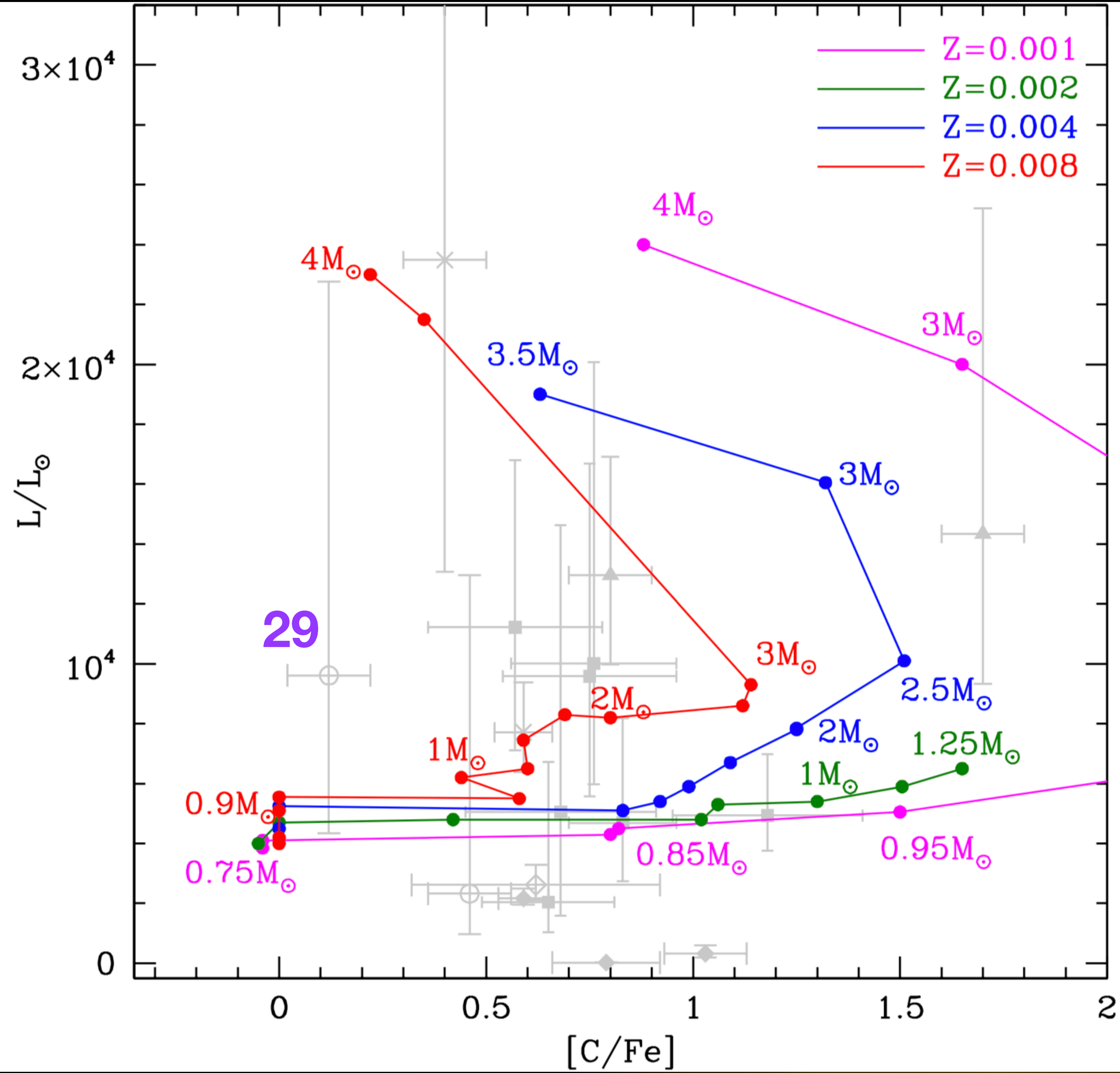

- **Case 1: First Dredge-Up (FDU)**
- **Progenitor mass below ~1 Msun**
  - Few thermal pulses before envelope is lost
  - Evolve as M-stars
  - Little to no C and *s*-process
  - Some N (~0.5 dex) from FDU

Index	Object	T_{eff}	$L/L_\odot$	[C/Fe]	[N/Fe]	[O/Fe]	Flag	M_{init}	chemistry
19	IRAS 01259+6823	5510 ± 250	340	0.18 ± 0.15	...	0.31 ± 0.06	Q1	$0.5 - 0.6\ M_\odot$	FDU
22	HD 107369	7533 ± 250	910	< -0.2	0.49 ± 0.3	0 ± 0.2	Q1	$0.5 - 0.6\ M_\odot$	FDU
24	HD 133656	8238 ± 250	5227	0.3 ± 0.2	0.5 ± 0.2	0.6 ± 0.2	Q1	$0.8 - 1\ M_\odot$	FDU
29	IRAS 19386+0155	6303 ± 250	9611	0.1 ± 0.2	...	...	Q2	$0.7 - 0.8\ M_\odot$	FDU
30	IRAS 19475+3119	8216 ± 250	6775	-0.09 ± 0.30	...	0.30 ± 0.02	Q1	$0.8 - 1\ M_\odot$	FDU
31	HR 7671	6985 ± 250	3579	-0.57 ± 0.13	0.51 ± 0.16	0.46 ± 0.05	Q1	$0.5 - 0.6\ M_\odot$	FDU

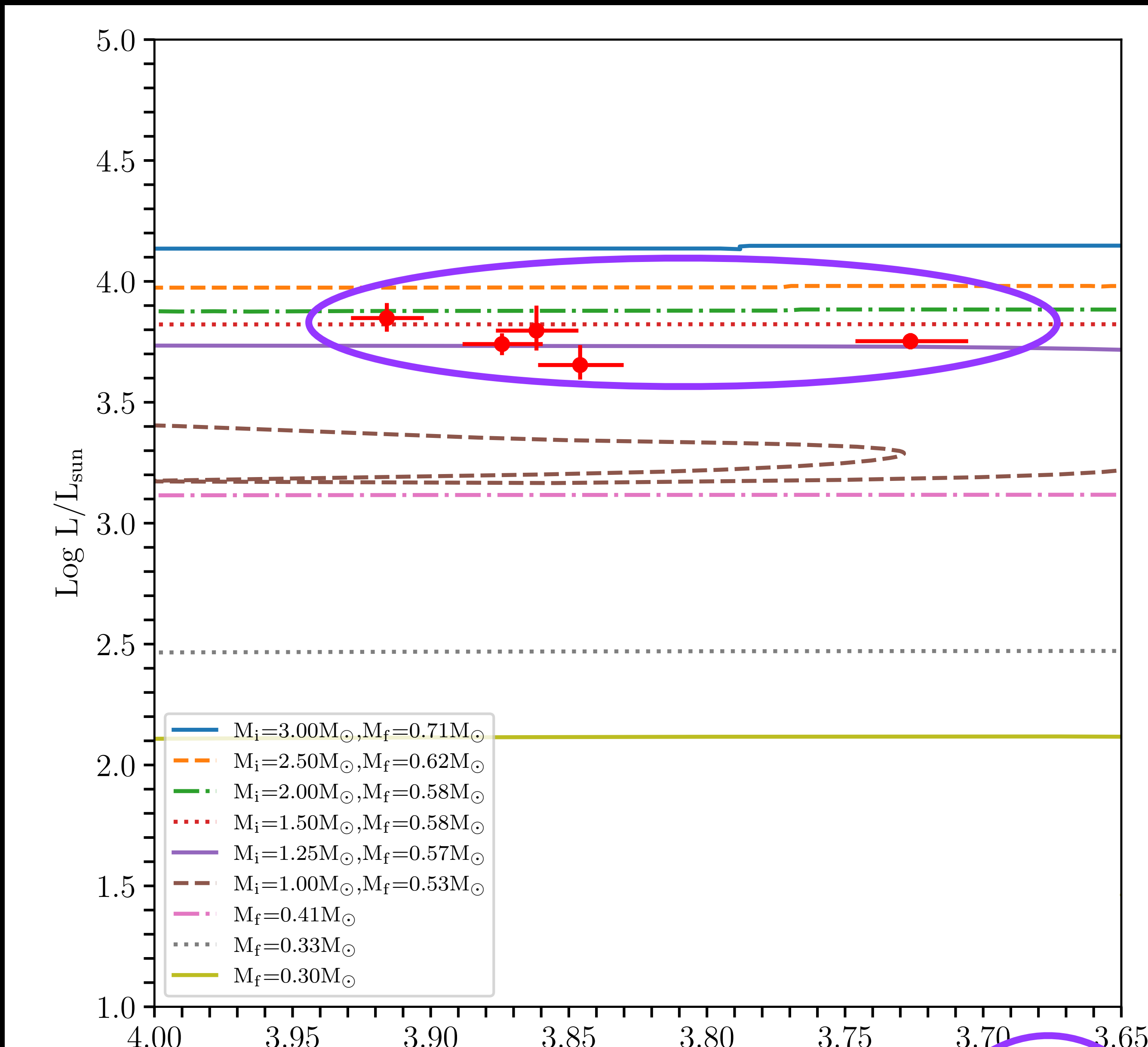

- **Case 2: Third Dredge-Up (TDU)**
- **Progenitor mass of ~1 - 3 Msun**
  - Series of thermal pulses
  - Evolve as C-stars
  - Significant C and *s*-process
  - Some N (from FDU), mild O-enrichment

	Object	T_{eff}	$L/L_\odot$	[C/Fe]	[N/Fe]	[O/Fe]	Flag	M_{init}	chemistry
8	IRAS 08143-4406	7013 ± 250	4509	0.71 ± 0.10	0.01 ± 0.22	0.19 ± 0.13	Q1	$1 - 1.5\ M_\odot$	TDU
9	IRAS 08281-4850	7462 ± 250	9584	0.75 ± 0.21	...	0.12 ± 0.11	Q2	$1.5 - 2\ M_\odot$	TDU
10	IRAS 12360-5740	7273 ± 250	6258	0.27 ± 0.18	0.22 ± 0.32	0.31 ± 0.05	Q1	$1 - 1.5\ M_\odot$	TDU
11	IRAS 13245-5036	9037 ± 250	11221	0.57 ± 0.21	...	0.26 ± 0.13	Q2	$1.5 - 2\ M_\odot$	TDU
12	IRAS 14325-6428	7256 ± 250	4935	1.18 ± 0.23	0.18 ± 0.20	0.57 ± 0.09	Q2	$1.5 - 2\ M_\odot$	TDU
13	IRAS 14429-4539	9579 ± 250	5049	0.68 ± 0.23	...	0.31 ± 0.12	Q2	$1.5 - 2\ M_\odot$	TDU
14	IRAS 19500-1709	8239 ± 250	7053	0.99 ± 0.06	0.41 ± 0.30	0.72 ± 0.04	Q1	$1.5 - 2\ M_\odot$	TDU

- **Case 2: Third Dredge-Up (TDU)**
- **Progenitor mass of ~1 - 3 Msun**
  - Series of thermal pulses
  - Evolve as C-stars
  - Significant C and *s*-process
  - Some N (from FDU), mild O-enrichment

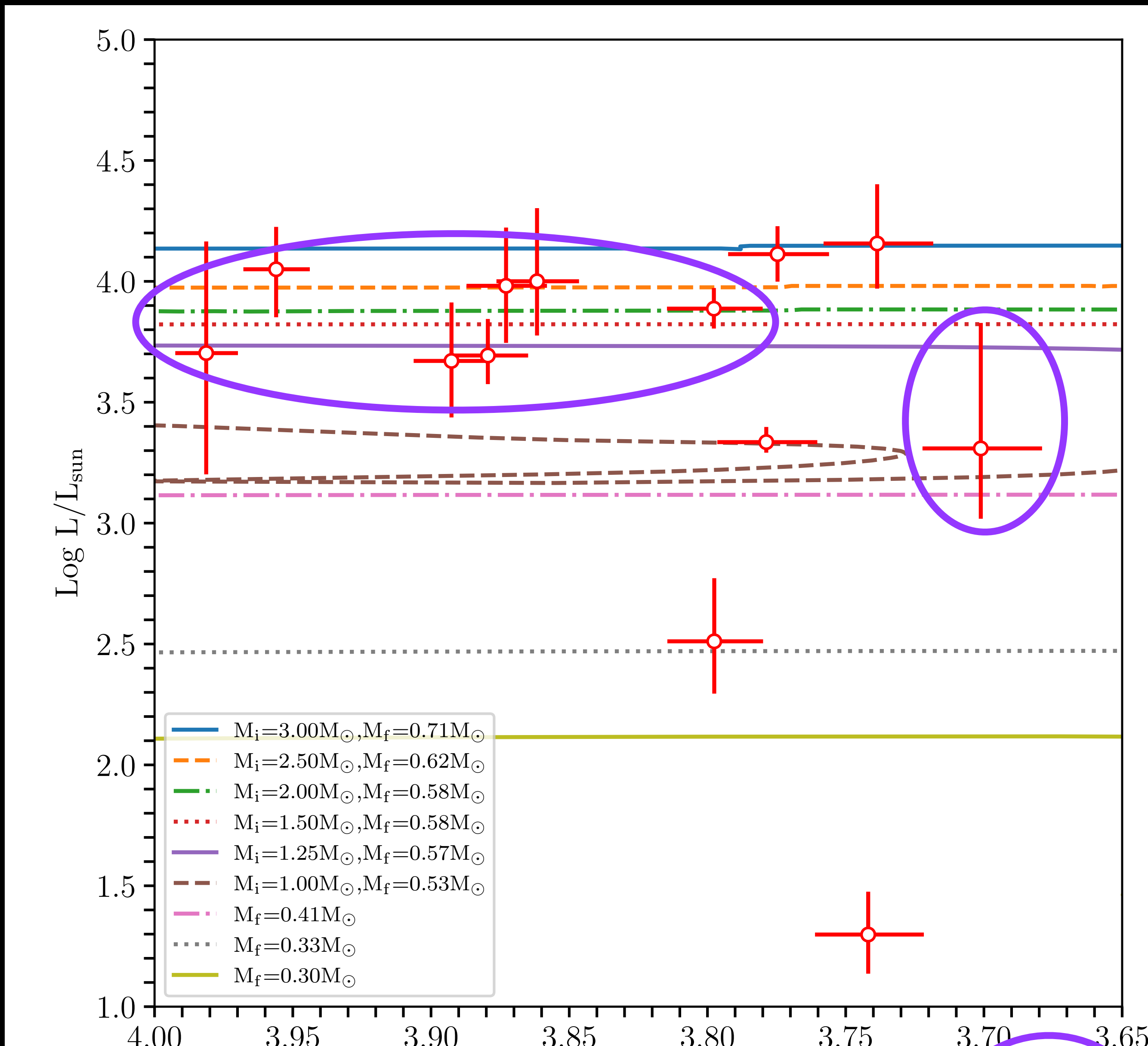

Object		T_{eff}	$L/L_\odot$	[C/Fe]	[N/Fe]	[O/Fe]	Flag	M_{init}	chemistry
8	IRAS 08143-4406	7013 ± 250	4509	0.71 ± 0.10	0.01 ± 0.22	0.19 ± 0.13	Q1	$1 - 1.5$ M$_\odot$	TDU
9	IRAS 08281-4850	7462 ± 250	9584	0.75 ± 0.21	...	0.12 ± 0.11	Q2	$1.5 - 2$ M$_\odot$	TDU
10	IRAS 12360-5740	7273 ± 250	6258	0.27 ± 0.18	0.22 ± 0.32	0.31 ± 0.05	Q1	$1 - 1.5$ M$_\odot$	TDU
11	IRAS 13245-5036	9037 ± 250	11221	0.57 ± 0.21	...	0.26 ± 0.13	Q2	$1.5 - 2$ M$_\odot$	TDU
12	IRAS 14325-6428	7256 ± 250	4935	1.18 ± 0.23	0.18 ± 0.20	0.57 ± 0.09	Q2	$1.5 - 2$ M$_\odot$	TDU
13	IRAS 14429-4539	9579 ± 250	5049	0.68 ± 0.23	...	0.31 ± 0.12	Q2	$1.5 - 2$ M$_\odot$	TDU
14	IRAS 19500-1709	8239 ± 250	7053	0.99 ± 0.06	0.41 ± 0.30	0.72 ± 0.04	Q1	$1.5 - 2$ M$_\odot$	TDU

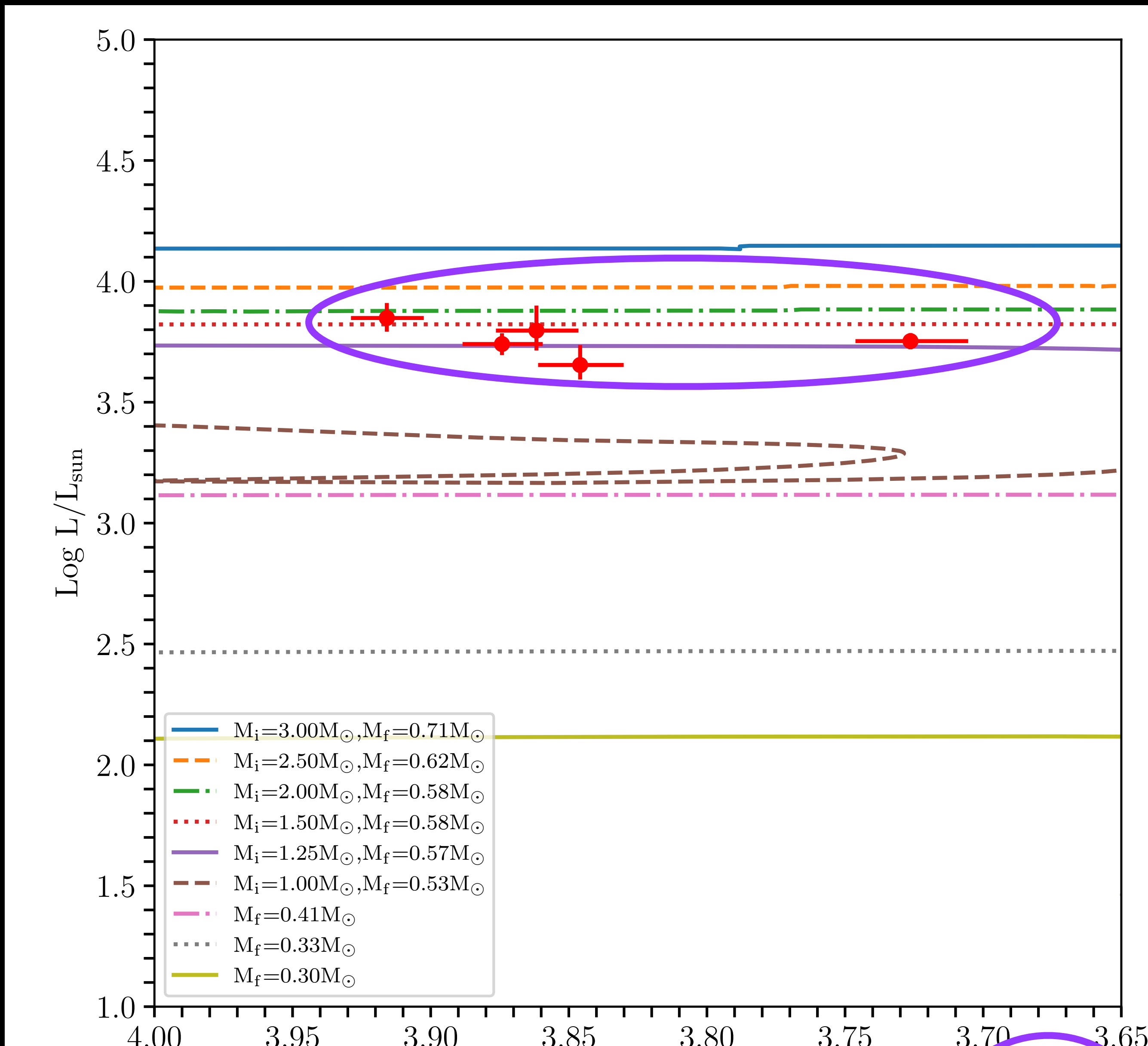

- ★ **Case 2: Third Dredge-Up (TDU)**
- ★ **Progenitor mass of ~1 - 3 Msun**
  - ★ Series of thermal pulses
  - ★ Evolve as C-stars
  - ★ Significant C and *s*-process
  - ★ Some N (from FDU), mild O-enrichment

Object		T_{eff}	$L/L_\odot$	[C/Fe]	[N/Fe]	[O/Fe]	Flag	M_{init}	chemistry
8	IRAS 08143-4406	7013 ± 250	4509	0.71 ± 0.10	0.01 ± 0.22	0.19 ± 0.13	Q1	$1 - 1.5\ M_\odot$	TDU
9	IRAS 08281-4850	7462 ± 250	9584	0.75 ± 0.21	...	0.12 ± 0.11	Q2	$1.5 - 2\ M_\odot$	TDU
10	IRAS 12360-5740	7273 ± 250	6258	0.27 ± 0.18	0.22 ± 0.32	0.31 ± 0.05	Q1	$1 - 1.5\ M_\odot$	TDU
11	IRAS 13245-5036	9037 ± 250	11221	0.57 ± 0.21	...	0.26 ± 0.13	Q2	$1.5 - 2\ M_\odot$	TDU
12	IRAS 14325-6428	7256 ± 250	4935	1.18 ± 0.23	0.18 ± 0.20	0.57 ± 0.09	Q2	$1.5 - 2\ M_\odot$	TDU
13	IRAS 14429-4539	9579 ± 250	5049	0.68 ± 0.23	...	0.31 ± 0.12	Q2	$1.5 - 2\ M_\odot$	TDU
14	IRAS 19500-1709	8239 ± 250	7053	0.99 ± 0.06	0.41 ± 0.30	0.72 ± 0.04	Q1	$1.5 - 2\ M_\odot$	TDU